Microscopic Examination of the Effects of Ptr (*Pyrenophora tritici-repentis*) ToxA on Wheat

BY

EYMOND DONALD TOUPIN

A Thesis
Submitted to the Faculty of Graduate Studies
in Partial Fulfillment of the Requirements
for the Degree of

MASTER OF SCIENCE

Department of Plant Science
University of Manitoba
Winnipeg, Manitoba

THE UNIVERSITY OF MANITOBA

FACULTY OF GRADUATE STUDIES

*****

COPYRIGHT PERMISSION PAGE

Microscopic Examination of the Effects of Ptr (*Pyrenophora tritici-repentis*) ToxA on Wheat

BY

Eymond Donald Toupin

A Thesis/Practicum submitted to the Faculty of Graduate Studies of The University of Manitoba in partial fulfillment of the requirements of the degree of Master of Science

ACKNOWLEDGMENTS

I would like to thank my advisor, Dr. G.M. Ballance for his advice and support throughout the duration of this project. I have also greatly appreciated the suggestions and encouragement provided by the other members of my examining committee, Dr. M.J. Sumner, and Dr. L. Lamari.

Much valuable technical assistance and guidance was provided in the course of this research by Mr. Ralph Kowatsch, Ms. Lynn Burton, Mr. Ian Brown, Mr. Bert Luit, Ms. Susan Ramsey, and Mr. Richard Smith. Thank you for showing me how to do things, helping me overcome difficulties, and for performing some important tasks.

I am grateful to NSERC for the funding which was provided to conduct this research.

Lastly, I am especially thankful for the moral and emotional support of my wife Penny. She has been very patient in my pursuit of this Master's degree.

TABLE OF CONTENTS

Page

LIST OF TABLES

LIST OF FIGURES

ABSTRACT

Toupin, Eymond D. University of Manitoba, May 2000, Microscopic examination of the effects of Ptr (*Pyrenophora tritici-repentis*) ToxA on wheat. Major Professor; Dr. G.M. Ballance.

Tan spot is an important leaf-spotting disease of wheat which has become more prevalent due to the adoption of conservation tillage practices. Certain isolates of the ascomycete *Pyrenophora tritici-repentis*, the causal agent of tan spot, are known to produce host-selective toxins which are involved in pathogenesis. PtrToxA, which induces tan necrotic lesions in the leaves of sensitive wheat genotypes, was the first of these toxins to be characterized, and is a 14 kDa ribosomally-synthesized polypeptide. The purpose of this study was to examine the effects of PtrToxA on sensitive wheat leaf tissue using light, fluorescence, and transmission electron microscopy. The microscopic effects of the toxin were also compared to those of freezing and thawing, desiccation of detached leaves, and plasmolysis at the time of fixation. PtrToxA induces cell disruption and collapse in the mesophyll, epidermis and outer bundle sheath but not in the vascular bundle, including the inner bundle sheath, or in the stomatal guard cells. The walls of collapsed cells, although severely deformed, did not lose a significant amount of cellulose or polysaccharides with vicinal glycol groups, as indicated by calcofluor or PAS staining respectively. These severely collapsed cells seemed to have well-preserved thylakoidal membranes interspersed with large starch granules. This indicates that the chloroplasts were not the primary targets of toxin activity. Certain cells in the early stages of toxin-induced disruption appear to have a damaged tonoplast, as evidenced by the distribution of intact organelles throughout the cell volume. Wall appositions, deposited between the plasma membrane and cell wall of healthy-appearing cells in regions opposite toxin-affected cells, were often observed. These wall appositions were at least partially composed of callose as indicated by aniline blue staining. The wall appositions were frequently observed in the vicinity of plasmodesmata connecting healthy and toxin-affected cells. The

effect of PtrToxA on water relations, cell walls, and tonoplast are discussed with respect to the potential site and mode of action of this toxin in sensitive wheat leaf tissue.

INTRODUCTION

It is estimated that humans are consuming about 40% of the total net photosynthetic productivity on land (Raven *et al.*, 1992). The human population depends on plants for the production of food, fibre, energy and chemicals. Wheat is one of six crop plants which provides more than 80% of the total calories consumed by human beings (Raven *et al.*, 1992). Plant diseases, like tan spot of wheat, can cause significant crop losses and are therefore detrimental to the health and well-being of the world population.

Tan spot of wheat, caused by the ascomycete *Pyrenophora tritici-repentis*, seems to have become more prevalent since the adoption of conservation tillage practices because infected stubble may be a source of inoculum (Rees and Platz, 1979). Tan spot development appears to depend on the ability of the fungus to produce host-specific toxins (Lamari and Bernier, 1989b, and DeWolf *et al.*, 1998). PtrToxA, also known as the Ptr necrosis toxin because of the type of symptom it induces in sensitive wheat genotypes, was the first toxin characterized in this pathosystem (Ballance *et al.*, 1989). PtrToxA is unique because it is a 14 kDa ribosomally synthesized polypeptide, whereas most host-specific toxins of fungal origin are low molecular weight secondary metabolites (Walton, 1996).

There is very little understanding of the activity of PtrToxA in sensitive wheat leaf tissue. When infiltrated into sensitive wheat leaves, the toxin induces a tan coloured necrotic lesion which appears desiccated. Sensitive wheat plants maintained at temperatures above 27°C are insensitive to the toxin (Lamari and Bernier, 1994). Electrolyte leakage, a common result of toxin activity in plant cells which supposedly indicates plasma membrane lesion, is detected only after 10 hours of toxin exposure (Kwon *et al.*, 1996). Necrotic activity of the toxin seems to require active cell metabolism such as mRNA transcription and protein translation (Kwon *et al.*, 1998). It has also been suggested that toxin activity inhibits or retards defense response in plants, which can include lignification of cell walls (Dushnicky *et al.*, 1998), and this in turn facilitates fungal invasion of sensitive wheat leaf tissue.

Elucidating the mode and site of action of host-specific toxins is an important and potentially rewarding scientific endeavour. It is important as it provides a better understanding of the interaction between plants and pathogens. This, therefore, provides us with more tools to combat plant diseases. However, mode of action studies also reveal some of the important physiological mechanisms which sustain plant life. For example, studying the activity of T-toxin, the toxin produced by *Cochliobolus heterostrophus* race T which was responsible for the catastrophic southern corn leaf blight epidemic of 1970, has contributed to an understanding of mitochondrial function during pollen development and its potential effect on male sterility (Tadege and Kuhlemeier, 1997 and Roel and Kuhlemeier, 1997).

Microscopy is a useful and informative means of examining the effects of toxin activity in plant cells and tissues. The observation of mitochondrial swelling as a result of T-toxin activity was significant because it confirmed the site of action suggested by the maternal inheritance of toxin-sensitivity (Gengenbach *et al.*, 1973) and created a basis for the valuable research which followed. The microscopic effects of the toxin can also be compared to those induced by other fatal treatments which are better understood. For example, toxin treatments can be compared to the effect of a freeze-thaw cycle which draws water into the intercellular spaces and damages cell membranes. Also, the effect of the toxin can be contrasted to the developmental and relatively organized processes of senescence, and programmed cell death. Ultimately, microscopic examination of toxin-treated tissues may suggest the toxin site of action via the pattern of cellular disruption.

The purpose of this study is therefore to utilize light, fluorescence, and transmission electron microscopy to examine the effect of PtrToxA on sensitive wheat leaf tissue. This will involve the characterization and comparison of the pattern of cellular disruption induced by each of the following treatments: PtrToxA toxin infiltration, a freeze-thaw cycle, desiccation caused by leaf detachment, and plasmolysis at the time of fixation. The effect of toxin activity on specific tissues, water relations, cell walls, and organelles, such as chloroplasts and vacuoles, will be discussed.

LITERATURE REVIEW

Introduction

The ever growing human population is placing increasing pressure on the resources the planet can provide. Our population has exceeded 6 billion, and it is expected to reach 8.5 billion by the year 2025 (Alexandratos, 1995). About one quarter of the global human carrying capacity estimates surveyed by Cohen (1995) predict that the planet can sustain less than 8 billion people and almost half predict a carrying capacity of less than 16 billion. Most of these estimates are based on our ability to feed the human population. For example, a large estimate of 40 billion (Revelle, 1976) assumes a vegetarian diet of 2,500 kcal per day, a tripling of current cropping area, pest losses and non-food uses under 10% of the harvest, expansion of nitrogen and phosphorous fertilizer use, and irrigation of a land area equivalent to two-thirds the size of the total area presently cropped.

From the above, it seems imperative that agricultural production be not only maintained but increased. One of the threats to agricultural production is losses to plant diseases. In the United States it is estimated that plant diseases cause losses of 15% annually (Roberts, and Boothroyd, 1984). However, depending on the crop, pathogen present, and environmental conditions, diseases losses can vary significantly from this estimate.

Each year there are more tonnes of wheat produced worldwide than any other crop, making it one of the most important crops for food production (Gooding and Davies, 1997). In fact, because of its protein, energy, nutrient, and fibre content, wheat can provide more than half of the calorie requirements in a healthy diet (Dukes *et al.*, 1995). In terms of grain tonnage produced in western Canada, wheat accounts for half and its harvest is nearly twice that of the second most important crop (Anonymous, 1999).

Tan spot

Tan spot is a foliar disease of wheat which has caused significant losses in many parts of the world such as Australia (Rees and Platz, 1979), South America

(Mehta *et al.*, 1992) and North America (Hosford, 1972, Tekauz *et al.*, 1982, Luz and Bergstrom, 1986). In a 12 year survey of plant diseases in Kansas, Sim IV *et al.* (1988) estimated that tan spot caused losses of less than 0.1 up to 3.5% annually and that on average it was the third most important disease in terms of losses. Luz and Bergstrom (1986) found that infections of *Pyrenophora tritici-repentis* (Ptr), the causal agent of tan spot, and powdery mildew could cause losses of 15 to 20% in the north-eastern U.S.. Tekauz *et al.* (1982) predicted that losses of 5 to 20% could be expected in individual fields in the Canadian Prairies if environmental conditions were favorable.

The discovery of the ascomycete which incites tan spot, *Pyrenophora tritici-repentis* (Died) Drechs., is credited to Diedicke who isolated it in 1902 (DeWolf *et al.*, 1998). The sexual state of this fungus has also been known as *Pleospora tritici-repentis* Died., *Pleospora trichostoma* f. sp. *tritici-repentis* (Died.) Noack, *Pyrenophora tritici-vulgaris* Dickson, and *Pyrenophora trichostoma* (Fr.) Fckl. (DeWolf *et al.*, 1998, Tekauz, 1976). Anamorph nomenclature includes *Helminthosporium graminearum* f.sp. *tritici-repentis* (Rab. ex Schlecht) Died., *H. tritici-repentis* (Died.) Died., *H. tritici-vulgaris* Nisikado, *Dreschlera tritici-vulgaris* (Nisikado) Ito, and *D. tritici-repentis* (Died.) Shoem. (DeWolf *et al.*, 1998).

Drechsler (1923) described Ptr as having relatively long (45-175 µm) and straight cylindrical conidia which are 1 to 9 septate. The conidia, with conical shaped basal cells, grow from olivaceous sporophores. According to Shoemaker (1962), the small (400-500 µm diameter) dark brown ascocarps produced by Ptr overwinter on straw. These setose pseudothecia produce bitunicate, cylindric, 8-spored asci. The light yellowish brown ascospores, like the conidia, can germinate from any or all of the segments.

Ptr has a wide host range and has been found on both wild and domesticated grasses in Canada and in the U.S.A. (Shoemaker, 1962). Ptr isolates collected from infected wheat plants were able to infect many species of wheat (*Triticum*), wheatgrass (*Agropyron*), wildrye (*Elymus*), as well as barley (*Hordeum vulgare* L.), rye (*Secale cereale* L.) and smooth bromegrass (*Bromus inermis*

Leyss.) (Hosford, 1971, Krupinsky, 1982).

Tan spot epidemics can be initiated in the spring when infected grass residues release conidia and ascospores (Morrall and Howard, 1975). This supports the hypothesis that the increased incidence of tan spot which occurred in the 1970's and 1980's was partly due to the adoption of conservation tillage practices (Rees and Platz, 1979). However, in two separate experiments, where local primary inoculum significantly affected tan spot disease severity, there was no significant influence on yield (Adee and Pfender, 1989, and Stover *et al.*, 1996). Seed transmission can also be a minor source of inoculum and may be responsible for the introduction of the disease to new areas (Schilder and Bergstrom, 1995). Secondary inoculum, in the form of conidia, can be released from diseased leaf tissue during the cropping season (Hosford, 1972, and Rees and Platz, 1980) and this may lead to polycyclic epidemic development.

The infection process of Ptr in wheat and the accompanying symptom development of tan spot have been described. At a temperature of 20°C, 95% of conidia sprayed onto wheat leaves will have germinated after 6 hours of exposure to continuous leaf wetness (Larez *et al.*, 1986). Using light and electron microscopy, Dushnicky *et al.*, (1996), found that germinating conidia formed two to four germ tubes, which in turn produced appressoria usually at stomata, junctions of epidermal cells, and above epidermal cells. From the appressoria the penetration peg grew into an epidermal cell, and produced a vesicle. Ptr then usually generated secondary hyphae which would ramify in the intercellular spaces of the mesophyll tissue. There was no observable effect of host tissue resistance or susceptibility on the initial infection processes described above. Macroscopically, the infection site is visible as a dark brown necrotic spot, which has been characterized as a hypersensitive response by Lee and Gough (1984).

In susceptible wheat leaf tissue, lesions develop beyond the necrotic fleck region and create a halo-like symptom. The rating system developed by Lamari and Bernier (1989a) distinguished two lesion types, chlorotic and necrotic, and permitted Ptr isolates to be classified into one of three pathotypes using a differential set of

wheat cultivars (Lamari and Bernier, 1989b). Isolates which could cause both necrosis and chlorosis on susceptible cultivars, were designated as pathotype 1, isolates which could induce only necrosis on susceptible cultivars were designated as pathotype 2, and isolates which could cause only chlorosis on susceptible tissues were placed in pathotype 3. In 1991, the avirulent pathotype, pathotype 4, was identified by Lamari *et al.* and added to the classification system. Correspondingly, wheat cultivars could be sorted according to their reaction to the isolates from each of the pathotypes. Therefore, wheat cultivars could be resistant to both necrosis- and chlorosis-inducing isolates, susceptible to both, or susceptible only to either chlorosis- or necrosis-inducing isolates.

Ptr necrosis toxin

Tomás and Bockus (1987) were the first to suggest that toxic compounds produced by the fungus were involved in tan spot disease development. They discovered that cell-free culture filtrates of pathogenic Ptr isolates could induce symptoms similar to those observed in inoculated tissues when infiltrated into wheat leaves. It was also found that there was a strong correlation between sensitivity to culture filtrates and susceptibility to isolates. The Ptr necrosis toxin, the first Ptr toxin characterized, was identified by Lamari and Bernier (1989c). As its name suggests, this toxin induces only tan necroses in sensitive infiltrated leaves. Their experiments indicated that necrosis-inducing isolates produced the necrosis toxin and that wheat lines that had the gene conferring sensitivity to the toxin were also susceptible to necrosis-toxin-producing isolates. The detection of toxin in the intercellular washing fluids of leaves infected with toxin-producing isolates provided further evidence for toxin involvement in disease development. (Lamari *et al.*, 1995). However, although absence of toxin production does not prevent fungal penetration of tissue, it does restrict its spread into the intercellular spaces of the mesophyll (Lamari and Bernier, 1989b). The Ptr necrosis toxin, later designated Ptr ToxA (Ciuffetti *et al.*, 1998), can be regarded as a pathogenicity factor as defined by Yoder (1980), because the absence of tan necroses is used to identify resistance

(Lamari and Bernier, 1989a).

In addition to the necrosis toxin, the existence of two separate chlorosis toxins has been either confirmed; Ptr ToxB (Strelkov *et al.*, 1999), or suggested; Ptr ToxC (Effertz *et al.*, 1998). In wheat, three independent loci which confer sensitivity/insensitivity to each of the toxins (and susceptibility/resistance to the isolates which produce them) have been discovered so far (Gamba *et al.*, 1998). It appears that to be fully resistant a wheat cultivar must carry insensitivity genes for both chlorosis and necrosis (Lamari and Bernier, 1991). This means that the wheat-Ptr system does not fit the gene-for-gene incompatibility model (Loegering, 1978) in which the interaction of a pathogen avirulence gene with the corresponding host resistance gene confers resistance despite the presence of any compatibility factors (Lamari and Bernier, 1991).

Purification and characterization of the Ptr ToxA toxin revealed its proteinaceous nature (Ballance *et al.*, 1989). Unlike other host-selective toxins, which are low molecular weight secondary metabolites (Walton, 1996), Ptr ToxA is a 14 kD ribosomally synthesized monomeric protein. The genetic sequence, which codes for the toxin, and the corresponding amino acid sequence, were first determined by Ballance *et al.* (1996). Southern analyses reinforced the validity of the toxin model by indicating that hybridization with the toxin gene only occurred in Ptr races which induce necrosis. Furthermore, cloning and expression of the Ptr ToxA in *E. coli* yielded a toxin which produced necrotic symptoms on wheat in a host-selective manner consistent with the naturally produced toxin.

Database searches for similar protein or DNA sequences produced no significant matches which could hint at an activity or function of this toxin. Phosphorylation consensus sites were identified by Ciuffetti *et al.* (1997) and Zhang *et al.* (1997). Sites within the toxin protein were also identified which could be involved in binding to a potential receptor (Ciuffetti *et al.*, 1997) or to the plasma membrane of host cells (Zhang *et al.*, 1997).

Genetic studies repeatedly indicated that only one gene was involved in sensitivity/insensitivity to Ptr ToxA and that sensitivity was dominant (Lamari and

Bernier, 1991, Stock *et al.*, 1996, Faris *et al.*, 1996, and Anderson *et al.*, 1999). Although there is agreement that the locus for this gene is located on the long arm of chromosome 5B, there is disagreement on whether the gene codes for resistance or for susceptibility. Genetic studies involving an aneuploid series of a resistant cultivar, Chinese Spring, indicated that removal of the 5B chromosome made the plants sensitive to the toxin (Stock *et al.*, 1996). In other words it suggested that an active resistance process was involved. Conversely, another group of researchers using a similar approach found that insensitivity was conferred by the lack of expression of a gene for sensitivity (Anderson *et al.*, 1999). This passive recessive resistance is more consistent with the existence of a putative toxin receptor in sensitive wheat cells.

To date there are very few clues pointing to a site or mode of action for Ptr ToxA in sensitive wheat tissue. Deshpande (1993) did not observe any significant detrimental effect of the toxin on cell suspension or callus cultures initiated from either toxin sensitive or insensitive cultivars. This lack of response could be due to insufficient toxin exposure in the callus and suspension systems. In the callus system, the toxin may not have been taken up from the media in significant quantities. In the cell suspension system, the effective toxin concentration to which the cells are exposed may be significantly less than it is in intact infiltrated leaves. Also, the cells in both these systems are characteristically undifferentiated and may therefore be insensitive to the toxin (Deshpande, 1993). Lastly, the necrosis symptom is usually associated with severe drying and browning of leaf tissue. The callus and cell suspension environments which are moist and wet, respectively, will not permit tissues to dry and this might preclude the development of necrotic symptoms.

Ultrastructural studies conducted by Freeman *et al.* (1995) suggested that membranes were damaged by toxin activity. Within four hours of toxin infiltration, chloroplast membranes of susceptible plants were reported as evaginated or swollen. After twenty-four hours, all organelles of susceptible leaf cells were severely damaged. However, these researchers stated that resistant plants showed

a similar pattern of necrosis, although ultrastructural damage was limited to individual or small groups of cells. This last result is very unexpected as the leaves of resistant plants are visually unaffected by relatively high toxin concentrations (Ballance *et al.*, 1989).

Based on the study by Freeman *et al.* (1995), Kwon *et al.* (1996) developed an electrolyte leakage assay in order to rapidly quantify the reaction to Ptr ToxA. They found that the conductivity of a solution bathing toxin-infiltrated toxin sensitive leaves would begin to increase significantly after the leaves had been exposed to toxin for at least 10 hours compared to both toxin insensitive leaves and to water infiltrated leaves. Since electrolyte leakage has been used as a quantitative bioassay for a number of host-selective toxins differing in their mode of activity (Kwon *et al.*, 1996), it can be viewed as non-specific or secondary toxin reaction. Conversely, it has been suggested that toxins act directly on the plasmalemma (Yoder, 1980).

Three separate studies indicated that necrosis development in susceptible plants was sensitive to temperature (Lamari and Bernier, 1994, Kwon *et al.*, 1996, and Kwon *et al.*, 1998). Lamari and Bernier (1994) showed that at temperatures above 27°C necrosis failed to develop in sensitive leaves infiltrated with toxin. This high temperature insensitivity was confirmed by the electrolyte leakage bioassays conducted by Kwon *et al.* (1996). Temperature sensitivity of toxin activity supports the receptor model for toxin sensitivity (Walton and Panaccione, 1993, Yoder 1980, and Scheffer and Livingston, 1984). High temperature either prevents binding of the toxin with its putative receptor (Lamari and Bernier, 1994) or disrupts the signaling pathway downstream of toxin perception (Kwon *et al.*, 1996).

One recent report proposes that Ptr ToxA activity requires host metabolism (Kwon *et al.*, 1998). This proposition was based on the decreased level of electrolyte leakage, a symptom of toxin activity, of toxin-treated tissues which have been co-infiltrated with H+-ATPase, transcription, and translation inhibitors or which have been incubated at low temperatures which slow host metabolism. These results support the hypothesis that Ptr ToxA induces a kind of programmed cell

death which is typically associated with a plant defense response to pathogen infection. However, although the inhibitors were able to reduce or slow the leakage of electrolytes from toxin infiltrated tissues, only one of the inhibitors tested was able to prevent the development of necrosis. This indicates that the inhibitors were able to protect the susceptible tissues by delaying the onset of necrosis.

Histological studies describing the tan spot infection process can also provide some insight into the Ptr ToxA mode of action. Larez *et al.* (1986) characterized the infection process of a what appears to be a necrosis inducing isolate. At 72 hours post-inoculation, they found affected host cells beyond the zone of hyphal penetration, which is consistent with the diffusion of a fungal toxin. At the electron microscopy level, they observed the vesiculation and collapse of membranes in affected host cells. These cells were characterized by either the rupture of the tonoplast, the breakdown of chloroplasts, the vesiculation of the plasmalemma, or, in severe cases, the almost complete destruction of ultrastucture with only remnants of chloroplasts discernable.

Similar results were obtained by Dushnicky *et al.* (1998) who compared the infection process of a Ptr ToxA producing isolate in resistant leaves to that in susceptible leaves. The infected susceptible tissues had collapsed mesophyll cells inside of which chloroplasts could not be distinguished because of the opacity of the protoplasm. Cell walls, stained with calcofluor to indicate the presence of 1,4-β-glucans, which include cellulose and hemicellulose, appeared to lose their fluorescence in affected tissues. The epidermis also seemed to lose cellular integrity but the inner bundle tissue appeared to remain intact. In resistant tissues, as was mentioned earlier, Ptr was able to penetrate the leaf but the ramification of hyphae within the intercellular spaces was limited. The affected, yet resistant, mesophyll cells did not collapse and their chloroplasts remained visible. The intercellular spaces between the affected cells were filled with a lignin-like compound which probably helped prevent the proliferation of hyphae in the resistant tissues. This leads to another hypothesis for toxin activity in which the toxin somehow disables the plant's ability to detect and/or respond to fungal invasion.

However, the fact that the resistant reaction was not observed in the susceptible tissues does not necessarily mean that it did not occur. The susceptible reaction is characterized by large coalescing tan necrotic lesions which have dark brown or black centres which may or may not be distinguishable (Lamari and Bernier, 1989a). These dark brown or black centres are likely very similar to the lesions observed in resistant tissues, but, since they are so small compared to the size of the necrotic lesions in susceptible tissues, they may not have been detected in the studies conducted by Dushnicky *et al.* (1998).

Most of the microscopic investigations carried out so far have been conducted with a Ptr ToxA producing isolate (Larez *et al.*, 1986, and Dushnicky *et al.*, 1998). However, there are a number of events which take place in fungal infected tissue which are not related to toxin activity. Firstly, there is the defense reaction (hypersensitive response) which is observed in response to fungal invasion. Also, fungi not only produce toxins, such as Ptr ToxA, but also secrete a number of degradative enzymes (Deacon, 1997a). These enzymes digest large proteins and polysaccharides into small soluble and absorbable units which the fungi require for their nutrition. Therefore in studies using toxin producing isolates, it is difficult to separate out the toxin effects from other effects caused by fungal infection.

The microscopic examination of the effects of Ptr ToxA in sensitive wheat tissue, and the comparison of these effects with other disruptive treatments could lead to an improved understanding of PtrToxA activity. Therefore, the mode-of-action studies of other host-specific toxins, and the microscopic changes taking place in dying plant cells will be presented in the following sections.

Host-selective toxins

Host-selective toxins (HST's), such as Ptr ToxA, are molecules produced by plant pathogens which confer pathogenicity (Yoder, 1980). In other words, the toxin activity is required for disease development and the absence of toxin production in the pathogen or loss of sensitivity to the toxin in the host will result in incompatibility. Unlike Ptr ToxA, most HST molecules are relatively small molecules which are the

products of specialized or secondary pathways (Walton, 1996). HST's can be polyketides, cyclic peptides, terpenoids, saccharides, polypeptides or compounds of unknown biogenesis (Walton, 1996).

It has been suggested that opportunistic saprophytic pathogens developed the ability to synthesize HST'S in order to overcome plant defense reactions (Scheffer, 1991, Otani *et al.*, 1991). Another postulated role for HST'S is the destruction of cellular integrity which would lead to the release of simple nutrients, such as sugars and amino acids, into the apoplasm for absorption by fungal mycelia (Walton, 1996).

Obviously, HST'S are toxic to cells and the activity of HST'S is associated with a number of gross physiologic reactions in host cells: changes in respiration, cell permeability, protein synthesis, and CO_2 fixation (Scheffer and Livingston, 1984), as well as necrosis, chlorosis, inhibition of root growth, and electrolyte leakage (Walton, 1996). However, since these reactions, such as electrolyte leakage, are quite general, they provide little insight into the modes of action of HST's.

There are essentially two main groups of fungal organisms which are known to produce HST's: *Cochliobolus* and *Alternaria*. *Cochliobolus* species, which are pathogens of grasses like oat and corn, produce three toxins which have been studied extensively: victorin, T-toxin, and HC-toxin. *Alternaria alternata* pathotypes also produce a number of well-researched HST's, such as AK-toxin, ACR-toxin, AM-toxin and AAL-toxin, but the pathogens which produce these toxins infect dicotyledonous plants such as pear, lemon, apple and tomatoes. The mode of action models developed for each of the above mentioned toxins is somewhat unique; however, they can provide a foundation for research into the activity of other toxins in terms of both methodology and theory.

Mode of action studies

Toxins produced by *Cochliobolus* species

Victorin. Although victorin was one of the first HST's isolated (Pringle and Braun, 1957), the elucidation of its mode of activity has not progressed until recently because of the difficult purification process involved. Early studies demonstrated the rapidity of response to the toxin; electrolyte leakage was detected within 2 minutes of toxin exposure in susceptible oat tissues (Scheffer and Samaddar, 1970). This finding suggested that the plasma membrane was the site of toxin activity or binding. Also, the decreased sensitivity of oat tissues treated with protective compounds indicated that a protein might be involved as a receptor substance (Scheffer and Yoder, 1970). Therefore it was proposed that toxin effects such as increased respiration and inhibition of protein synthesis were secondary to plasma membrane damage.

It was only in the mid-80's that the peptide, 12-membered ring structure of victorin was described (Wolpert *et al.*, 1988). The activity of the toxin was found to depend greatly on its structure; however, this did not lead to a greater understanding of its mode of activity.

Binding studies using ^{125}I-labeled toxin identified a 100 kDa protein as a potential toxin receptor (Wolpert and Macko, 1989). This protein was later identified as a subunit of the multi-enzyme glycine decarboxylase complex (GDC) (Wolpert *et al.*, 1994). The GDC is located in the mitochondrion and is involved in photorespiration. The product of photorespiration, phosphoglycolate, is a metabolite of little use, which needs to be recycled into phosphoglycerate such that it can be reintroduced into the Calvin cycle. The GDC is a component of this recycling pathway (Lehninger *et al.*, 1993).

Navarre and Wolpert (1995) suggest three possibilities for toxin activity based on the interaction with the GDC. First the toxin could be metabolized by the GDC of resistant genotypes into a non-toxic molecule. Conversely, the GDC of susceptible genotypes could convert victorin to a toxic compound. Thirdly, cell

death could be a direct result of victorin interaction with the GDC. However, Walton (1996) later suggested that the gene conferring sensitivity might control the uptake into the mitochondria or the metabolism of victorin even though there is strong evidence that the GDC is the site of action.

T-toxin. *Cochliobolus heterostrophus* race T, the causal agent responsible for the devastating southern corn leaf blight epidemic of 1970, produces T-toxin. Corn hybrids produced with the Texas type of cytoplasmic male sterility (cms-T) were very sensitive to T-toxin (Miller and Koeppe, 1971); and this sensitivity was inherited extrachromosomally.

The site of action of the toxin was quickly narrowed to the mitochondria for the following reasons. Firstly, mitochondria, along with chloroplasts, are known to contain DNA and are inherited maternally. In addition, it was observed that isolated mitochondria from susceptible corn seedlings had decreased respiration and swelled when they were exposed to T-toxin compared to resistant mitochondria (Miller and Koeppe, 1971, Gengenbach *et al.*, 1973). The electron microscopy observation of mitochondrial swelling was therefore an important step towards an understanding of the T-toxin mode of action.

Genetic studies of mitochondrial DNA from cms-T corn identified a unique open reading frame which encodes for a 13 kD polypeptide (Dewey *et al.*, 1986). Male fertile maize, which are also insensitive to the toxin, fail to produce or produce a truncated form of this polypeptide (Wise *et al.*, 1987). *Escherichia coli* spheroplasts expressing this 13 kD polypeptide from male sterile corn demonstrated the same symptoms as isolated cms-T mitochondria when exposed to T-toxin; their respiration was inhibited and they swelled (Dewey *et al.*, 1988).

This 13 kD polypeptide identified above was later designated the pore-forming protein. The pore-forming protein, as its name suggests, increases the permeability of the mitochondrial membrane due to the interaction with T-toxin by the formation of a trimer (Levings and Siedow, 1992). The formation of these pores might explain the mitochondrial swelling phenomenon observed in response to toxin

exposure in early experiments.

One of the most interesting discoveries resulting from the investigations into T-toxin activity is the role of the pore-forming protein in male sterility. It appears that fermentation is employed to satisfy the high rate of metabolism required in the process of pollen development (Tadege and Kuhlemeier, 1997). It has been suggested that the interaction between one of the products of fermentation, acetaldehyde, and the pore-forming proteins weakens the mitochondrial membrane and leads to male sterility (Tadege and Kuhlemeier, 1997). This hypothesis is supported by the finding that one of the genes which restores male fertility is likely an aldehyde dehydrogenase (Roel and Kuhlemeier, 1997).

HC-toxin. *Cochliobolus carbonum*, the causal agent of leaf spot of maize, produces the HST HC-toxin. The interaction of this toxin with its host is quite unusual. Firstly, host resistance is achieved by enzymic detoxification of HC-toxin (Meeley *et al.*, 1992). Secondly, the toxin is not toxic to cells but inhibits root growth (Walton, 1996). The toxin is therefore characterized as having a cytostatic effect (Walton and Panaccione, 1993). Similarly to other toxin research, the characterization of many crude physiological responses to toxin, such as increased electrolyte leakage, respiration, and dark fixation of CO_2 (Yoder and Scheffer, 1973), did not lead to an increased understanding of toxin activity.

The most recent hypothesis for HC-toxin activity is that it interferes with histone deacetylase activity (Brosch *et al.*, 1995). The path that lead to this discovery is fairly circuitous. Firstly, a molecule with a similar structure to HC-toxin, trapoxin, was found to detransform oncogene transformed mammalian cells (Yoshida and Sugita, 1992). This same effect was observed for a chemically unrelated antibiotic which inhibits histone deacetylase. Finally, this led to experiments which showed that HC-toxin does indeed inhibit histone deacetylase activity (Brosch *et al.*, 1995).

HC-toxin production by *C. carbonum* may facilitate its infection process by suppressing defense response activation in the host corn tissue. Since histone acetylation and deacetylation is involved in the expression of certain genes

(Taunton *et al.*, 1996), HC-toxin activity may prevent the expression of defense response genes which would otherwise have been activated by the elicitors released by the invading hyphae (Walton, 1996). Reduced production of defense proteins and chemicals would allow this pathogen to proliferate more easily in the host leaf tissue.

Toxins produced by *Alternaria* species

AK-toxin. Microscopy was an integral component of toxin site of action studies for most of the HST'S produced by *Alternaria* species. Electron microscopy has been used extensively to characterize the effect of AK-toxin on susceptible pear tissues (Park, 1977a, Park 1977b, Park, 1977c, Park *et al.*, 1976, Park *et al.*, 1987). As with most other toxins, the first reported cellular toxin effect was electrolyte leakage (Otani *et al.*, 1973). Park *et al.* (1976) studied the ultrastructural changes caused by AK-toxin activity, and found that cells had invaginated plasma membranes after one hour of exposure to the AK-toxin. These invaginations frequently occurred in the vicinity of plasmodesmata and often contained membrane fragments and darkly staining materials. Mesophyll cells, which were necrotic after ten hours of toxin exposure, had densely staining cytoplasm but appeared to have intact organelles with preserved membranes. Apparent leakage of sodium ions at plasmodesmata of toxin treated susceptible cells was later demonstrated using potassium antimonate (Park *et al.*, 1987). Therefore it was suggested that AK-toxin disrupts plasma membranes near plasmodesmata and causes leakage of electrolytes in these areas.

Crude binding studies supported the hypothesis for a plasma membrane bound receptor for AK-toxin in susceptible tissues (Otani *et al.*, 1989). In these studies, plasma membrane fractions were obtained from pear fruits of both resistant and susceptible plants and mixed with AK-toxin. Necrosis was reduced in susceptible leaves treated with the mixture containing susceptible fractions compared to leaves treated with the mixture containing the resistant fractions (Otani *et al.*, 1989). However, a receptor protein has not yet been identified.

In addition, electrolyte leakage does not always lead to the development of necrosis but may be required for fungal infection (Otani *et al.*, 1995). For example, pear leaves, which have been pretreated with inhibitors of mRNA or protein synthesis, leak electrolytes but are protected from necrosis development (Otani *et al.*, 1991). Also, since these pretreatments do not protect against fungal infection, it seems that the toxin induced plasma membrane disruption is a critical event in the infection process. This is further supported by the hypothesis that AK-toxin-induced membrane dysfunction could suppress the formation of papilla in susceptible cells (Otani *et al.*, 1995) and therefore facilitate fungal penetration.

ACR-toxin. ACR-toxin, like T-toxin described previously, seems to cause swelling of mitochondria (Kohmoto *et al.*, 1984). Electron micrographs of ACR-toxin affected cells show that mitochondria not only swell, but also their matrix becomes more electron-lucent and their cristae seem to form vesicles internally. Also, isolated susceptible mitochondria exposed to ACR-toxin had an increased rate of NADH oxidation and inhibited malate oxidation (Akimitsu *et al.*, 1989).

However, unlike most other toxins so far discussed, plasma membrane disruption was not considered to be the primary site of toxin activity. Plasma membrane modification only occurred following mitochondrial toxin effects if the leaves were not continously exposed to light (Kohmoto *et al.*, 1989). However, plasma membrane modification is necessary for both the development of necrosis and pathogen infection.

AM-toxin. Electron microscopy indicated that there were two sites of action for this toxin: the plasma membrane and the chloroplast (Park *et al.*, 1981). Although AM-toxin has a different chemical structure than AK-toxin, it appears to have similar effects on plasma membranes; it causes plasma membrane invaginations at plasmodesmata. Also, these membrane disruptions are associated with cell wall degradation. In chloroplasts of susceptible cells, vesicles are apparently produced from the tips of granae.

Light can inhibit the development of AM-toxin symptoms as it did for ACR-toxin (Tabira *et al.*, 1989, Shimomura *et al.*, 1992). Continuous irradiation following

toxin exposure will prevent the development of necrosis. However, light will not prevent the disruption of plasma membranes or chloroplasts and will not protect against the fungal infection.

AAL-toxin. AAL-toxin is an important factor in the development of Alternaria stem canker of tomato. Its mode of action is believed to be similar to that of a structurally related toxin. The latter toxin, fumonisin, is synthesized by certain *Fusarium* species, and it interrupts sphingolipid metabolism (Abbas *et al.*, 1995). Tomato tissues treated with AAL-toxin will accumulate free sphingoid bases such as sphinganine and sphingosine and will deplete complex sphingolipids (Abbas *et al.*, 1995). Apart from their structural role as membrane components, sphingolipids can act as second messengers affecting such processes as differentiation and growth.

Apoptosis or programmed cell death, is a developmental and orderly process which occurs in the cells of living organisms to remove unwanted cells which could be harmful to the organism (Mittler and Lam, 1997, Schwartzmann and Cidlowski, 1993). This process could also be beneficial in diseased plant tissues if the sacrificed cells were able to contain the invading organism. A characteristic sign of apoptosis in animal cells is DNA fragmentation into multimers of about 180 base pairs (Wyllie *et al.*, 1984) and the vesiculation of these fragments into so-called apoptotic bodies (Martin *et al.*, 1994).

Therefore, since AAL-toxin disrupts the metabolism of sphingolipids which are involved in signalling pathways, and since apoptosis is a regulated process, it was suggested that AAL-toxin might be triggering some sort of programmed cell death to facilitate infection of susceptible tissues (Wang *et al.*, 1996). This hypothesis was substantiated by research indicating that AAL-toxin treated tissues have fragmented DNA typical of apoptosis and that this DNA seems to form the small nuclear bodies mentioned above (Wang *et al.*, 1996). However, stronger evidence, such as the triggering of specific apoptotic enzymes by AAL-toxin treatment, is required to legitimately validate this hypothesis.

Summarizing the findings of toxin studies

A number of observations can be made regarding the toxin studies described above. Firstly, it is often hypothesized that HST's have a detrimental effect on the plasma membrane and that this is the primary site of action. However, the fact that all toxins seem to cause electrolyte leakage suggests that this may be a general secondary effect.

Mode of action studies have resulted in the development of a number of different toxin models. Toxins like HC-toxin and AK-toxin seem to disrupt plant cells in order to prevent defense responses and facilitate the infection process. AAL-toxin seems to induce a type of programmed cell death. Other toxins such as victorin and T-toxin disrupt specific enzymes within the mitochondria which ultimately lead to cell death. Therefore, the models developed to explain toxin activity not only increase our understanding of host-pathogen interactions, which will make us better equipped to deal with crop pathogens, but also provide a better understanding of plant physiology.

In the case of T-toxin, AK-toxin, ACR-toxin, and AM-toxin, microscopy has helped to resolve the site of action of HST's. However, in some cases, more sensitive molecular methods have been required. For example, binding studies using labelled toxin were important for the study of victorin activity. Enzyme assays or metabolism studies were helpful in examining the activities of AAL-toxin and HC-toxin. Nonetheless, microscopic examination of toxin effects, even through the observation of secondary effects, can help pin-point the site of toxin activity.

Ultrastructure of moribund or stressed plant cells

As discussed in the previous section, a number of studies have examined the ultrastructural changes which occur in toxin-affected plant cells. However, ultrastructural studies have also examined the changes which take place in tissues which are dying due to chemical treatments, environmental stresses, senescence, or to a developmental program such as xylem maturation. These descriptions are useful in identifying the patterns of degradation which occur in moribund plant cells.

Comparison of these patterns with those which occur in toxin-affected tissues may be helpful in separating the secondary from the primary toxin effects and may therefore assist in identifying the site and mode of action of toxins such as Ptr ToxA.

Xylem maturation

One of the last steps in the process of xylem maturation, which follows wall deposition, involves the digestion of the cytoplasm to create a hollow cylinder for water-conduction (Wodzicki and Humphreys, 1973). In pine stems tracheid maturation, prior to autolysis, there is a close association between the vacuole and the cytoplasm in the form of complex vacuolar invaginations. In the process of autolysis, the cytoplasm and organelles bud-off into vesicles inside the vacuole and are eventually digested (Wodzicki and Humphreys, 1973). Srivastava and Singh (1972) described the differentiation of vessel elements in corn. In the late stages of differentiation, the previously active endoplasmic reticulum (ER) and Golgi dilate, invaginate and become lobed. A number of vesicle remnants of the ER and Golgi can be seen, ribosomes are lost, and the mitochondrial cristae become less discrete. In the nucleus, the nucleoplasm becomes more electron-lucent with scattered clumps of dense chromatin and the nucleolus becomes more compact (Lai and Srivastava, 1976). The cytoplasm and the plasma membrane (PM) appear to be the last structures to survive as the disintegration of the PM results in the dissolution of end walls (Srivastava and Singh, 1972).

Senescence

Another process which seems to be developmentally regulated is senescence. In senescing mesophyll cells of *Phaseolus,* the degradation of thylakoid stacks accompanied by the accumulation of lipid globules in chloroplasts appeared to be the first indication of cell disruption (Barton, 1966). The degradation of other structures, such as the mitochondria and vacuoles, appeared to be secondary to the chloroplast disruption. The chloroplasts of senescing wheat leaves also seem to be primary sites of degradation (Mittelheuser and Steveninck, 1971). In this study, the accumulation of plastoglobuli and the loss of chloroplast

ribosomes were early signs of degeneration. These are contrary to the findings of Shaw and Monocha (1965) which suggested that tonoplast rupture is an important senescence event which releases hydrolytic vacuolar contents released into the cytoplasm and initiates the degradation process.

Hypersensitive reaction

The hypersensitive reaction, which appears as a dark brown necrotic spot, is an attempt by plant cells to prevent the spread of an invading pathogen by dying (Deacon, 1997b), and is therefore also a type of programmed cell death. Meyer and Heath (1987b) studied the incompatible reaction between cowpea epidermal cells and the plantain powdery mildew fungus. The first sign of cell death they observed was the cessation of cytoplasmic streaming. This was followed by the loss of polyribosomes, golgi and ER, the disruption of mitochondrial cristae and outer envelopes, the loss of microtubules, the general degeneration of membranes, the collapse of the protoplasm, and finally the accumulation of membranous structures between the cell wall and the cytoplasm. These researchers did not use the fragmentation of tonoplast or plasma membrane as indicators of cell death because they were often fragmented in control tissues by the fixation process. However, Jones *et al.* (1975) found that hypersensitively reacting pepper cells had disrupted tonoplast membranes and fragments of cytoplasm inside the vacuole. They suggested that these two changes were precursors of cell death.

Environmental stresses

The stress caused by changes in environmental conditions, such as drought and frost, can also damage plant cells and cause death. Desiccation tolerant, or so-called resurrection plants, are able to survive long periods of drought. Ultrastructural studies of desiccated *Selaginella lepidophylla*, a type of resurrection plant, showed that although the cellular contents were highly condensed, all structures were preserved (Thomson and Platt, 1997). Cell walls were highly folded but remained tightly bound to the plasma membrane. It was suggested that a coating of granular material protected cellular membranes such as the tonoplast

and plasma membrane from damage. This observation is supported by Quartacci *et al.* (1997) who suggested that starch was lost in dried desiccant-tolerant plants and that this starch was converted to soluble sugars which could protect cells and their membranes. Also, in these dehydrated tissues, the vacuole was fragmented into a large number of vesicles (Thomson and Platt, 1997). This vacuolar fragmentation seems to be an essential survival mechanism in desiccant-tolerant plants (Quartacci *et al.*, 1997). In tissues which did not survive drying, vacuoles remained whole and thylakoid membranes were visibly damaged (Quartacci *et al.*, 1997). Also, rehydration of the drought-sensitive tissues brings about further degradation of chloroplasts and membranes, which is likely due to the reactivation of catabolic enzymes.

Freezing is another process that can damage tissues by extracting water from cells and forming ice crystals which can disrupt cellular structures. Pearce and McDonald (1977) examined the effect of a freeze-thaw cycle on tall fescue leaf cells. They observed three main effects; the disruption of membranes and the concomitant accumulation of osmiophilic material, the swelling of organelles, and the contraction of the nucleus. It was suggested that the osmiophilic materials were lipid fragments originating from the disrupted membranes. The membranes may have been damaged by their dehydration. The swelling and bursting of organelles, which may have occurred during the thawing process, is a sign that the plasma membrane may have been damaged by freezing because the organelles would have been exposed to a hypotonic environment during rehydration.

Chemical treatments

The last type of plant cell disruption that will be described is caused by exposure to chemicals of either inorganic or biological nature. Meyer and Heath (1987a) examined the microscopic effects of copper chloride induced cell death in cowpea epidermal cells and compared them to the hypersensitive effects described above. Essentially it was found that in $CuCl_2$ treated tissue, symptoms developed fairly similarly to those in hypersensitively reacting tissue. There were two main

differences, first it appeared that Golgi and microtubules degenerated more slowly, and secondly, the membranes were less disorganized in the $CuCl_2$ treated tissue.

Exposure of wheat leaves to ozone causes a series of changes which resembles senescence (Ojanpeä *et al.*, 1992). In wheat plants fumigated with O_3, there is a decreased amount of cytoplasm and an increased vacuolation of cells. However, the most evident changes typical of senescence occurred in the chloroplast where there was an accumulation of plastoglobuli, the formation of vesicles between grana thylakoids, and a general decrease in chloroplast area. A common symptom of dying tissue was also observed in the withdrawal of the plasma membrane from the cell wall. This plasma membrane withdrawal may be due to the net loss of membrane material by pinocytosis which is not replaced by membrane synthesis and exocytosis in disrupted cells (Hanchey and Wheeler, 1968).

The microscopic effects of bromine, another gas pollutant harmful to plant tissues, has been studied (Strauss *et al.*, 1982). Bromine had localized effects on epidermal cells and on mesophyll cells adjacent to the sub-stomatal chamber. Unlike ozone which affected primarily the chloroplasts, bromine caused general cellular disorganization such as plasmolysis, cell wall collapse, cytoplasmic vacuolation, and disappearance of the cellular membrane system. Interestingly, in mesophyll cells, the loss of the tonoplast preceeded cell collapse and necrotic symptoms. The loss of a large central vacuole resulted in the scattering of chloroplasts in the cell's interior compared to their normal organized positions on the cell periphery. In severely collapsed mesophyll cells the only remaining recognizable structures were the granal stacks.

Degradative enzymes secreted by fungi are very important for their nutrition because they breakdown large polymers of their host or substrate, such as cellulose, into small soluble and absorbable ones (Deacon, 1997a). However, enzymes, such a pectin lyase, which attack primarily wall materials, have detrimental effects on the health of plant cells. There are three potential means by which pectin lyase can kill plant cells; first the pectin fragments released by enzyme

activity may signal fungal invasion and trigger defense responses such as the hypersensitive reaction; second the degradation of pectin may weaken the cell wall and therefore make the cell susceptible to bursting; and third the pectin lyase activity may release disruptive enzymes which are compartmentalized in the cell wall (Keon, 1985). The ultrastructural changes caused by pectin lyase on cultured apple cells included common disruptive changes described earlier such as the shrinkage of the protoplast from the cell wall, increased vacuolation, and the accumulation of vesicles between the cell wall and the plasma membrane (Keon, 1985). However, it was still not evident how the enzymatic activity of pectin lyase results in plant cell death.

Summary of structural changes observed in stressed or dying plant cells

Programmed or developmental death processes seem to cause a more orderly degradation of plant cell ultrastructure. There is a progression of events which probably involve a gradual slowing of metabolism and a recycling of cellular materials. For example xylem maturation involves an intravacuolar digestion of the cytoplasm, a loss of ribosomes and degradation of the nucleus. In senescence the degradation of thylakoids seems to be a primary effect although there is evidence that tonoplast rupture might initiate the process. The cessation of cytoplasmic streaming, the loss of ribosomes and microtubules, and the alteration of Golgi and endoplasmic reticulum, are all signs of slowed metabolism in hypersensitively responding epidermal cells. In all these programmed processes it seems that the plasma membrane is the last structure to disintegrate and that cell death is a gradual, internal, and regulated process.

Environmental stresses and chemical treatments are described as more catastrophic events causing a relatively disorderly destruction of cellular structure. For example freezing causes membrane disruption and the loss of osmotic regulation. Dehydration damages membranes and decompartmentalizes catabolic enzymes which are reactivated upon rehydration. Bromine gas causes plasmolysis, wall collapse and damages membranes. Pectin lyase treatment also causes plasmolysis, increased vacuolation and the accumulation of membrane

fragments outside the cell.

A number of microscopic changes have been observed in plant cells in response to environmental stresses, development, pathogens, toxins, or other chemical treatments. Each of these treatments causes a unique pattern of structural transformation which seems to be indicative of the underlying molecular processes involved.

MATERIALS AND METHODS

Toxin production and purification

Ptr ToxA, the necrosis-inducing toxin, was purified from liquid cultures of monoconidial, *Pyrenophora tritici-repentis*, race 2 isolate, 86-124, obtained from Dr. L. Lamari, Department of Plant Science, University of Manitoba. Inoculum was prepared as described by Lamari and Bernier (1989a).

Leaves infected with isolate 86-124 were cut into approximately 1 cm segments and placed in petri plates on moistened filter paper to maintain high humidity. These plates were then placed under continuous fluorescent lighting at room temperature (20-25°C) for a period of 18 to 24 hours. The plates were incubated in a dark environment at a temperature of 20°C for another 24 hour period. Single conidia were harvested using a flame-sterilized needle and transferred to 9 cm petri plates containing 30 mL of V8-potato dextrose agar (PDA) medium. This medium consisted of 150 mL of V8-juice, 10g of Difco PDA, 3g of $CaCO_3$, 10g of Bacto agar, and 850 mL of distilled water and was autoclaved for 20 minutes and poured into plates. The single-conidia cultures were incubated in the dark at a temperature of 20°C until they reached a diameter of approximaterly 2 cm.

The cultures were increased by singly transferring 5.0 mm diameter plugs, cut from the single-spore cultures with a flame-sterilized cork borer, to V8-PDA medium. These cultures were incubated for 4-5 days in darkness at a temperature of 20°C to allow the mycelium to spread over much of the plate. The plates were then flooded with sterilized distilled water and the mycelia flattened with the bottom of a flamed test tube. The water was decanted and the plates were placed under continuous light at room temperature for 24 hours followed by 24 hours of darkness at 20°C to initiate the production of conidiophores and conidia.

The conidia were harvested by flooding the plates with 10-15 mL of sterile distilled water and then lightly scraping the surface of the cultures with a flamed wire loop. The liquid spore suspension was then decanted into a common beaker. The inoculum concentration was measured using a Fuchs Rosenthal haemocytometer

(Hausser Scientific, Blue Bell, PA) and adjusted to a concentration of 5000 spores/mL by dilution with distilled water. Five millilitres of conidia suspension were transferred to 1 litre Roux bottles containing 150 mL of Fries medium which had been autoclaved for 20 minutes and allowed to cool. A 1 litre solution of Fries medium consisted of 5 g ammonium tartrate, 1 g NH_4NO_3, 0.5 g $MgSO_4.7H_2O$, 1.3 g KH_2PO_4, 2.6 g K_2HPO_4, 30 g sucrose, 1.0 g yeast extract, 2.0 mL trace element stock, and brought to 1 litre with distilled water (Dhingra and Sinclair, 1985). The trace element stock contained 167 mg $LiCl_3$, 107 mg $CuCl_2.H_2O$, 34 mg H_2MoO_4, 72 mg $MnCl_2.4H_2O$, and 80 mg $CoCl_2.4H_2O$ in 1 litre of solution and was autoclaved for 20 minutes. The liquid cultures were incubated for three weeks in the dark at a temperature of 20°C without agitation. The cultures were then vacuum-filtered through a Whatman No. 1 filter and the filtrates were kept at -20°C until processed.

The toxin purification used was based on a procedure described by Ballance *et al.* (1989). The culture filtrates were thawed, vacuum-filtered through a Whatman No. 1 filter and subsequently through a 0.45 µm millipore membrane filter. This filtrate was bioassayed for toxin activity by infiltration into the second or third leaves of toxin-sensitive cultivar, Glenlea, using a 'Hagborg' device (Hagborg, 1970) at dilutions of 1:1, 1:10, 1:100, and 1:1000 in deionized distilled water.

The culture filtrate was diluted to reduce its conductivity and to ensure binding to the ion exchange matrix by adding 150 mL of filtrate to 1000 mL of 10 mM sodium acetate buffer at a pH of 5.0. The diluted filtrate was mixed with 150 mL of CM-cellulose matrix equilibrated with the same acetate buffer in a 2 litre Erlenmeyer flask on a rotary shaker for 40 minutes. The matrix solution was vacuum-filtered using Whatman No.1 filter paper and the eluate collected and stored at 4°C. The matrix wash, vacuum-filtration, and eluate collection steps were repeated for the following sequence of solutions (except the solutions were only shaken for 15 minutes): two consecutive 200 mL solutions of buffer, one 100 mL solution of 0.25 M NaCl, one 200 mL solution of 0.5 M NaCl, and one 200 mL solution of 2.0 M NaCl. All these solutions were buffered with 10 mM of sodium acetate at a pH of 5.0.

The eluate from the 0.25 and 0.5 M NaCl washes were pooled and dialysed with Spectra/Por 3,500 molecular weight cut off dialysis tubing (Spectrum, Houston, Tx) against the 10 mM acetate buffer. The dialysed eluate was applied to a 40 mL ion exchange CM-cellulose column also equilibrated to 10 mM sodium acetate at a pH of 5.0. Effluent from the column was continuously monitored at 280 nm. The column was washed with approximately 200 mL of buffer to remove the unbound fraction. A 300 mL linear salt gradient (0 to 0.3 M NaCl in the pH 5.0 buffer) was applied to elute the bound material into 5 mL fractions. Every fifth fraction was bioassayed for toxin activity as described above. The fractions which contained most of the toxin activity were pooled and dialysed using the same tubing as above against deionized, distilled water at 4°C. The pooled dialysed fractions were freeze-dried and then dissolved into 1 mL of sterile, deionized, distilled water. The absorbance (280 nm) of the sample was measured using a Hewlett Packard model 8452A diode array spectrophotometer with a 1 cm cuvette and this value was multiplied by 0.8 (A_{280}) to obtain the concentration of protein in mg/mL. The stock was diluted to a concentration of 1 mg/mL and stored at -20°C until required. The A_{280} value of 0.8 g/L, provides an estimate of protein concentration since the A_{280} of most proteins is between 0.5 and 1.5 g/L (Kirschenbaum, 1975). However, it should be noted that the use of this factor overestimated the toxin concentration used in all the experiments described herein by 20% because the correct A_{280} for PtrToxA, as determined by Ballance *et al.* (1989), is 0.668 g/L.

The purity of the Ptr ToxA stock was determined by SDS-PAGE using a 12.5% separating gel and a 5% stacking gel with the buffer system of Fling and Gregerson (1986) at pH 8.5. Stock sample (10 µg) and protein molecular markers (Pharmacia LKB Biotechnology Inc.) were prepared in 10 µL of sample buffer which consisted of 0.2 M TRIS, pH 8.8, 0.5 M sucrose, 0.01% bromophenol blue, 10 mM EDTA. Prior to placing the samples in boiling water for 5 minutes, 4 µL of 10% SDS and 1 µL of 0.25 M dithiothreitol were added. After cooling on ice, 5 µL of 0.5 M iodoacetamide was added to the samples. The samples were loaded onto the 0.75-mm-thick mini-gel which was run at 100 V for 2 hours. The mini-gel was fixed for

30 minutes in methanol-acetic acid-water (5:1:5), stained with Coomassie brilliant blue (0.05% wt/vol in fix solution) for 1 hour, and destained in methanol-acetic acid-water (2:0.8:7.2, vol:vol:vol). The molecular weight marker set consisted of the following proteins: phosphorylase B (94 kDa), bovine serum albumin (67 kDa), ovalbumin (43 kDa), carbonic anhydrase (30 kDa), soybean trypsin inhibitor (20.1 kDa), and α-lactalbumin (14,4 kDa).

Plant material and toxin infiltration

Glenlea and Erik were the two cultivars of wheat used in this study. Glenlea is a Ptr ToxA-sensitive, Canadian-bred spring wheat (Evans *et al.*,1972), and Erik is an American semi-dwarf spring wheat which is insensitive to Ptr ToxA (Lamari and Bernier, 1989b). The wheat plants were grown in 110 mm plastic pots filled with a 2:1:1 soil:sand:peat mixture fertilized with 11-48-0 NPK pellets at a rate of 9 to 11 seeds per pot. The plants used for all the studies were grown in a growth room, with a photoperiod of 18 hours at 250 $\mu E/m^2/s$, a light period temperature of 22°C, a dark period temperature of 17°C and were watered every second day. In all the experiments, the second or third fully expanded leaf of 2 to 3 week old plant were used.

Toxin, at a concentration of 2 µg/mL, or water was infiltrated into the wheat leaves using a hagborg device (Hagborg, 1970) until the infiltrated region, which appears darker and more translucent than the uninfiltrated portions of the leaf, was approximately 8.0 cm long (Fig. 1). The edges of the infiltration zone were demarcated with a permanent felt marker and the centre of the hagborg device usually left a pin prick in the leaf.

Once infiltrated, the plants were either returned to the same growth chamber or were placed in a small humidity chamber within another growth chamber with the same light and temperature conditions. The humidity chamber consisted of a polyvinyl chloride tubing frame with dimensions of 2.5 m x 1 m x 1.4 m which was covered with a clear polyethylene wrap. High humidity was maintained in this chamber by two ultrasonic humidifiers running continuously.

Leaf samples were harvested at 18, 24, 48, 96 hours after toxin infiltration.

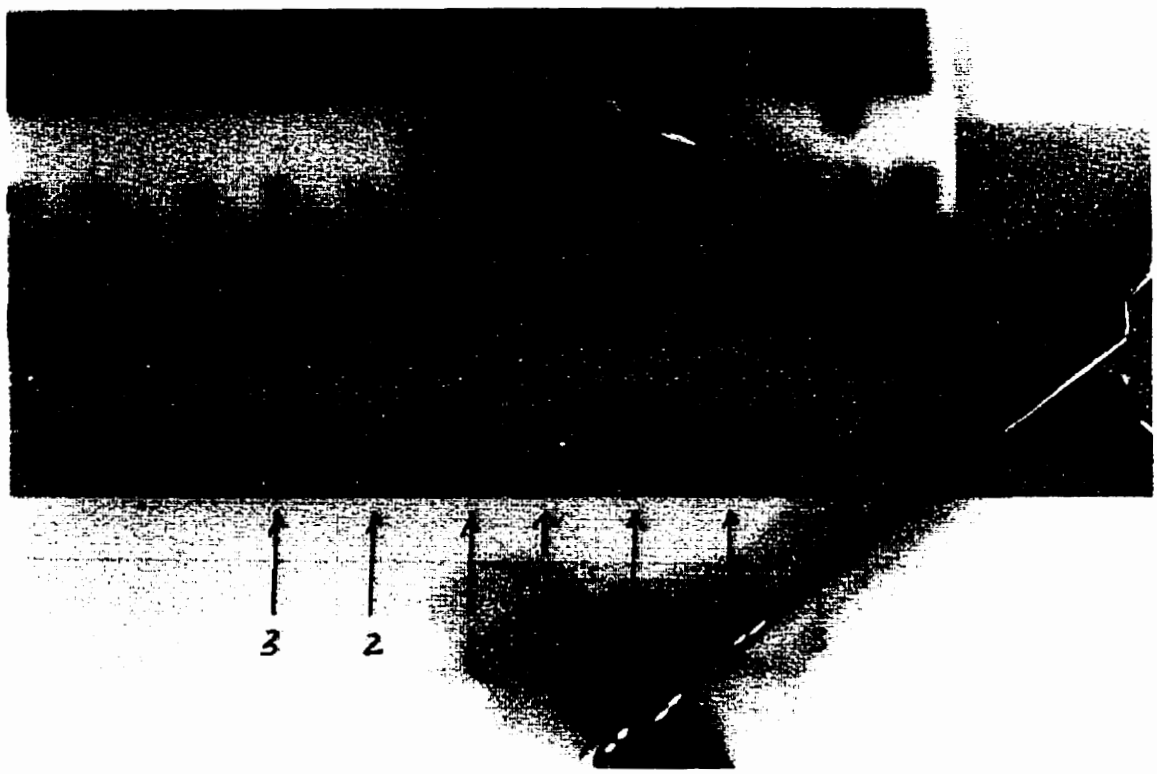

Figure 1. Hagborg device, infiltration zone demarcated by felt pen marks (< and >) and tissue sampling positions at bull's eye, and 1, 2, and 3 cm from bull's eye.

Leaf pieces, 0.5 mm wide, were cut under fixative at four different positions within the infiltration zone; at the 'bull's eye', which is where the hagborg leaves a pin-prick in the leaf at the centre of the infiltration zone, and at positions approximately 1, 2, and 3 cm away from the 'bull's eye' (Fig. 1). The cut leaf pieces were placed in labelled glass vials and immersed in 5 mL of fixative as described below. The fixative was infiltrated into the leaf pieces by placing the vials under vacuum for periods of 1 to 2 hours. The vials were then stored at a temperature of 4°C until processed for microscopy.

Comparison disruptive treatments

Leaves or leaf pieces were also exposed to three other disruptive treatments for comparison against the toxin treatment. The first treatment involved desiccating Glenlea leaves by removing them from the plant and allowing them to dry in the normal growth room environment described above for periods of 2, 4, 6, 8, 16, 24, and 48 hours. The leaves were weighed immediately before being cut and following their desiccation period to determine their fresh and partially dried weights respectively. The weighed leaves were cut and fixed in the phosphate buffered 3% gluteraldehyde solution described below. The water content of fresh wheat leaf tissue, estimated by weighing leaves before and after freeze-drying, was determined to be approximately 90%. This proportion was then used to estimate the percentage water remaining following the 7 desiccation periods with the following formula:

$$\%\text{moisture remaining} = \frac{\text{Desiccated wt} - 0.1 \times \text{Fresh wt}}{\text{Fresh wt} \times 0.9} \times 100\%$$

The second disruptive treatment consisted of freezing three-week old Erik plants in a freezer at -20°C for 10 minutes and subsequently returning them to the normal growth chamber for a period of 24 to 48 hours before harvesting and fixing leaf pieces in the cacodylate buffered 3.75% gluteraldehyde fixative.

The final disruptive treatment consisted of plasmolyzing leaf pieces at the time of fixation using either sucrose or sodium chloride. A hyperosmotic fixative was made by adding either 1 M sucrose or 2 M NaCl to the phosphate buffered 3% gluteraldehyde fixative. Leaf pieces were harvested as for the toxin treated tissues and placed in the hyperosmotic fixative. The remainder of the processing procedure was unchanged from that described for the infiltrated tissues.

Processing for microscopy

Three different types of fixation and post-fixation procedures were used in the course of this experiment. The first fixation procedure consisted of a 3% gluteraldehyde 0.025 M potassium phosphate buffered primary fixative at pH 6.8, three 20-minute washes in buffer, a 4-hour post-fix in buffered 2% osmium tetroxide at 4°C, and three 20-minute washes in deionized filtered water. The second and third fixation procedures both consisted of a cacodylate buffered (0.025M), 3.75% gluteraldehyde, 7 mM $CaCl_2$, primary fix at pH 7.0, followed by three 20-minute washes in buffer with 7 mM $CaCl_2$. The second and third fixation procedures differed in their post-fixation procedures, the second post-fix consisted of buffered 2% osmium tetroxide, 0.8% potassium ferrocyanide with 5 mM $CaCl_2$ for 4 hours at 4°C, the third post-fix consisted of buffered 6% potassium permanganate with 5 mM $CaCl_2$. For all procedures the primary fixation was conducted at room temperature for 4 hours followed by storage in the same fixative solution at 4°C for at least 16 hours and until further processing could be resumed. Both the second and third fixation procedures were completed by three 20-minute deionized filtered water washes followed by uranyl acetate (1% w/v) *en bloc* staining for 20 minutes at 4°C.

Following the water washes or the *en bloc* staining, all the leaf pieces were dehydrated in a graded series of ethanol: 20 minutes each in 30, 50, 70, 90, and 95%. The tissues were then further dehydrated for 10 minutes each in 100% ethanol (3 times), a 1:1 mixture of 100% ethanol:propylene oxide, and propylene oxide (3 times). The tissues were then infiltrated with a series of 4 Spurr solutions each for a period of 1 to 2 days on a rotator. The Spurr resin including the accelerator consisted of 10:7:26:0.4 vinylcyclohexene dioxide (ERL

4206):diglycidylether of polypropylene glycol (DER 736):nonenyl succinic anhydride (NSA):dimethylaminoethanol (DMAE accelerator) (w:w:w:w). The first solution consisted of a 1:1 mixture (v:v) of Spurr (without accelerator):propylene oxide, the second of a 3:1 mixture (v:v) of Spurr (without accelerator):propylene oxide, the third of 100% Spurr (without accelerator) and the fourth of 100% Spurr (with accelerator). The leaf pieces were then embedded in aluminum pans and polymerized in a 65°C oven overnight (12-16 hours).

Tissue sectioning for light and fluorescence microscopy

Once cooled, the molds were removed from the aluminum pans and tissue blocks were cut from them using a coping saw. The blocks were epoxy-glued to small cylinders (5 mm diameter x 10 mm length) of polymerized Spurr. The blocks were trimmed with disposable double-edged razor blades. Thin sections (2 µm) were cut using a Reichert Om U2 microtome and placed on a drop of deionized distilled water on a glass slide. The sections were stretched by exposing them to vapours from a chloroform soaked swab and then dried onto the glass slide at 75°C on a slide warmer. The sections were stained as described below for examination by light and fluorescence microscope.

Toluidine blue O stainining

Toluidine blue O (CI 52040 British Drug Houses Ltd) buffered with borax was used as a general stain (Ruzin, 1999). It is a metachromatic stain which can be used to indicate, DNA (blue), RNA (purple), polycarboxylic acids (red), or polyphenols or lignin (green) (O'Brien and McCully, 1981). A drop of 0.5% toluidine blue solution was placed on the sections and the slide placed on a 75°C slide warmer for 1 to 2 minutes or until the edges of the stain drop had dried. The stain was then rinsed off the slide under running tap water until all the excess stain had been removed. The sections were mounted in 60% sucrose solution, overlaid with a coverslip, and examined under brightfield microscopy.

Calcofluor staining

Calcofluor White M2R (Polysciences) was used to visualize 1,4-β-glucans

including cellulose and hemicellulose (Hughes and McCully, 1975, and Maeda and Ishida, 1967). In order to properly stain with Calcofluor, the resin had to be extracted by exposing the sections to a saturated solution of sodium methoxide (sodium hydroxide pellets dissolved in methanol) for 12 minutes followed by three consecutive 2 minute rinses in 95% ethanol (Sutherland and McCully, 1976). The sections were then dried on the slide warmer and then stained with a 0.1% solution of Calcofluor for 2 minutes. The stain was then briefly rinsed in tap water, allowed to dry, covered with a drop of glycerin, and examined by fluorescence microscopy using ultraviolet excitation (Nikon UV excitation filter cassette; excitation filter U 330-380 nm, dichroic mirror DM 400 nm, and eyepiece-side absorption filter slide 420W).

Periodic Acid Schiff (PAS) staining

PAS staining was used to stain compounds which contain vicinal glycol groups such as starch, pectin, hemicellulose but it is not an effective stain for cellulose (McCully and O'Brien, 1981, and Pearse, 1968). The resin was removed as described for Calcofluor staining to enhance the staining reaction. The sections were then placed in a saturated solution of DNPH (2,4-dinitrophenyl-hydrazine) in 15% acetic acid for 30 minutes to block the aldehyde groups present from the fixation process, rinsed for 10 minutes in running water, exposed to a 1% solution of periodic acid (G Frederick Smith Chemical Company) for 20 minutes to oxidise vicinal glycol groups to aldehydes, rinsed in running water for another 5 minutes, placed in Schiff's reagent (Fisher Scientific) for 30 minutes to allow the reagent to complex with the newly formed aldehydes, rinsed a final time in running water for 5 minutes, and dried. The sections were covered with a drop of glycerin and viewed by fluorescence microscopy using green light excitation (Nikon G excitation filter cassette; excitation filter G 535-550 nm, dichroic mirror DM 575 nm, and eyepiece-side absorption filter slide 580W).

Aniline blue callose staining

Aniline blue was used to indicate callose, a 1,3-β-glucan, in the cell walls

(Smith and McCully, 1978a, Smith and McCully, 1978b, and Eschrich and Currier, 1964). The resin was removed using sodium methoxide as previously described for Calcofluor staining. The sections were stained by mounting them in a 0.05% solution of aniline blue in 0.067 M phosphate buffer, pH 8.3. A drop of glycerin was placed on the coverslip and the sections were examined by fluorescence microscopy using ultraviolet light excitation (Nikon UV excitation filter cassette; excitation filter U 330-380 nm, dichroic mirror DM 400, and eyepiece-side absorption filter slide 420W).

Light and fluorescence microscopy and photomicroscopy

A Nikon Optithot brightfield microscope equipped with EF fluorescence and AFX photomicrographic attachements was used for fluorescence and light microscopy examination and microphotography. A high pressure 50W mercury lamp was used as a fluorescence source. Glycerin immersion objective lenses Nikon CF UV-F were used for fluorescence microscopy and Nikon CF Plant Achromat dry objective lenses were used for light microscopy. Both fluorescent and light micrographs were recorded with the Nikon Microflex AFX control box and photomicrographic attachment and FX-35 plain dark box on Kodak Select Series Elite Chrome 160 tungsten colour slide film.

Transmission electron microscopy

A Reichert-Jung Ultracut microtome equipped with a Diatome diamond knife was used to cut 90 nm thick sections of wheat leaf tissue. The sections were mounted on 300-mesh copper grids, dried overnight, stained in a saturated solution of uranyl acetate for 15 minutes in a dark container, rinsed by dipping the grids 9 times in boiled deionized water, stained in a solution of lead citrate for 15 minutes in a closed container inside of which was placed potassium hydroxide pellets to remove carbon dioxide, rinsed again as described above and dried. The sections were examined at 75 kV with a Hitachi H-7000 transmission electron microscope and the images recorded onto Kodak electron microscope film 4489.

RESULTS

Toxin purification

The bioassay of the 86-124 culture filtrate from which the toxin was purified indicated a toxin concentration of approximately 10 µg/mL. In other words, the necrotic lesion size induced by neat culture filtrate two days after infiltration was roughly equivalent to that caused by a 10 µg/mL solution of purified toxin. It should be noted that the bioassay is a crude quantification method which can only distinguish toxin concentrations differing by a factor of 10 or more.

All of the toxin activity in the batch ion exchange process was contained in the 0.25 and 0.5 M NaCl eluate; 1:10 dilutions of the 0.25 and 0.5 M NaCl eluate indicated a toxin concentration of 10 µg/mL and no activity was found in the 2 M eluate. The 0.25 and 0.5 M NaCl eluate were pooled, dialyzed, and loaded onto the CM-cellulose ion exchange column. The column was washed initially with equilibration buffer, and then eluted with a 300 mL NaCl linear salt gradient while the eluate was continuously monitored at 280 nm (Fig. 2). Every fifth fraction was bioassayed at a 1:10 dilution and activity was found in fractions 35, 40, 45 and 50. Fractions 28, 32, 35, and 45 were run on a polyacrylamide gel; a bright and a faint 14 kDa band were found in the lanes corresponding to fractions 32 and 35, respectively. No bands were visible in the lanes corresponding to fractions 28 and 45. Fractions 31 to 45 were pooled, dialysed against deionized, distilled water at 4°C, lyophilized, and resolubilized in 1 mL of sterile, deionized, distilled water.

The absorbance of the purified toxin solution in a 1 cm cuvette at 280 nm was 3.040, which is equivalent to a protein concentration of 2.432 mg/mL. A sample of this solution was run on a SDS polyacrylamide gel and the only band observed had a molecular weight equivalent to the 14 kDa expected for Ptr ToxA (Fig. 3). Therefore, the protein concentration calculated from the spectrophotometer reading was used as the toxin concentration, and all dilutions used in the experiments were made from this stock solution.

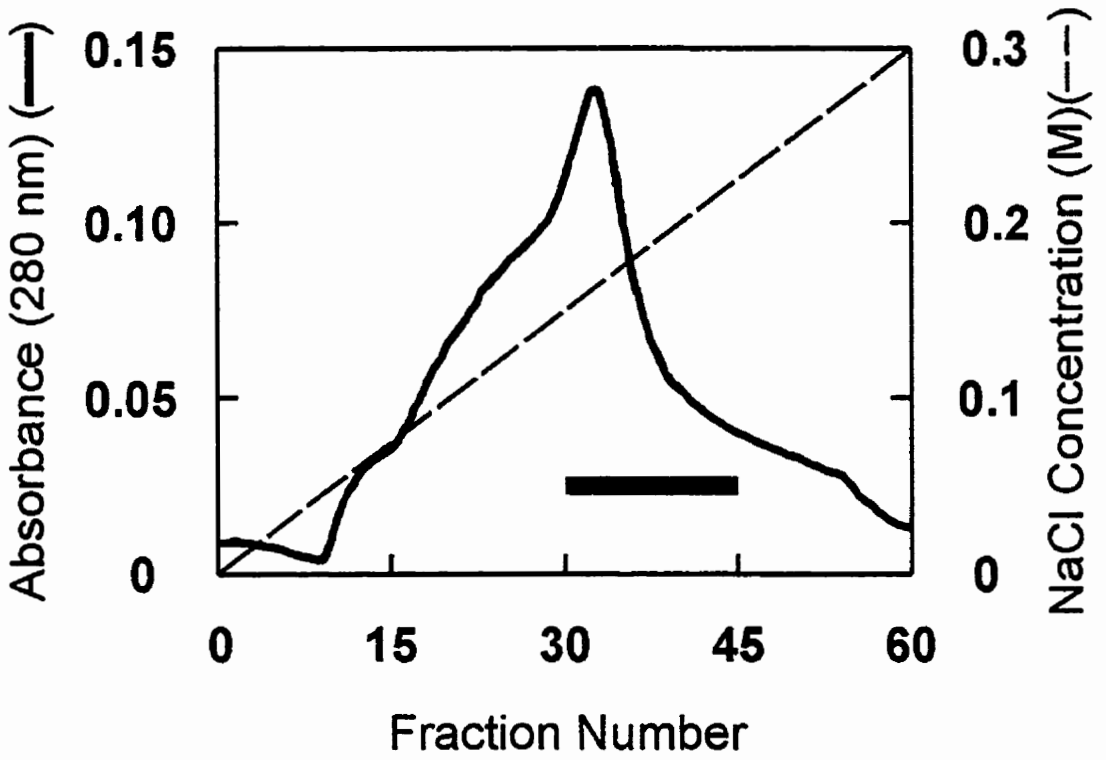

Figure 2. CM-cellulose ion exchange chromatographic profile of the pooled fractions (0.25 and 0.5 M NaCl) eluted from the batch ion exchange. A 0.3 M NaCl linear salt gradient in 10 mM sodium acetate buffer, pH 5.0 was run to elute the toxin. Fraction 31-45, which are indicated by the solid horizontal bar were pooled, dialysed, lyophilized, and dissolved in water.

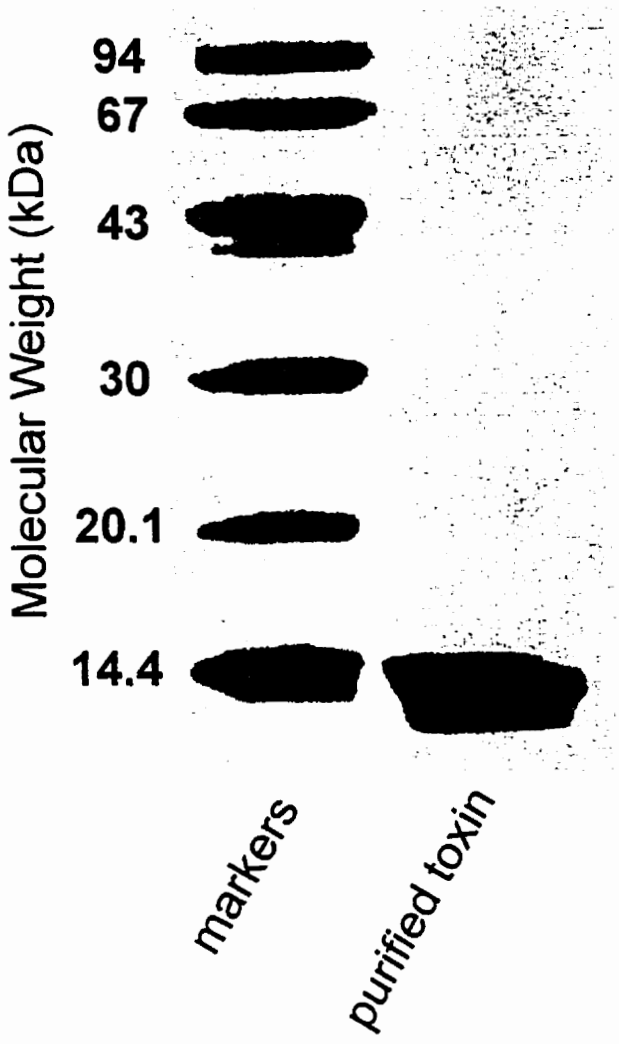

Figure 3. SDS-polyacrylamide gel electrophoresis of purified PtrToxA. The molecular weight markers were run in the left lane and 10 µg of purified toxin was run in the right lane. The gel was stained with Coomassie brillant blue.

Toxin bioassay

The progression of necrosis development in sensitive Glenlea leaf tissue infiltrated with 1 µg/mL PtrToxA is shown in Figures 4 to 7. Forty eight hours after infiltration, the lesions were relatively small, covering only about 10% of the infiltrated region, which corresponded to a lesion size of about 1 cm in length by half a leaf width. The lesion grew to cover approximately 30% of the infiltrated region after 96 hours, or roughly 3 to 4 cm in length by the width of the leaf, and about 60 to 70% after 144 to 336 hours, or approximately 5 to 6 cm in length by the width of the leaf. The lesion did not only grow in size but became more desiccated and tan coloured over time.

Therefore, Glenlea leaves infiltrated with a 1 µg/mL solution of PtrToxA, would have been necrotic in the bull's eye region after 48 hours. Sections harvested from region 1 (1 cm away from bull's eye) would have been on the edge of the necrotic lesion after 48 hours, and inside the lesion area after 96 hours. Sections from region 2 (2 cm away from the bull's eye) would have been on the edge of the lesion after 96 hours and sections from region 3 (3 cm away from the bull's eye) would have been on the edge or more likely outside the lesion area after 96 hours.

Leaves treated as controls are shown in Figures 8 to 10. Erik leaves were unaffected by water or PtrToxA toxin (1 µg/mL) infiltration and Glenlea leaves were unaffected by water infiltration. The only symptom visible on control leaves was the pinprick caused by the needle in the hagborg device which marked the centre of the infiltration region.

Light microscopy

Cells of water-infiltrated Glenlea leaves had a healthy appearance (Figs. 11 and 12). Toluidine blue stained cross sections of these water control leaves showed turgid mesophyll cells with lightly staining chloroplasts appressed to the interior of the cell walls and densely staining blue nuclei. The bundle sheath cells were very similar in appearance to the parenchyma cells of the mesophyll tissue.

Figure 4. Necrotic symptoms induced in toxin-sensitive wheat leaves (cultivar Glenlea) 48 hours after infiltration with 1 µg/mL PtrToxA.

Figure 5. Necrotic symptoms induced in toxin-sensitive wheat leaves (cultivar Glenlea) 96 hours after infiltration with 1 µg/mL PtrToxA.

Figure 6. Necrotic symptoms induced in toxin-sensitive wheat leaves (cultivar Glenlea) 144 hours after infiltration with 1 µg/mL PtrToxA.

Figure 7. Necrotic symptoms induced in toxin-sensitive wheat leaves (cultivar Glenlea) 336 hours after infiltration with 1 µg/mL PtrToxA.

Figure 8. Lack of necrotic symptom development in toxin-insensitive wheat leaves (cultivar Erik) 96 hours after infiltration with 1 µg/mL PtrToxA.

Figure 9. Lack of necrotic symptom development in toxin-insensitive wheat leaves (cultivar Erik) 96 hours after infiltration with distilled water.

Figure 10. Lack of necrotic symptom development in toxin-sensitive wheat leaves (cultivar Glenlea) 96 hours after infiltration with distilled water.

The < and > marks on the leaves indicate the edge of the infiltration region.

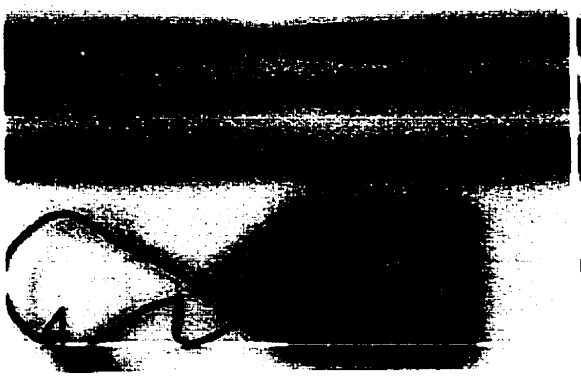

4

5

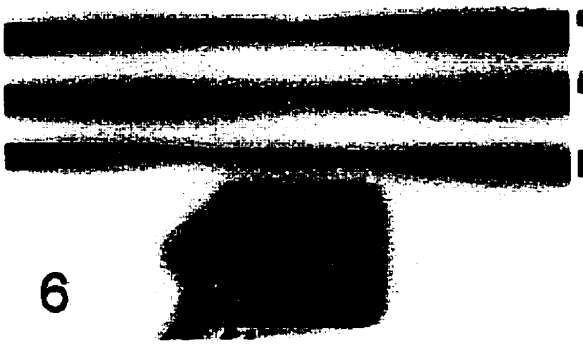

6

7

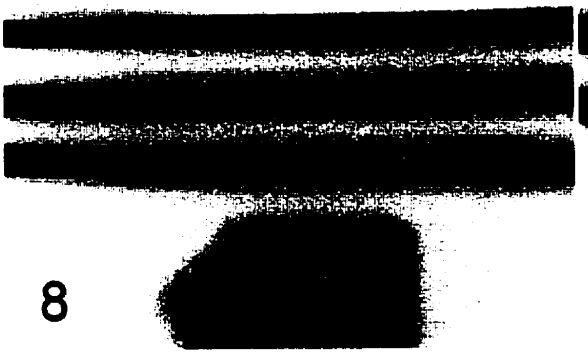

8

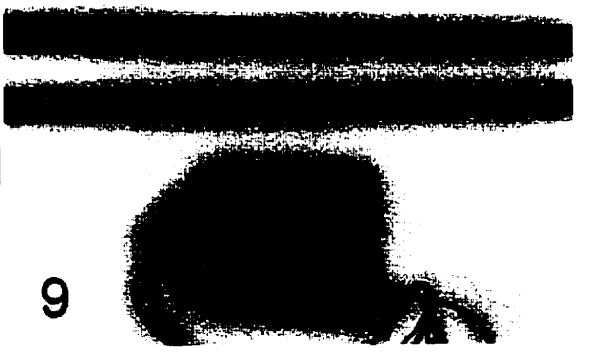

9

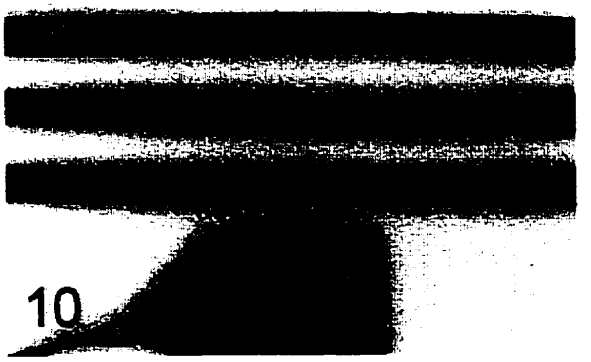

10

Epidermal cells were generally fairly turgid and were very rarely severely collapsed or deformed. The guard cells of the stomates, the mestome sheath (the inner bundle sheath) and the phloem tissue usually stained fairly densely.

The severity of cellular disruption observed by light microscopy increased with proximity to the bull's eye region and with the length of exposure to the toxin (Figs. 13 to 17). After 18 hours of toxin exposure in region 1, some of the leaf tissue had been affected (Fig. 13). Certain mesophyll cells had become collapsed and their contents stained densely blue or purple; portions of the upper epidermis had also collapsed; and bundle sheath cells had not collapsed but often stained dense purple. In the bull's eye region after 48 hours of toxin exposure a larger proportion of mesophyll cells and epidermal cells had collapsed (Fig. 15) but some relatively healthy mesophyll and epidermis remained. Finally after 96 hours, almost all the mesophyll and epidermal cells in region 1 were severely collapsed and densely stained (Fig. 17).

In region 3, even after 96 hours of toxin exposure, there were few signs of toxin activity; mesophyll cells appeared healthy and only a few epidermal cells on the adaxial surface had collapsed (Fig. 14). There was an intermediate level of cellular disruption in region 2 after 96 hours of toxin exposure (Fig. 16); most of the epidermis had collapsed, some bundle sheath cells were uncollapsed but stained densely, some of the mesophyll cells had collapsed and stained densely and some of the mesophyll appeared disrupted. The disrupted mesophyll cells had not collapsed and their chloroplasts could not be seen tightly appressed to the cell walls but appeared to be distributed throughout the entire cellular volume. These disrupted cells, which seemed to be at an intermediate stage of necrosis, were generally found near vascular bundles, whereas the collapsed mesophyll cells were generally found near substomatal chambers. The severe level of disruption observed in region 1 at this time period has already been described.

Occasionally, the earliest toxin symptom observed at the light microscope level was the collapse of epidermal cells (Figs. 18 and 19). In Figure 19, the epidermal cells are collapsed but the underlying mesophyll cells appear intact. In

Figure 11. Light micrograph of transverse section of water-infiltrated wheat leaf showing healthy and turgid tissues. Stained with toluidine blue. Cultivar Glenlea, 24 h, p.i., 1 cm from bull's eye. Bar = 20 µm.

Figure 12. Light micrograph of transverse section of water-infiltrated wheat leaf showing turgid mesophyll cells with chloroplasts and nuclei. Stained with toluidine blue. Cultivar Glenlea, 24 h, p.i., 1 cm from bull's eye. Bar = 50 µm.

Figure 13. Light micrograph of transverse section of toxin-infiltrated wheat leaf demonstrating a relatively low level of toxin-induced disruption. There are few collapsed mesophyll and epidermal cells and some bundle sheath cells stain densely. Stained with toluiding blue. Cultivar Glenlea, 18 h, p.i., 1 cm from bull's eye. Bar = 50 µm.

Figure 14. Light micrograph of transverse section of toxin-infiltrated wheat leaf showing very little toxin-induced disruption. There are no collapsed mesophyll cells and very few collapsed epidermal cells. Stained with toluidine blue. Cultivar Glenlea, 96 h, p.i., 3 cm from bull's eye. Bar = 50 µm.

Figure 15. Light micrograph of transverse section of toxin-infiltrated wheat leaf illustrating an intermediate level of toxin-induced disruption. There are many collapsed epidermal cells and a moderate number of collapsed mesophyll cells. Stained with toluidine blue. Cultivar Glenlea, 48 h, p.i., bull's eye. Bar = 50 µm.

Figure 16. Light micrograph of transverse section of toxin-infiltrated wheat leaf with an intermediate level of disruption. Affected mesophyll cells are either collapsed or have a disrupted cytoplasm. Stained with toluidine blue. Cultivar Glenlea, 96 h, p.i., 2 cm from bull's eye. Bar = 50 µm.

Figure 17. Light micrograph of transverse section of toxin-infiltrated wheat leaf with a severe level of disruption. Most epidermal and mesophyll cells are collapsed and stain densely. Stained with toluidine blue. Cultivar Glenlea, 96 h, p.i., 1 cm from bull's eye. Bar = 50 µm.

cE - collapsed epidermis, cM - collapsed mesophyll, dM - disrupted mesophyll, E - epidermis, lvb - large vascular bundle, M - mesophyll, sBS - stained bundle sheath, svb - small vascular bundle. (p.i. - post-infiltration)

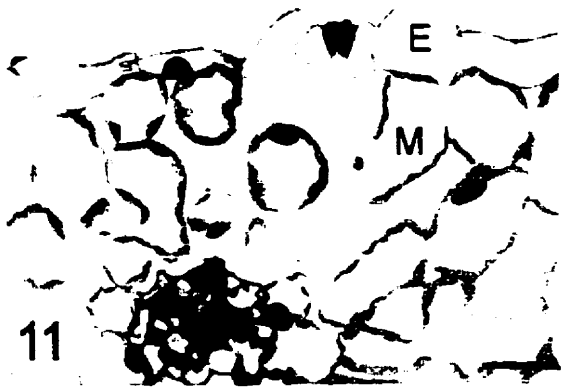

11

12

13

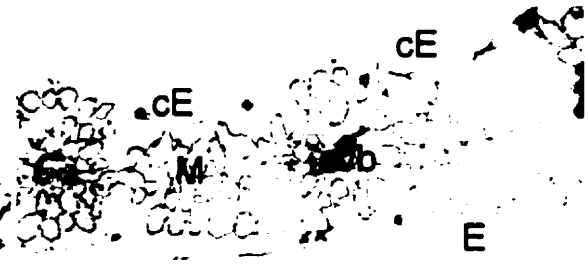

14

15

16

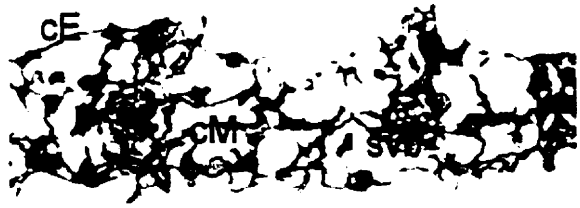

17

some cases however, the mesophyll underlying turgid epidermis was collapsed (Fig. 21). In contrast to the sensitive epidermal cells, the guard cells of the stomatal apparatus appeared to be more insensitive to PtrToxA. These latter cells were often the last recognizable structures in severely collapsed toxin-treated tissue.

Within the mesophyll there was also a differential reaction to the necrosis toxin. It appeared that the mesophyll cells nearest the adaxial side of the leaf were usually affected by PtrToxA before the mesophyll cells nearest the abaxial side (Fig. 21). The cells contained within the vascular bundle were unaffected by PtrToxA even when the surrounding mesophyll had collapsed (Fig. 20). The bundle tissues including: the phloem, the xylem, the parenchyma, and the mestome sheath (inner bundle sheath) but not including the outer bundle sheath did not appear to be affected. This is consistent with the observation that leaf tissue, distal to a necrotic lesion which spans the width the leaf, remains green and turgid (Figs. 5,6, and 7). This tissue would require a healthy and functional vascular system in order to remain healthy.

The epidermal and outer bundle sheath cells of toxin-treated tissues often reacted strongly to the toluidine blue stain (Fig. 22 and 23). In these tissues, very few cells had collapsed, suggesting that the toxin had not yet had a significant effect in that region of the leaf. However, many epidermal and bundle sheath cells, which also had not yet collapsed, were very densely stained by toluidine blue. This reaction was also observed in water-infiltrated control tissues but much less frequently and when it did occur the level of staining was not as pronounced (Fig. 24).

Fluorescence microscopy

Calcofluor, and PAS, which stain 1,4-β-glucans and polysaccharides with vicinal glycol groups respectively, were used to characterize potential changes in the composition of cell walls due to toxin activity, particularly in cells which had collapsed.

In water-infiltrated control tissues (Figs. 25 and 27), calcofluor stained the outer epidermal wall and the walls of the vascular tissues brightly, whereas the walls

Figure 18. Light micrograph of transverse section of toxin-infiltrated wheat leaf showing early signs of toxin activity. There are a few collapsed epidermal cells overlaying mostly healthy mesophyll. Stained with toluidine blue. Cultivar Glenlea, 96 h, p.i., 2 cm from bull's eye. Bar = 50 µm.

Figure 19. Light micrograph of transverse section of toxin-infiltrated wheat leaf showing a close-up of the collapsed epidermis. Stained with toluidine blue. Cultivar Glenlea, 48 h, p.i., 2 cm from bull's eye. Bar = 10 µm.

Figure 20. Light micrograph of transverse section of toxin-infiltrated wheat leaf showing unaffected bundle tissues surrounded by collapsed mesophyll. Stained with toluidine blue. Cultivar Glenlea, 48 h, p.i., bull's eye. Bar = 10 µm.

Figure 21. Light micrograph of transverse section of toxin-infiltrated wheat leaf displaying collapsed and healthy mesophyll in the adaxial and abaxial regions of the leaf respectively. Stained with toluidine blue. Cultivar Glenlea, 18 h, p.i., 1 cm from bull's eye. Bar = 50 µm.

Figure 22. Light micrograph of transverse section of toxin-infiltrated wheat leaf exposed to a humid environment demonstrating relatively intact mesophyll and densely staining outer bundle sheath cells and epidermis. Stained with toluidine blue. Cultivar Glenlea, 48 h, p.i., 1 cm from bull's eye. Bar = 50 µm.

Figure 23. Light micrograph of transverse section of toxin-infiltrated wheat leaf demonstrating relatively intact mesophyll and densely staining outer bundle sheath cells and epidermis. Stained with toluidine blue. Cultivar Glenlea, 24 h, p.i., 1 cm from bull's eye. Bar = 50 µm.

Figure 24. Light micrograph of transverse section of water-infiltrated wheat leaf exposed to a humid environment demonstrating intact mesophyll and moderately densely staining outer bundle sheath cells and epidermis. Stained with toluidine blue. Cultivar Glenlea, 24 h, p.i., bull's eye. Bar = 50 µm.

cE - collapsed epidermis, cM - collapsed mesophyll, E - epidermis, lvb - large vascular bundle, M - mesophyll, sBS - stained bundle sheath, sE - stained epidermis, svb - small vascular bundle. (p.i. - post-infiltration)

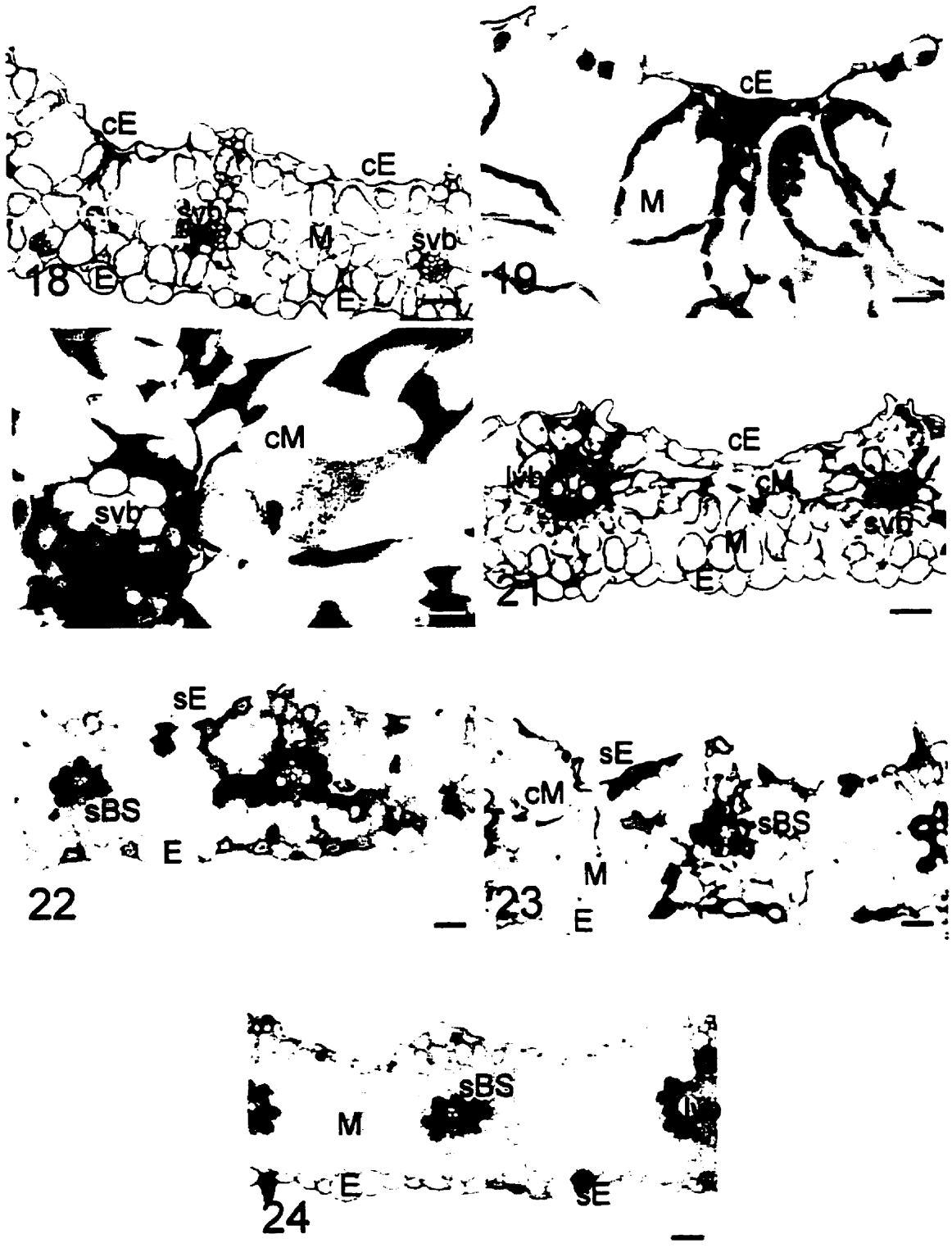
cE
cE
svb
M
svb
E
E
18
cE
M
19
cM
svb
cE
svb
cM
svb
M
E
21
sE
sBS
E
22
sE
cM
M
E
sBS
23
sBS
M
E
sE
24

of the mesophyll were stained relatively lightly. In toxin-treated tissues where both epidermal and mesophyll cells had collapsed (Figs. 26 and 28), calcofluor staining does not seem significantly reduced in the epidermal, mesophyll or vascular walls.

As with calcofluor, PAS staining was most conspicuous in the walls of the vascular tissues and the outer epidermis and less striking in the walls of mesophyll cells. Staining of wall material was not significantly reduced in toxin-treated cells which had collapsed (Figs. 30 and 32). In addition, it appeared that some PAS-positive material had accumulated inside the collapsed mesophyll cells.

Comparison disruptive treatments

The first set of disruptive treatments consisted of allowing detached Glenlea leaves to desiccate for up to 40 hours. Table 1 shows the amount of moisture remaining at each of 7 time periods following leaf detachment. After 6 hours of desiccation, the leaf had lost approximately 20% of its original moisture. However, there was little damage caused to these leaf tissues (Fig. 34) compared to the uninfiltrated control (Fig. 33). There were no collapsed cells and the order prevalent in healthy tissue seemed to be maintained. However, when comparing this desiccated tissue (Fig. 34) with the water infiltrated control (Fig. 11) it appeared that the cells had begun to shrink in size and that this had caused the leaf to deform and curl very slightly. The cell shrinkage appeared to be due to a contraction of the vacuole and a concomitant increase in the proportion of cellular volume occupied by chloroplasts and protoplasm.

There was only 42% of the original moisture remaining in leaves which had been detached for 16 hours. The mesophyll cells in these leaves had shrunken further and become less vacuolated (Fig. 35). Some of the mesophyll, especially towards the edge of the leaf, had desiccated to the point that none of the internal cellular structure could be distinguished.

The detached leaves lost an additional 20% of the original moisture between 16 and 24 hours of desiccation. Cellular structure, such as nuclei and chloroplasts, were still discernable at this point in mesophyll cells (Fig. 36). Most epidermal cells had not collapsed and still appeared to maintained their turgor, although they may

Figures 25 and 27. Fluorescence micrographs of transverse sections of water-infiltrated wheat leaves showing the relative abundance of cellulose in the vascular bundle and epidermal outer walls compared with the mesophyll cell walls. Stained with calcofluor. Cultivar Glenlea.

Figure 25: 18 h, p.i., 1 cm from bull's eye. Bar = 20 µm.

Figure 27: 24 h. p.i., 1 cm from bull's eye. Bar = 20 µm.

Figures 26 and 28. Fluorescence micrographs of transverse sections of toxin-infiltrated wheat leaves showing a similar abundance of cellulose in collapsed mesophyll as in the healthy mesophyll cell walls from Figs. 25 and 27. Stained with calcofluor. Cultivar Glenlea.

Figure 26. 24 h, p.i., bull's eye. Bar = 20 µm.

Figure 28. 18 h, p.i., 1 cm from bull's eye. Bar = 20 µm.

Figures 29 and 31. Fluorescence micrographs of transverse sections of water-infiltrated wheat leaves showing the relative abundance of PAS-positive material in the vascular bundle and epidermal outer cell walls compared with the mesophyll cell walls. Stained with PAS. Cultivar Glenlea.

Figure 29: 18 h, p.i., 1 cm from bull's eye. Bar = 20 µm.

Figure 31: 96 h, p.i., 2 cm from bull's eye. Bar = 20 µm.

Figures 30 and 32. Fluorescence micrographs of transverse sections of toxin-infiltrated wheat leaves showing a similar abundance of cellulose in collapsed mesophyll as in the healthy mesophyll cell walls from Figs. 29 and 31. Note: The cytoplasm of some collapsed cells has a moderate level of fluorescence. Stained with PAS. Cultivar Glenlea.

Figure 30. 24 h, p.i., bull's eye. Bar = 20 µm.

Figure 32. 24 h, p.i., bull's eye. Bar = 20 µm.

cE - collapsed epidermis, cM - collapsed mesophyll, E - epidermis, lvb - large vascular bundle, M - mesophyll,, svb - small vascular bundle. (p.i. - post-infiltration)

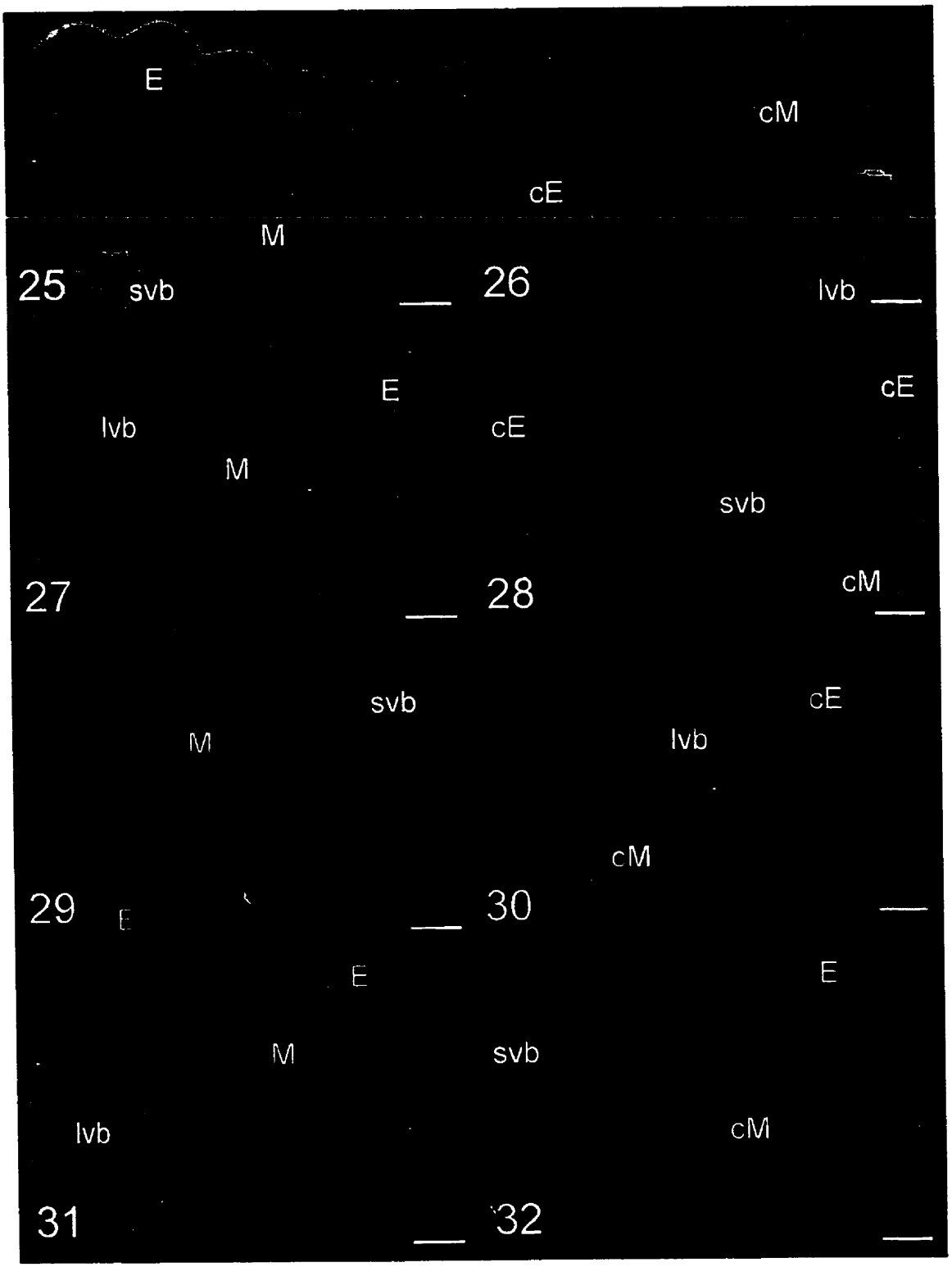
E
cM
cE
M
25
svb
26
lvb
E
cE
lvb
cE
M
svb
27
28
cM
svb
cE
M
lvb
cM
29
30
E
E
M
svb
lvb
cM
31
32

have been somewhat deformed.

Finally, after forty hours of desiccation, the leaf was very severely curled towards the adaxial side (Figs. 37 and 38), and only 15% of the original moisture remained in the tissue. Mesophyll cells were severely collapsed, their contents stained densely and chloroplasts or nuclei could no longer be identified. Epidermal cells were severely deformed and almost completely collapsed.

Table 1. The amount of moisture remaining in leaves which have been removed from a wheat plant and allowed to desiccate

Desiccation time (hrs)	Moisture remaining (%)
2	87
4	75
6	78
8	75
16	42
24	23
40	15

The second comparison treatment, which consisted of freezing Erik plants, allowing them to thaw, and then returning them to the growth chambers for 24 and 48 hours, was extremely damaging to the leaves and tissues. Upon thawing the leaves were wilted and had a dark green coloration indicating that the intercellular spaces had been wetted. Once returned to the growth chamber, the leaves quickly dried out, became brittle, but maintained a level of green pigmentation. At the microscopic level there was little difference between the 24 and 48 hour treatments (Figs. 39 and 40). In both these tissues the mesophyll was severely collapsed and

Figure 33. Light micrograph of transverse section of uninfiltrated wheat leaf with turgid epidermal and mesophyll cells. Note: The chloroplast are relatively compact and are appressed to the cell wall. Stained with toluidine blue. Cultivar Glenlea. Bar = 20 µm.

Figure 34. Light micrograph of transverse section of wheat leaf detached from plant for 6 hours. Note: The tissue is compacted due to vacuolar contraction and there are no collapsed cells. Stained with toluidine blue. Cultivar Glenlea. Bar = 50 µm.

Figure 35. Light micrograph of transverse section of wheat leaf detached from plant for 16 hours showing the leaf edge. Note: The tissue is further compacted and deformed due to vacuolar contraction and some of the mesophyll cells appear disrupted. Stained with toluidine blue. Cultivar Glenlea. Bar = 50 µm.

Figure 36. Light micrograph of transverse section of wheat leaf detached from plant for 24 hours. Note: Most of the cytoplasm of mesophyll cells stains moderately densely and vacuoles are very small or absent. Stained with toluidine blue. Cultivar Glenlea. Bar = 50 µm.

Figures 37 and 38. Light micrographs of transverse sections of wheat leaves detached from plant for 40 hours. Note: The tissue is severely deformed and mesophyll cells appear completely collapsed. Stained with toluidine blue. Cultivar Glenlea. Figure 37. Bar = 50 µm.
Figure 38. Bar = 20 µm.

Figures 39 and 40. Light micrographs of transverse sections of wheat leaves frozen at -20°C and then returned to normal growth conditions for 24 and 48 hours respectively. Tissue is completely collapsed and individual mesohyll cells are indistinguishable. Stained with toluidine blue. Cultivar Erik.
Figure 39. Bar = 50 µm.
Figure 40. Bar = 50 µm.

cE - collapsed epidermis, cM - collapsed mesophyll, dM - disrupted mesophyll, E - epidermis, lvb - large vascular bundle, M - mesophyll, svb - small vascular bundle.

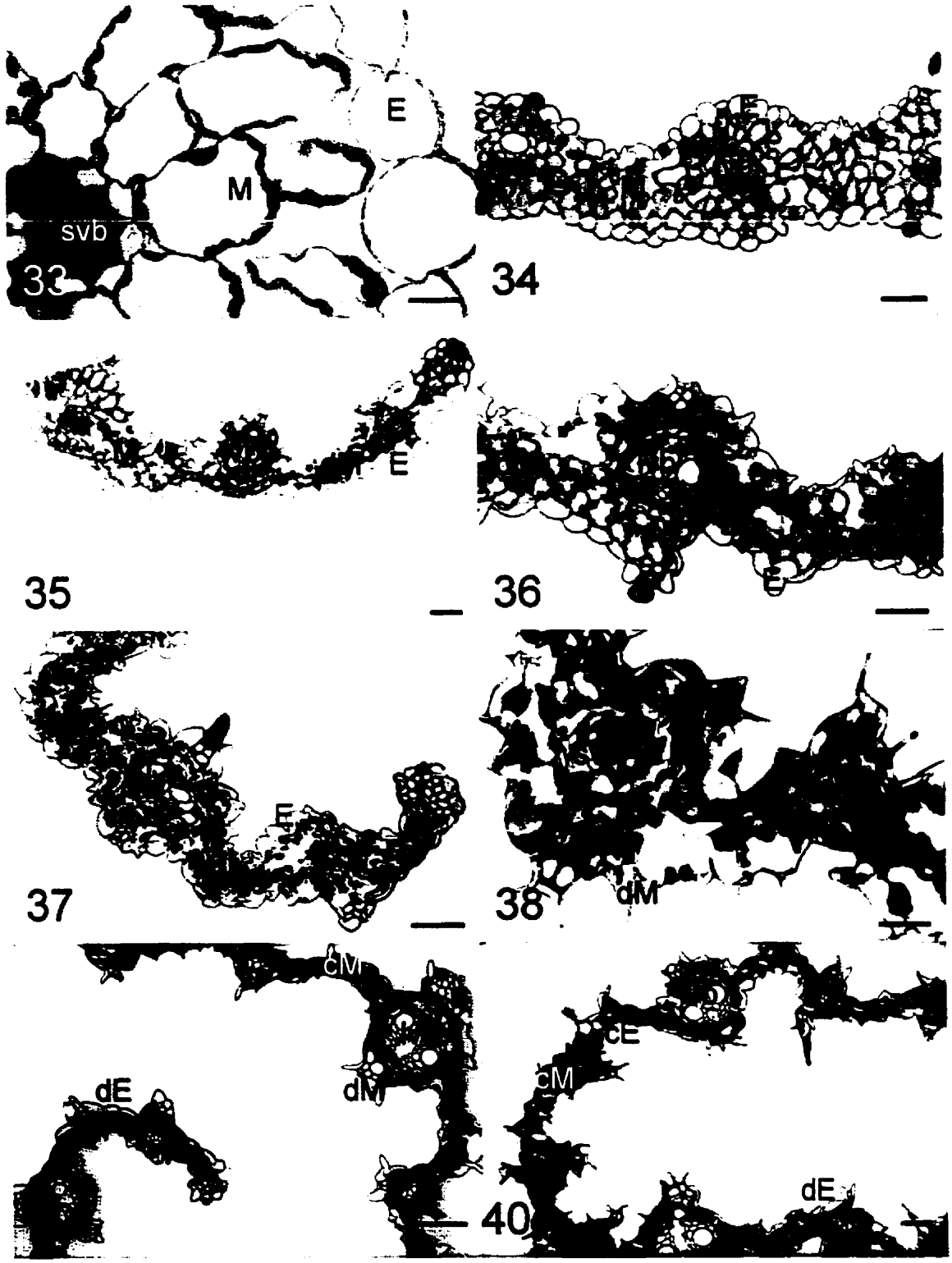
E
M
svb
33
34
35
36
37
38
dM
cM
dE
40
cE

densely stained. Unlike the 40 hour desiccation treatment, no individual parenchyma cells could be distinguished within the mesophyll leaf tissue of the freeze-treated Erik plants. The epidermal cells were severely deformed but were not completely collapsed.

The tissues plasmolyzed at the time of fixation in either 1 M sucrose (Fig. 41) or 2 M sodium chloride (Fig. 42) comprised the third and final treatment. This treatment had very little detrimental effect on the leaf tissues. The leaves were deformed or curled as they were for the other two disruptive treatments. The mesophyll cells were plasmolyzed but otherwise their internal structure remained unchanged; chloroplasts were still present and they remained appressed to the plasma membranes and nuclei could still be distinguished in some of the cells. Most epidermal cells maintained their rounded turgid shapes, and although some were slightly deformed, none of the epidermal cells completely collapsed.

Representative tissues from each of the plasmolysis, desiccation and freezing treatments were stained with PAS and calcofluor to examine their effects on the cell walls (Figs. 43 to 48). Plasmolysis and desiccation did not change the amount of carbohydrates containing vicinal glycol groups or 1,4-β-linkages in the cell walls compared to the controls (Figs. 27 and 29). Cell shape, as defined by the outline of the cell wall, was significantly affected by desiccation but not by plasmolysis. The freezing treatment caused significant distortion of the cell walls in all of the leaf tissues. A significant amount of PAS positive material was detected inside the cells of the freeze-treated Erik tissues.

It should be noted that in the PAS staining process of the freeze treated Erik tissues, the periodic acid reaction, which oxidizes vicinal glycol groups to aldehydes, was allowed to proceed for a longer period of time than for the other tissues (45 minutes versus 30 minutes). This explains the increased intensity of the PAS-fluorescence observed in Figure 47.

Figures 41 and 42. Light micrographs of transverse sections of wheat leaves plasmolyzed at the time of fixation with 1 M sucrose and 2 M NaCl respectively. Stained with toluidine blue. Cultivar Glenlea.
Figure 41. Bar = 50 µm.
Figure 42. Bar = 50 µm.

Figures 43 and 44. Fluorescence micrographs of transverse sections of wheat leaves plasmolyzed at the time of fixation with 2 M NaCl. Note: The cell walls have not deformed significantly. Cultivar Glenlea.
Figure 43. Stained with PAS. Bar = 50 µm.
Figure 44. Stained with calcofluor. Bar = 50 µm.

Figures 45 and 46. Fluorescence micrographs of transverse sections of wheat leaves detached from the plant for 16 hours. Note: The cell walls of both the mesophyll and epidermis have been severely deformed but have not lost a significant amount of staining. Cultivar Glenlea.

Figure 45. Stained with PAS. Bar = 50 µm.
Figure 46. Stained with calcofluor. Bar = 50 µm.

Figure 47. Fluorescence micrograph of transverse section of wheat leaf frozen at -20°C and then returned to normal growth conditions for 24 hours. Note: The cells are severely deformed and the cytoplasm of collapsed cells is fluorescent. The overall relative high fluorescence of this tissue is due to the extended periodate reaction in the staining process. Stained with PAS. Cultivar Erik. Bar = 20 µm.

Figure 48. Fluorescence micrograph of transverse section of wheat leaf frozen at -20°C and then returned to normal growth conditions for 48 hours. Note: The mesophyll cell walls are not only collapsed but appear to have partially disintegrated. Stained with calcofluor. Cultivar Erik. Bar = 20 µm.

cE - collapsed epidermis, cM - collapsed mesophyll, E - epidermis, lvb - large vascular bundle, M - mesophyll, pM - plasmolyzed mesophyll, svb - small vascular bundle.


E
E
41
42

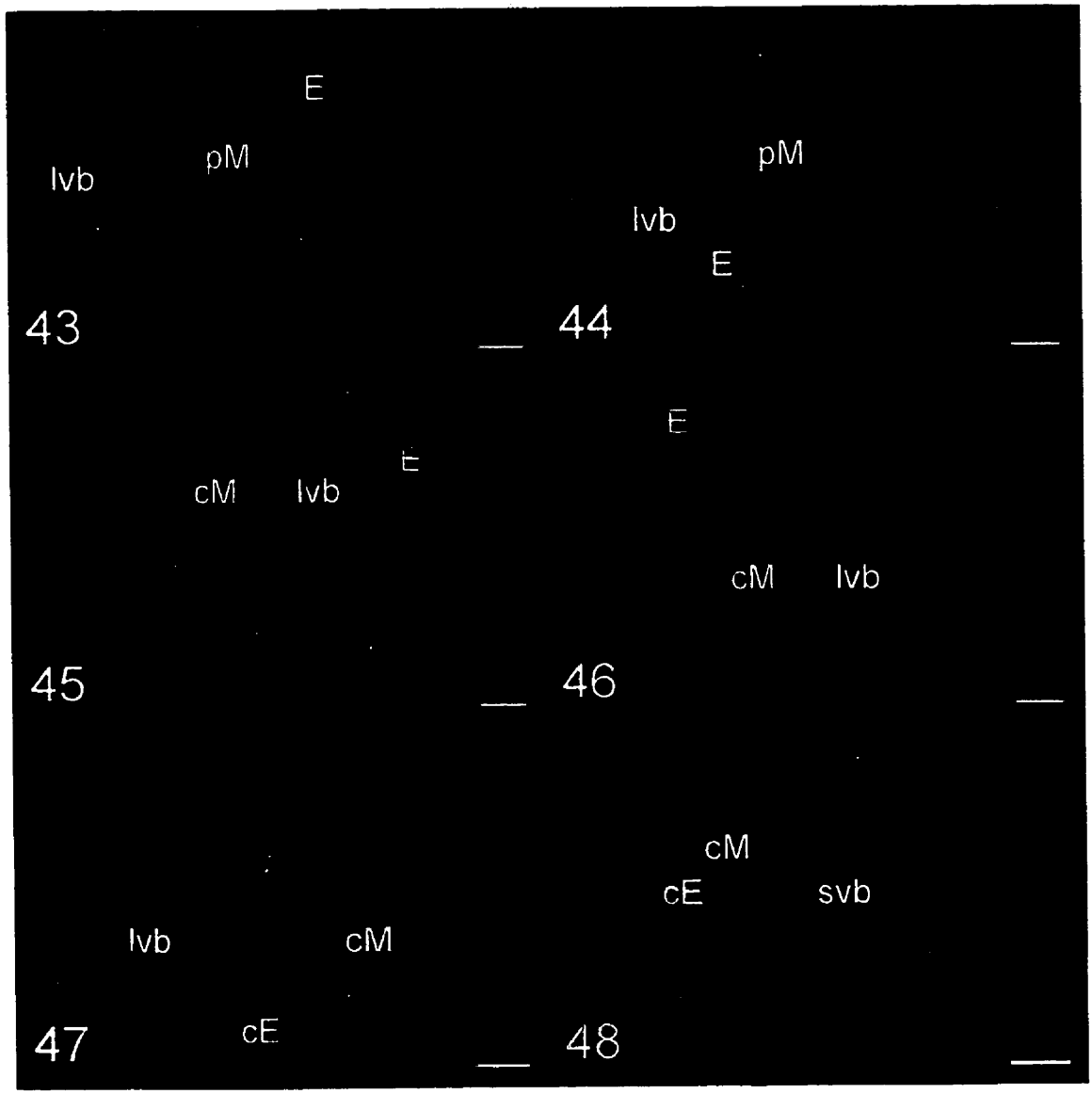
E
lvb
pM
43
pM
lvb
E
44
E
E
cM
lvb
45
cM
lvb
46
cM
cE
svb
lvb
cM
47
cE
48

Effect of humidity on lesion development

The humidity level to which toxin-infiltrated Glenlea plants were exposed, affected the development of necrosis lesions in the leaves (Figs. 49 and 50). Lesions which developed under normal humidity conditions were dry and tan-brown in colour and caused the leaf to curl and twist lengthwise. In comparison, lesions which developed in a relatively humid environment are yellow or green and did not cause the leaf to deform because their cells remained turgid. Although high humidity may have slowed or mediated lesion development it did not appear to prevent it.

At the microscopic level, PtrToxA-treated tissue also had a slightly different appearance depending on the humidity level to which the leaves were exposed (Figs. 51 to 56). In the normal growth chamber environment which was relatively dry, mesophyll and epidermal cells which had been exposed to PtrToxA tended to collapse and stain very densely (Figs. 51,53, and 55). Conversely, toxin-treated tissues exposed to high humidity for the same period of time and harvested from the same regions of the necrotic lesions tended to have little or no collapsed mesophyll or epidermal cells (Figs. 52, 54, and 56). However, cells from toxin treated-leaves placed in a humid environment had a disrupted internal structure; in some cases chloroplasts were no longer appressed to interior of the cell walls of mesophyll cells but were scattered or floating throughout the cell volume (Figs. 52 and 54), elsewhere cells stained lightly to moderately with toluidine blue but not as densely as collapsed toxin-treated cells exposed to the relatively dry environment of a regular growth chamber (Figs. 52 and 54).

Transmission electron microscopy

Control tissues

Examination of tissues by TEM confirmed the preservation of structures observed by light microscopy as well as structures that were not discernable at that lower magnification.

Representative healthy mesophyll cells from water-infiltrated leaf tissue had

Figure 49. Necrotic symptoms induced in toxin-sensitive wheat leaves (cultivar Glenlea) 72 hours after infiltration with 2 µg/mL PtrToxA. Leaves on the left were exposed to a 'normal' growth environment while leaves on the right were exposed to a humid environment following toxin infiltration.

Figure 50. Necrotic symptoms induced in toxin-sensitive wheat leaves (cultivar Glenlea) 120 hours after infiltration with 2 µg/mL PtrToxA with a portion of the infiltrated region sealed with packing tape to prevent moisture loss. The edges of the tape are outlined in black.

Figures 51, 53 and 55. Light micrographs of transverse sections of toxin-infiltrated wheat leaves exposed to a normal environment following toxin infiltration. Note: There are more collapsed mesophyll and epidermal cells in these tissues. Stained with toluidine blue. Cultivar Glenlea. Bar = 50µm.
Figure 51. 24 h, p.i., 1 cm from bull's eye.
Figure 53. 24 h, p.i., bull's eye.
Figure 55. 48 h, p.i., 1 cm from bull's eye.

Figures 52, 54 and 56. Light micrographs of transverse sections of toxin-infiltrated wheat leaves exposed to a humid environment following toxin infiltration. Note: There are fewer collapsed mesophyll and epidermal cells in these tissues and more mesophyll cells with a disrupted cytoplasm. Stained with toluidine blue. Cultivar Glenlea. Bar = 50 µm.
Figure 52. 24 h, p.i., 1 cm from bull's eye.
Figure 54. 24 h, p.i., bull's eye.
Figure 56. 48 h, p.i., 1 cm from bull's eye.

cE - collapsed epidermis, cM - collapsed mesophyll, dM - disrupted mesophyll, E - epidermis, lvb - large vascular bundle, mv - midvein, M - mesophyll,, svb - small vascular bundle. (p.i. - post-infiltration)

49

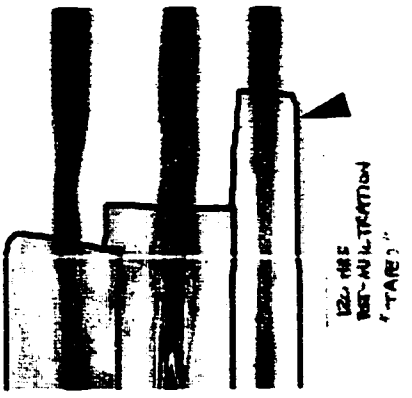

50

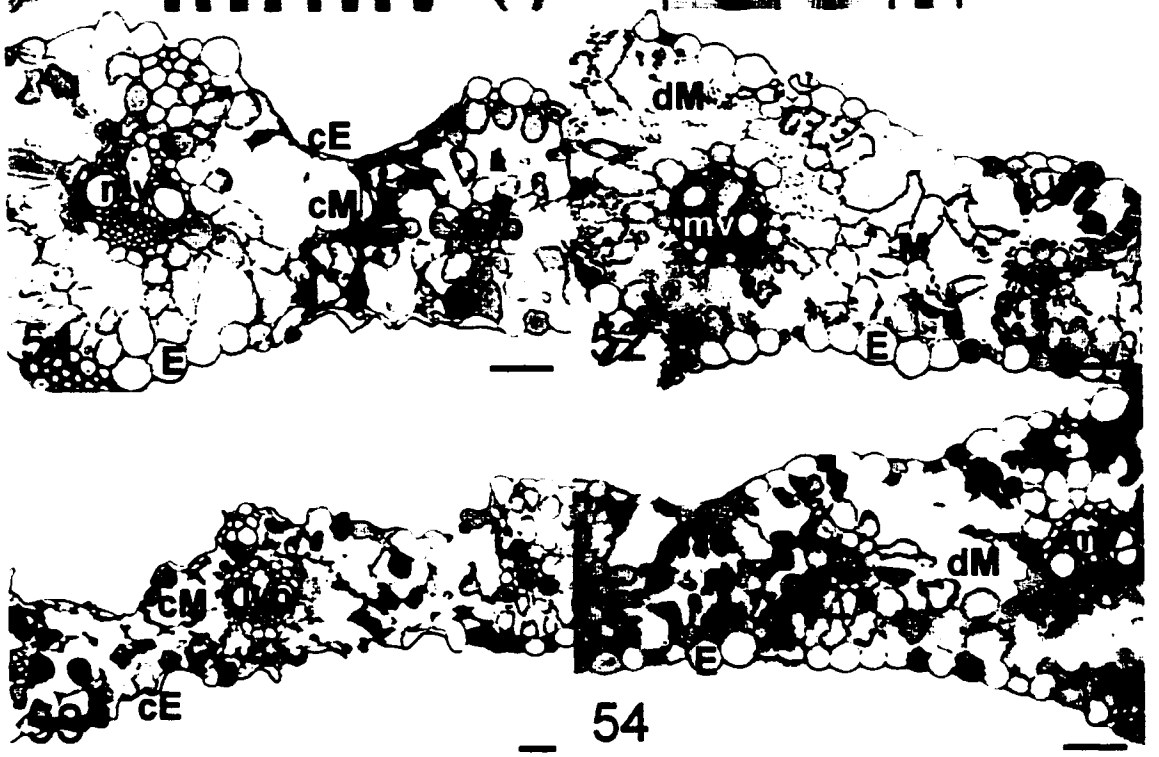

51 52

53 54

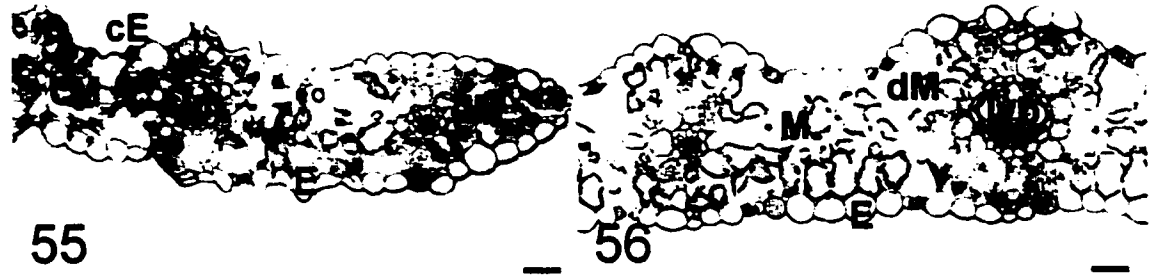

55 56

chloroplasts which were appressed to the cell walls (Fig. 57). These chloroplasts had well-preserved thylakoid membranes both in the stacks or grana and between grana, as well as a plastid envelope (Fig 57 and 58). In the mitochondria, which were usually tucked in between chloroplasts, both the inner membrane, which forms the cristae, and the outer membrane were visible in healthy control cells (Fig 57 and 59).

Nuclei, delimited by the double membrane nuclear envelope, contained a nucleoplasm which normally had a heterogeneous appearance with a relatively even distribution of dense and light staining patches (Fig 58 and 59). Nucleoli were sometimes observed in sections containing nuclei (Fig. 58).

The vacuole delimiting tonoplastic membrane, the Golgi apparatus, and the plasma membrane could be distinguished in the control tissues (Fig 57, 58, and 59). However, the plasma membrane was usually not tightly appressed to the interior of the cell wall but was typically slightly undulating (Fig. 59). Plasmodesmata connecting adjacent cells were often observed in the cell walls (Fig. 59). Endoplasmic reticulum was infrequently observed in mesophyll cells but was relatively abundant in cells of vascular tissues. Microbodies were also occasionally observed in control tissues.

The protoplasm, the mitochondrial matrix, and the chloroplastic stroma all stained relatively densely or were electron-opaque, whereas the vacuolar contents, the intercellular space and the cell wall stained relatively lightly or were electron-lucent.

Collapsed toxin-treated cells

The ultrastructure of toxin-treated mesophyll cells, which appeared collapsed and were densely stained with toluidine blue at the light microscope level, was revealed by TEM. The only discernable ultrastructure remaining in these cells appeared to be the granal and intergranal thylakoid membranes (Fig 60 to 64). Large starch grains were also usually associated with these thylakoid remnants. The plastid envelope, other organelles, or the plasma membrane could not be detected in these collapsed cells. However, the relatively-homogeneous and dense-staining

Figure 57. Transmission electron micrograph of transverse section of water-infiltrated leaf showing a control mesophyll cell with chloroplasts and mitochondria. Post-fixed with potassium permanganate. Cultivar Glenlea, 24 h, p.i., bull's eye. Bar = 2 µm.

Figure 58. Transmission electron micrograph of transverse section of water-infiltrated leaf showing a well-preserved chloroplast with thylakoid membranes and envelope, nucleus with nucleolus and double membrane nuclear envelope, tonoplast, and plasma membrane. Post-fixed with potassium permanganate. Cultivar Glenlea, 24 h, p.i., bull's eye. Bar = 1 µm.

Figure 59. Transmission electron micrograph of transverse section of water-infiltrated leaf showing well-preserved mitochondria, Golgi apparatus, plasmodesmata, double membrane nuclear envelope and plasma membrane of a bundle cell. Post-fixed with osmium and potassium ferrocyanide. Cultivar Glenlea, 48 h, p.i., bull's eye. Bar = 0.5 µm.

ch - chloroplast, cw - cell wall, g - Golgi apparatus, it - intergranal thylakoid membrane, mi - mitochondrion, ne - nuclear envelope, no - nucleolus, pd - plasmodesmata, pm - plasma membrane, to - tonoplast, ts - thylakoid stack, v - vacuole (p.i. - post-infiltration)

ch
ne
ne
to
ne
58
59

Figure 60. Transmission electron micrograph of transverse section of toxin-infiltrated leaf showing a collapsed mesophyll cell. Note: The walls are invaginate, there are large starch granules in the chloroplastic remnant, the cell contents are densely stained. Post-fixed with osmium and potassium ferrocyanide. Cultivar Glenlea, 24 h, p.i., bull's eye. Bar = 1 µm.

Figure 61. Transmission electron micrograph of transverse section of toxin-infiltrated leaf showing a magnification of the chloroplast remnant from Fig. 60. Note: The thylakoid membrane appears to be relatively intact but no other membranes are discernable. Post-fixed with osmium and potassium ferrocyanide. Cultivar Glenlea, 24 h, p.i., bull's eye. Bar = 0.5 µm.

Figure 62. Transmission electron micrograph of transverse section of toxin-infiltrated leaf showing a collapsed mesophyll cell adjacent to relatively intact one. Note: There are large starch granules in the collapsed cell, its walls are invaginate, and some wall material (apposition) has accumulated in the healthy cell opposite the collapsed one. Post-fixed with osmium and potassium ferrocyanide. Cultivar Glenlea, 48 h, p.i., 1 cm from bull's eye. Bar = 2 µm.

Figure 63. Transmission electron micrograph of transverse section of toxin-infiltrated leaf showing a magnification of a portion of the collapsed mesophyll cell in Fig 62. Note: The only recognizable structures are the thylakoid membranes and starch granules interspersed between them. Post-fixed with osmium and potassium ferrocyanide. Cultivar Glenlea, 48 h, p.i., 1 cm from bull's eye. Bar = 0.5 µm.

Ch - chloroplast, cw - cell wall, it - intergranal thylakoid membrane, pd - plasmodesmata, s - starch granule, ts - thylakoid stack, wa - wall apposition (p.i. - post-infiltration)

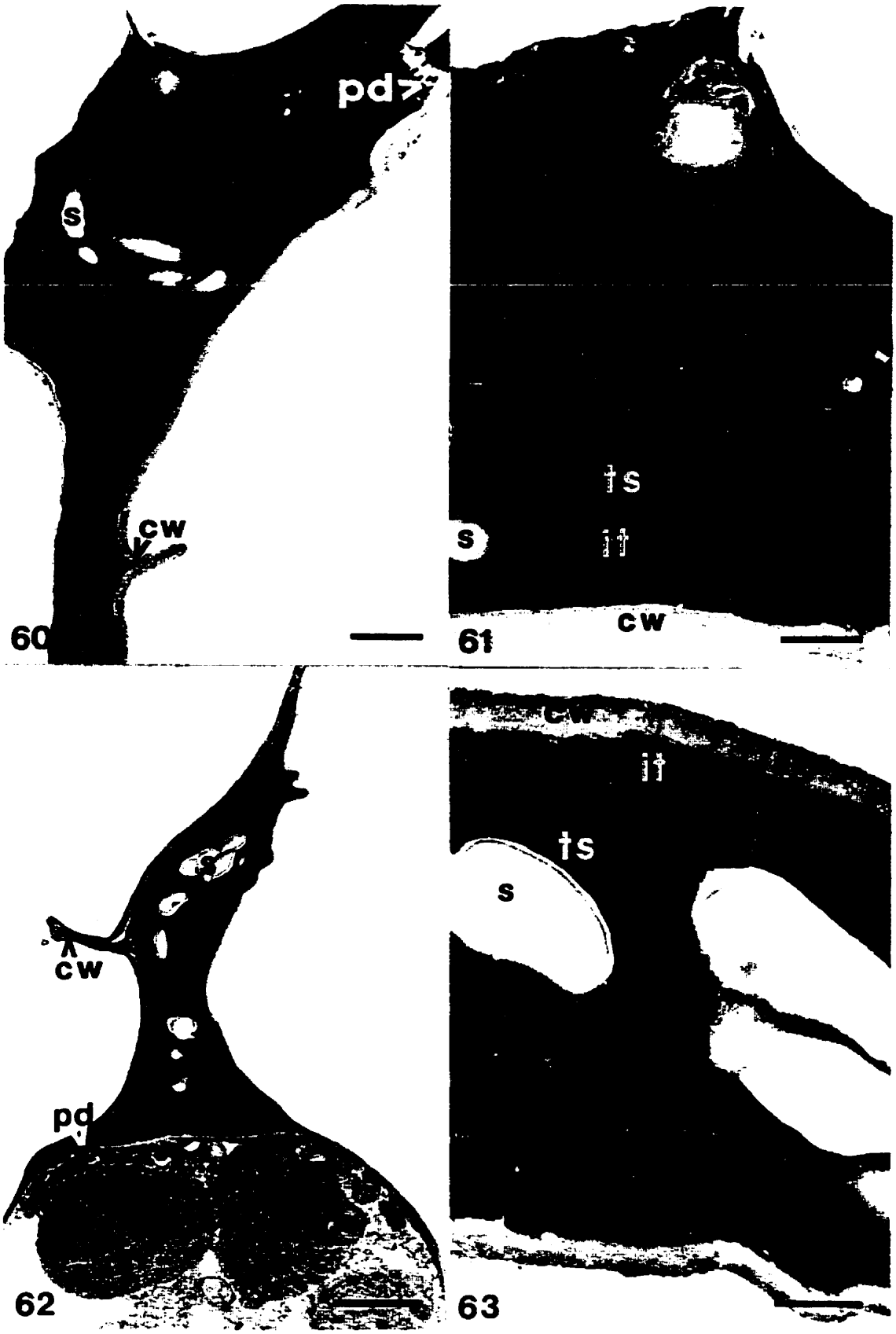
pd
s
cw
60
ts
s
cw
61
cw
62
pd
cw
ts
s
63

contents of these collapsed cells may have sufficiently reduced the contrast required to detect these structures. Also, the severe wall deformations or invaginations of collapsed cells are particularly conspicuous in the electron micrographs (Fig 60 and 62).

Disrupted toxin-treated cells

Cell collapse, as was described in the light microscopy section above, was the most severe toxin symptom and it was usually observed in tissues which had been exposed to PtrToxA for the longest period of time. However, many cells in toxin-infiltrated leaves displayed an intermediate level of damage which can be described as a disruption of cellular ultrastructure without complete cell collapse (Fig 64 to 67).

The least disruptive toxin-induced symptom consisted of chloroplast scattering within the volume of mesophyll and bundle sheath cells (Fig. 64). The chloroplasts of these cells did not appear do have been damaged by toxin activity. These organelles had retained their normal elliptical shape and size, as well as their intricate internal thylakoid ultrastructure. Structures resembling mitochondria were also scattered in the cellular volume and a wavy plasma membrane could be seen appressed to the interior of the cell wall. Also, as in the mesophyll cells of control tissues, microbodies were sometimes observed. Strands of membranous material could be seen interspersed with the above mentioned organelles and the protoplasm seemed to have disappeared. The overall appearance of these cells suggested that the tonoplast had disintegrated releasing the organelles from the cell wall and allowing them to move towards the interior of the cell and also dispersing the protoplasm.

Mesophyll cells, which had a moderate level of disruption compared to that described above, had distorted chloroplasts dispersed within the cellular volume (Fig 65 to 67). In these cells, the chloroplasts were swollen and had irregular outlines compared to their healthy appearance (Fig 65 and 67). However, their stroma still stained moderately densely and granal and intergranal thylakoids were still visible. One of the two membranes which formed the plastid envelope must still

Figure 64. Transmission electron micrograph of transverse section of toxin-infiltrated leaf showing bundle sheath cells with scattered chloroplasts and a disintegrated tonoplast. Note: A wavy plasma membrane against the cell wall and mitochondrial-like remnants are present in these disrupted cells. Post-fixed with osmium and potassium ferrocyanide. Cultivar Glenlea, 24 h, p.i., bull's eye. Bar = 4 µm.

Figure 65. Transmission electron micrograph of transverse section of toxin-infiltrated leaf mesophyll cell with cytoplasm which has pulled away from the cell wall. Note: There are chloroplast and mitochondria-like remnants in this disrupted cell but there is no tonoplast. Post-fixed with osmium and potassium ferrocyanide. Cultivar Glenlea, 24 h, p.i., bull's eye. Bar = 2 µm.

Figure 66. Transmission electron micrograph of transverse section of toxin-infiltrated leaf showing a magnification of the cell in Fig. 65. Note: The thylakoid membrane and one of the plastid envelope membranes is still present. Cristae in mitochondria can still be discerned but no tonoplast or plasma membrane remain. Post-fixed with osmium and potassium ferrocyanide. Cultivar Glenlea, 24 h, p.i., bull's eye. Bar = 0.5 µm.

Figure 67. Transmission electron micrograph of transverse section of toxin-infiltrated leaf showing collapsed and disrupted mesophyll cells. Note: Starch granules are present in the collapsed cell but not in the chloroplast remnants of the disrupted cell. Post-fixed with osmium and potassium ferrocyanide. Cultivar Glenlea, 24 h, p.i., bull's eye. Bar = 4 µm.

BS - outer bundle sheath cell, ch - chloroplast, cM - collapsed mesophyll cell, cr - chloroplast remnant, cw - cell wall, dM - disrupted mesophyll cell, it - intergranal thylakoid membrane, me - inner bundle sheath cell (mestome sheath), mi - mitochondrion, pm - plasma membrane, s - starch granule, ts - thylakoid stack (p.i. - post-infiltration)

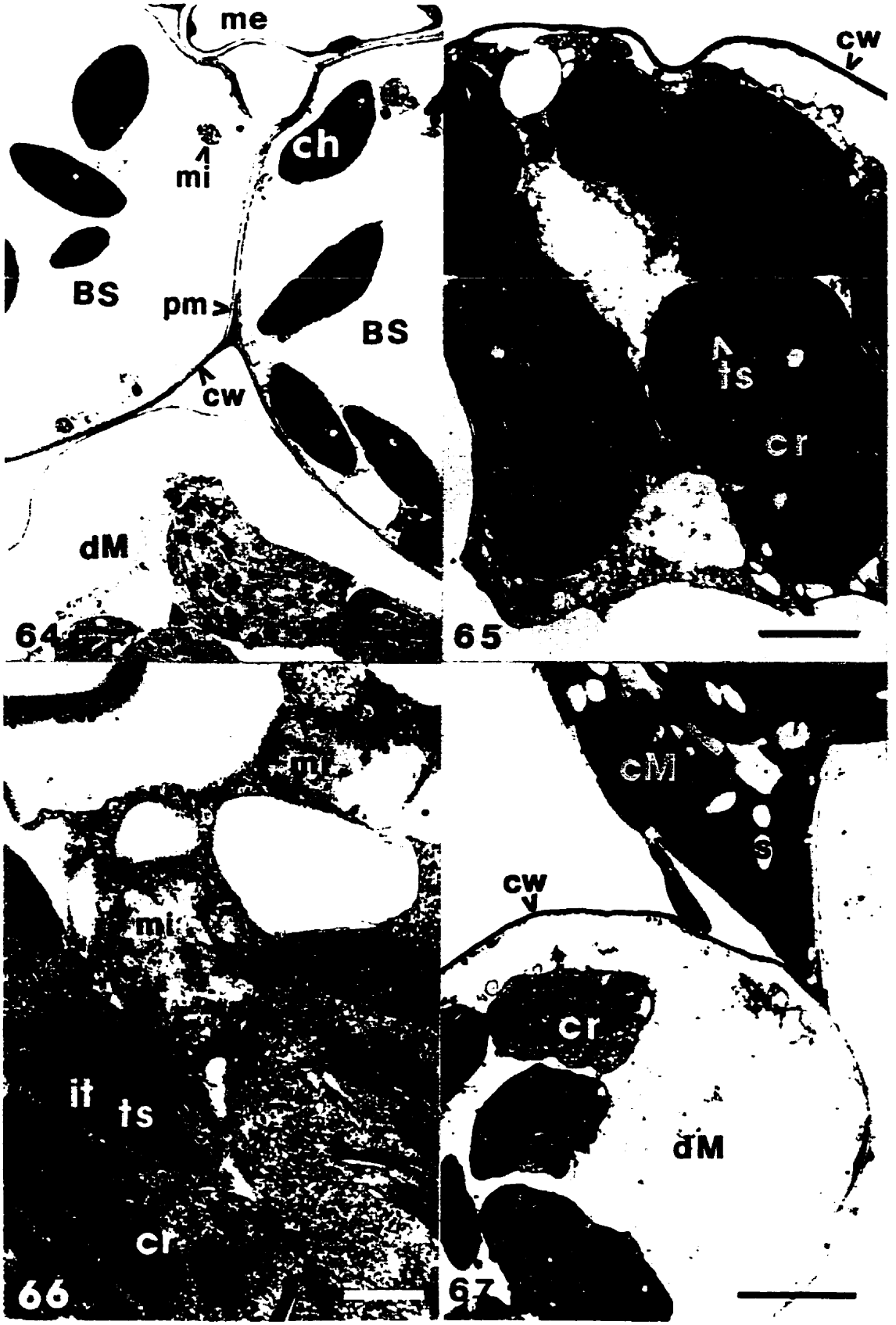
me
ch
mi
BS
pm
BS
cw
dM
64
cw
ts
cr
65
mi
mi
it
ts
cr
66
cM
s
cw
cr
dM
67

have surrounded these chloroplasts (Fig. 66) otherwise the stroma would have likely been lost to the surrounding medium. Structures which resemble mitochondria were also visible within these disrupted cells (Fig. 66).

The appearance or presence of the plasma membrane in the moderately disrupted cells was variable. Some cells had a plasmolyzed appearance where cytoplasmic contents seemed to be contained within an envelope (Fig. 65). In other cells there was no sign of the plasma membrane remaining (Fig. 67).

Toxin effect on epidermal and vascular bundle tissues

Epidermal cells, as described earlier, were sensitive to PtrToxA (Fig. 68). The epidermal cells collapsed, sometimes before the mesophyll tissue underneath it (Fig. 68). Collapsed epidermal cells had very little recognizable ultrastructure remaining; there were only a few strands of membrane and protoplasm and no structures resembling organelles of any sort. Conversely, Figure 71 shows healthy epidermal cells with a nucleus, endoplasmic reticulum, and mitochondria above collapsed mesophyll tissue. Therefore, epidermal collapse did not always preceed the collapse of the underlying mesophyll tissue.

Contrastingly, the ultrastructure of cells within the vascular bundle did not seem to be affected by PtrToxA (Fig 69 and 70). For example, Figure 69 shows a collapsed bundle sheath cell adjacent to a healthy vascular bundle. In this bundle both the mestome sheath cells and the parenchyma cell of the phloem tissue appear unaffected. A nucleus and its envelope, numerous mitochondria, endoplasmic reticulum and the plasma membrane were all well preserved within the phloem parenchyma cell (Fig. 69). The protoplasm of the two mestome sheath cells was contained between the plasma membrane and the tonoplast and mitochondria, and endoplasmic reticulum could be seen within it. Figure 70 illustrates the intricate ultrastructural detail preserved in a vascular bundle cell of toxin-treated tissue at a higner magnification.

Figure 68. Transmission electron micrograph of transverse section of toxin-infiltrated leaf showing collapsed epidermis above healthy-appearing mesophyll cell. Note: No tonoplast, plasma membranes or cytoplasm can be seen in the collapsed epidermal cells. Wall appositions are observed in the healthy mesophyll cell against the collapsed epidermal cell. Post-fixed with osmium and potassium ferrocyanide. Cultivar Glenlea, 48 h, p.i., bull's eye. Bar = 2 µm.

Figure 69. Transmission electron micrograph of transverse section of toxin-infiltrated leaf exposed to the humid environment with healthy-appearing bundle cells adjacent to a severely disrupted outer bundle sheath cell. Post-fixed with osmium and potassium ferrocyanide. Cultivar Glenlea, 48 h, p.i., bull's eye. Bar = 2 µm.

Figure 70. Transmission electron micrograph of transverse section of toxin-infiltrated leaf showing an unaffected bundle cell with well-preserved ultrastructure including endoplasmic reticulum, mitochondria, and plasma membrane. Post-fixed with osmium and potassium ferrocyanide. Cultivar Glenlea, 48 h, p.i. 1 cm from bull's eye. Bar = 1 µm.

cE - collapsed epidermal cell, ch - chloroplast, cr - chloroplast remnant, cw - cell wall, dBS - disrupted outer bundle sheath cell, er - endoplasmic reticulum, me - inner bundle sheath cell (mestome sheath), mi - mitochondrion, nu - nucleus, pm - plasma membrane, to - tonoplast, wa - wall apposition. (p.i. - post-infiltration)

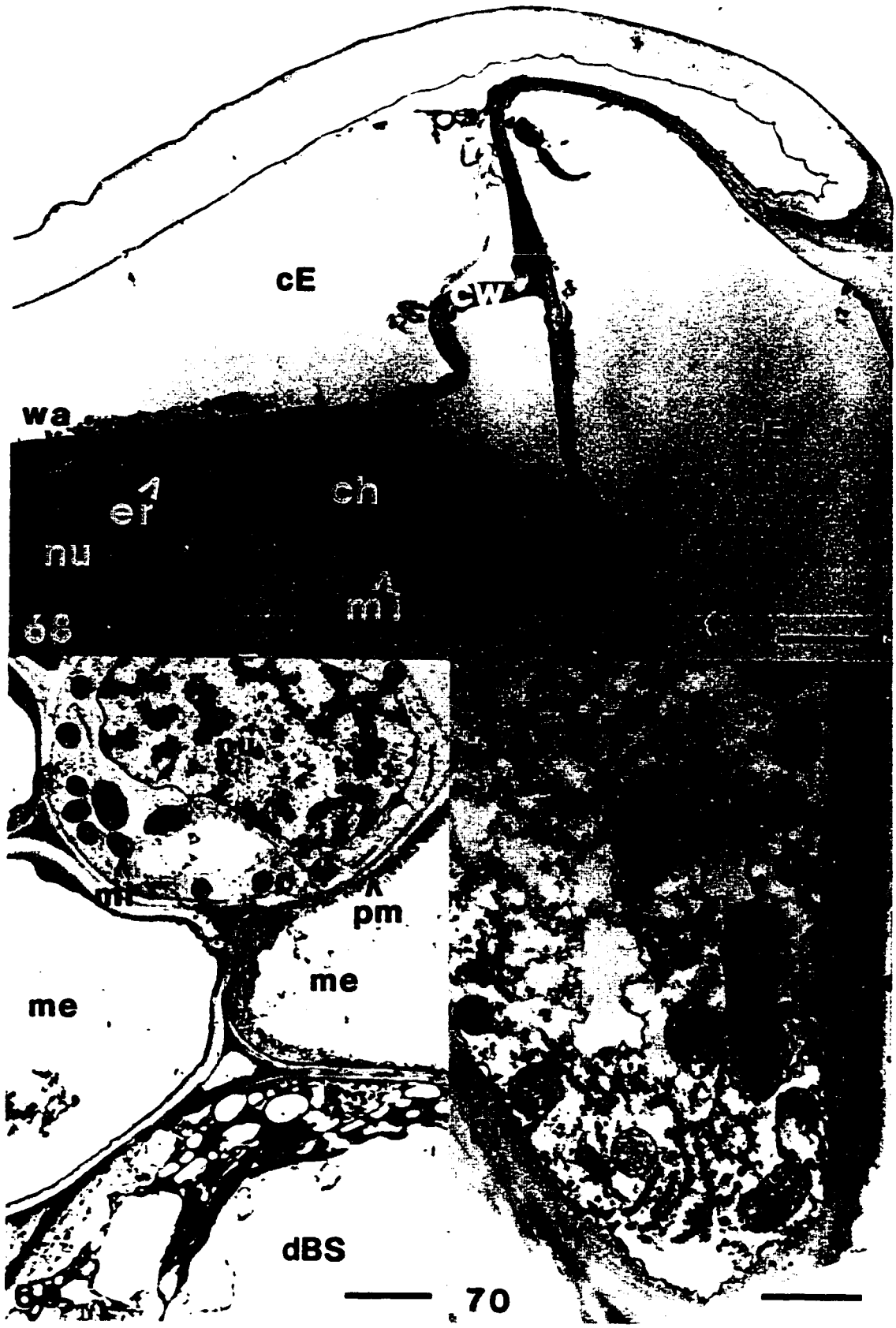

70

Starch granule accumulation in toxin-treated tissues

Starch granules often accumulated in toxin-affected cells, especially in mesophyll cells which had collapsed (Figs. 60, 62, 63, 67, 71, 72, and 73). The presence of these starch granules however was not observed in chloroplasts of healthy cells.

Figures 71 to 73 show collapsed mesophyll cells which contain large starch granules adjacent to healthy looking mesophyll cells with chloroplasts which did not contain any starch granules. Tissues processed for microscopy were harvested from plants throughout an 18 hour light period. If the tissues had been harvested late in the day, the healthy chloroplasts adjacent to the collapsed cells would likely also have contained starch granules. The lack of such granules in the healthy chloroplasts suggests that the collapsed cells had accumulated the starch during a previous light period and that this starch had not been mobilized into neighbouring mesophyll tissue. The size of the starch granules in the collapsed cells, some are approximately the same size as healthy chloroplasts, suggests that starch synthesis continued for a significant period of time.

Accumulation of densely-staining material in vacuole

Light microscopy revealed that uncollapsed epidermal and bundle sheath cells in toxin-infiltrated tissue sometimes stained moderately densely with toluidine blue (Figs. 22 and 23). A similar observation was made with transmission electron microscopy where a densely staining precipitate seemed to accumulate in the vacuolar region or at the centre of certain mesophyll or bundle sheath cells of toxin-treated tissues (Fig 74). In these mesophyll cells with densely stained vacuoles, chloroplasts remained in their normal positions, appressed to the interior of the cell wall, and had partially preserved thylakoid ultrastructure. However, the plastid envelope, other organelles or membranes such as the tonoplast or plasma membrane were not distinguishable in these cells.

Dehydration of cell walls

Severely collapsed cells, which were likely completely dehydrated, were usually poorly infiltrated with Spurr resin, especially when they had been post-fixed with potassium permanganate (Fig. 75). The poorly resin-infiltrated regions, which were very densely stained black and shattered during the sectioning process, were therefore likely representative of very dehydrated regions of the leaf. Figure 75 depicts the junction between a collapsed, dehydrated and poorly infiltrated cell and a healthy cell with preserved chloroplast and mitochondria. The dehydration and corresponding poor resin infiltration extends from the collapsed cell into the wall of the healthy mesophyll cell and right up to the surface of its plasma membrane. This suggests that the toxin-induced cell collapse caused water to be pulled from the adjacent cell walls despite being in contact with a healthy and therefore hydrated cell.

Wall appositions

The deposition of wall material or apposition was frequently observed at the junction of toxin-affected and healthy cells (Figs. 62, 68, 73, 76, 77, 78, 79 and 91). These appositions were observed in toxin-treated tissues exposed to the dry or humid environments. These wall appositions were always deposited on interior wall of healthy cells in apparent response to the disruption or death of the adjoining cell. The appositions were stained differently than the normal wall material, either more lightly or more densely, and displaced the plasma membrane towards the interior of the healthy cell. Also, these appositions were often positioned opposite plasmodesmata joining the healthy and toxin-affected cells and might therefore have created a protective seal between the two cells.

Examination by fluorescent microscopy of aniline blue stained sections from toxin-treated tissues, which demonstrated the wall appositions by electron microscopy, indicated that these structures consisted of callose (Figs. 80-84). These micrographs showed relatively bright yellow staining in the walls of some mesophyll and bundle sheath cells in regions where cells had collapsed due to toxin

Figure 71. Transmission electron micrograph of transverse section of toxin-infiltrated leaf showing two unaffected epidermal cells above a partially collapsed mesophyll cell. Note: Large starch granules observed in collapsed cell are absent in the chloroplasts of the neighboring mesophyll cell. Post-fixed with potassium permanganate. Cultivar Glenlea, 48 h, p.i., bull's eye. Bar = 5 µm.

Figure 72. Transmission electron micrograph of transverse section of toxin-infiltrated leaf showing one collapsed outer bundle sheath cell with large starch granules, another outer bundle sheath cell apparently unaffected by the toxin with chloroplasts lacking starch granules, and unaffected mestome sheath and bundle cells. Post-fixed with osmium and potassium ferrocyanide. Cultivar Glenlea, 24 h, p.i., bull's eye. Bar = 4 µm.

Figure 73. Transmission electron micrograph of transverse section of toxin-infiltrated leaf showing severely disrupted mesophyll cell with chloroplast remnants and large starch granules adjacent to a healthy-appearing cell with chloroplasts lacking starch granules. Note: Wall appositions have been deposited in the cell wall of the healthy-appearing mesophyll cell. Post-fixed with osmium and potassium ferrocyanide. Cultivar Glenlea, 24 h, p.i., 1 cm from bull's eye. Bar = 2 µm.

Figure 74. Transmission electron micrograph of transverse section of toxin-infiltrated leaf showing an outer bundle sheath cell with moderately dense staining vacuolar precipitate. Note: The chloroplast remnants and starch granules are observed in this affected cell. Post-fixed with potassium permanganate. Cultivar Glenlea, 48 h, p.i., 1 cm from bull's eye. Bar = 4 µm.

Figure 75. Transmission electron micrograph of transverse section of toxin-infiltrated leaf showing an unaffected mesophyll cell surrounded by poorly resin-infiltrated, densely staining, and shattered wall material and adjacent collapsed cell. Post-fixed with potassium permanganate. Cultivar Glenlea, 48 h, p.i., 1 cm from bull's eye. Bar = 2 µm.

BS - outer bundle sheath cell, ch - chloroplast, cM - collapsed mesophyll cell, cw - cell wall, dBS - disrupted outer bundle sheath cell, E - epidermal cell, er - endoplasmic reticulum, M - mesophyll cell, me - inner bundle sheath cell (mestome sheath), mi - mitochondrion, nu - nucleus, pd - plasmodesmata, pm - plasma membrane, po - poorly infiltrated wall and collapsed cell, s - starch granule, to - tonoplast, vp - vacuolar precipitate, wa - wall apposition. (p.i. - post-infiltration)


E
M
mi
ch
71
cM
er
E
dBS
me
cw
s
me
wa
BS
ch
72
pd
wa
s
ch
73
VP
ch
po
to
er
mi
ch
75

Figure 76. Transmission electron micrograph of transverse section of toxin-infiltrated leaf indicating that a wall apposition has been deposited at the junction of collapsed and healthy mesophyll cells. Post-fixed with osmium and potassium ferrocyanide. Cultivar Glenlea, 48 h, p.i., 1 cm from bull's eye. Bar = 2 µm.

Figure 77. Transmission electron micrograph of transverse section of toxin-infiltrated leaf indicating that a wall apposition has been deposited at the junction of collapsed and healthy mesophyll cells. Post-fixed with osmium and potassium ferrocyanide. Cultivar Glenlea, 48 h, p.i., 1 cm from bull's eye. Bar = 2 µm.

Figure 78. Transmission electron micrograph of transverse section of toxin-infiltrated leaf indicating that a wall apposition has been deposited at the junction of collapsed and healthy mesophyll cells. Note: The wall appositions are opposite the plasmodesmata and wall material appears to have been deposited intercellularly. Post-fixed with osmium and potassium ferrocyanide. Cultivar Glenlea, 48 h, p.i., 1 cm from bull's eye. Bar = 1 µm.

Figure 79. Transmission electron micrograph of transverse section of toxin-infiltrated leaf showing a magnified view of wall appositions at plasmodesmata. Note: The wall apposition material stains less densely than the cell wall. Post-fixed with osmium and potassium ferrocyanide. Cultivar Glenlea, 48 h, p.i., 1 cm from bull's eye. Bar = 0.5 µm.

ch - chloroplast, cM - collapsed mesophyll cell, cr - chloroplast remnant, cw - cell wall, er - endoplasmic reticulum, fi - filling of intercellular space, mi - mitochondrion, pd - plasmodesmata, pm - plasma membrane, s - starch granule, to - tonoplast, wa - wall apposition. (p.i. - post-infiltration)

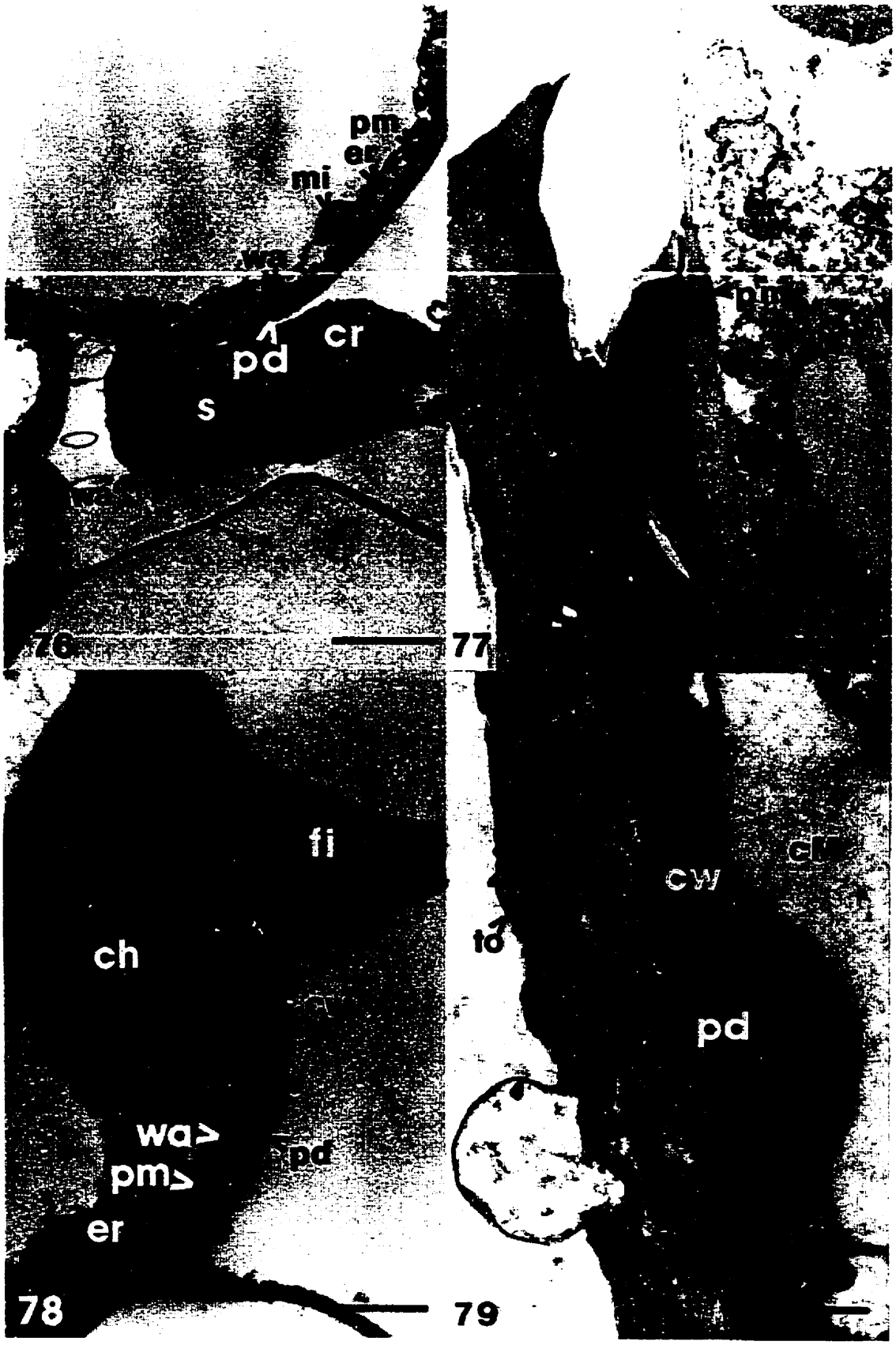
pm
mi
wa
cr
pd
s
76
77
fi
ch
cw
td
pd
wa
pm
er
pd
78
79

Figures 80 to 84. Fluorescence micrographs of transverse sections of toxin-infiltrated wheat leaves showing deposition of callose in the cell walls of toxin affected mesophyll. Note: Callose deposition can also be observed in phloem tissue. Stained with aniline blue. Cultivar Glenlea.

Figure 80. 24 h, p.i., bull's eye. Bar = 20 µm.
Figure 81. 48 h, p.i., bull's eye. Bar = 20 µm.
Figure 82. 48 h, p.i., 1 cm from bull's eye. Bar = 20 µm.
Figure 83. 24 h, p.i., bull's eye. Bar = 20 µm.
Figure 84. 24 h, p.i., bull's eye. Bar = 20 µm.

Figure 85. Fluorescence micrograph of transverse section of water-infiltrated wheat leaf exposed to a humid environment indicating that callose has not been deposited in the walls of healthy mesophyll cells. Stained with aniline blue. Cultivar Glenlea. 48 h, p.i., 1 cm from bull's eye. Bar = 20 µm.

cM - collapsed mesophyll, E - epidermis, lvb - large vascular bundle, M - mesophyll,, svb - small vascular bundle, arrowheads indicate callose depostion, (p.i. - post-infiltration)

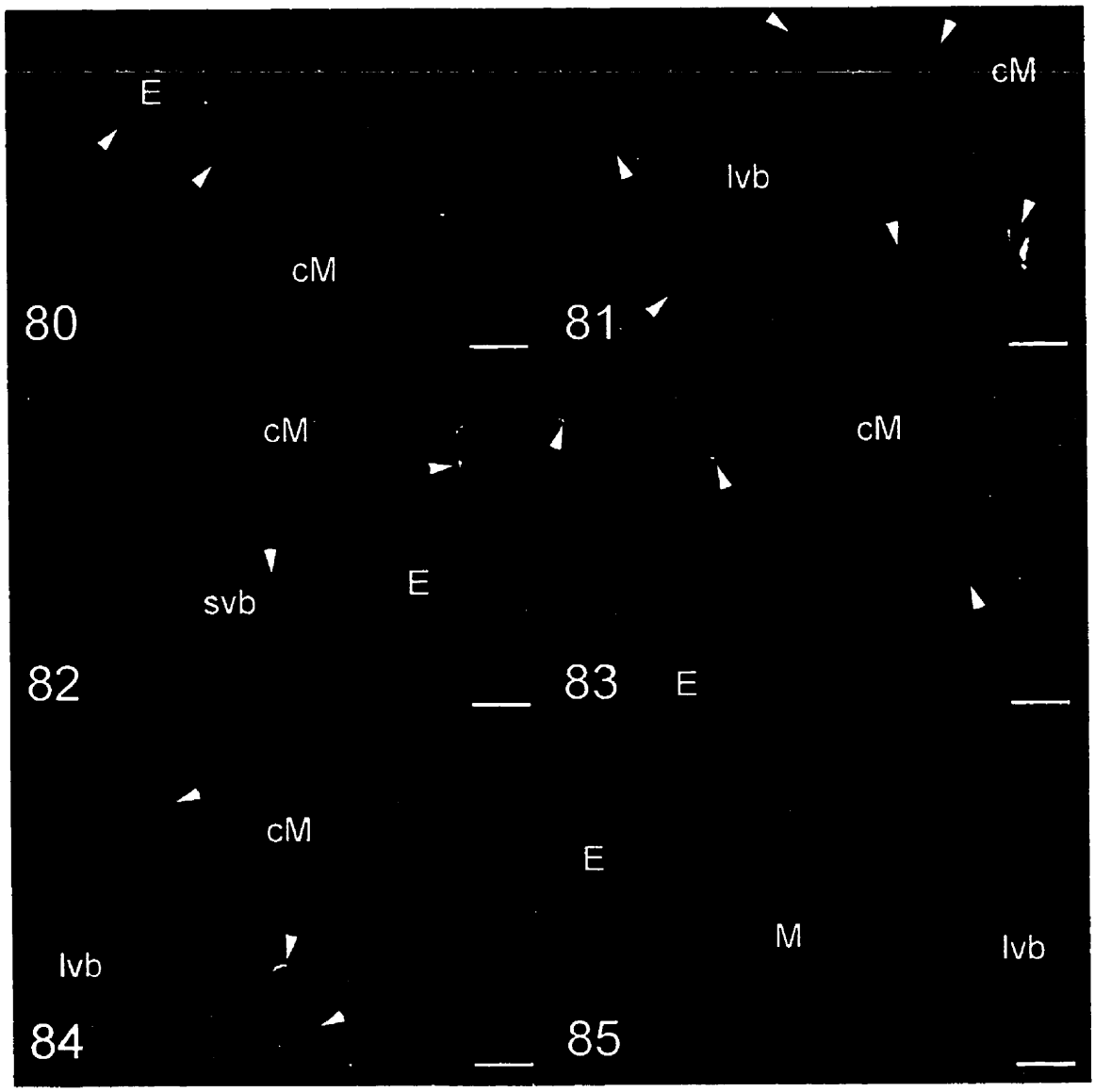
E
cM
lvb
cM
80
81
cM
cM
svb
E
82
83
E
cM
E
M
lvb
lvb
84
85

activity. Some staining was also observed in the interior wall of epidermal cells in these regions (Figs. 80 and 82). Conversely, in control tissue, there was no fluorescence indicative of callose in the cell walls; only autofluorescence of phenolic compounds such as lignin was observed (Fig. 85). Aniline blue staining of the freeze-treated tissues, which is not illustrated, also did not indicate any callose deposition in the wall of these cells.

Effect of humidity on cell disruption

The humid environment, as was mentioned earlier, prevented toxin-treated cells from collapsing and facilitated the examination of the ultrastructural disruption caused by toxin activity.

The first type of disruption, which appeared to be an early event in toxin activity, was very similar to the one previously described for toxin-treated plants exposed to the drier environment of the regular growth chamber (Fig. 16). In these disrupted cells, the organelles were no longer tightly appressed to the interior of the cell walls by the turgid centrally-positioned vacuole (Fig 86, 87, and 88). Also, the protoplasm of these cells seemed to have been diluted because it showed no staining in the electron micrographs (Fig 86 and 87). The break in the tonoplast shown in Figure 87 and the complete absence of the tonoplast in Figures 88 and 89 suggests that the rupture of this membrane had resulted in the loss of vacuole turgidity, cytoplasm dilution and the displacement of organelles from the periphery of the cell. However, the loss of tonoplast integrity in these cells did not seem to be accompanied by damage to the plasma membrane (Fig 86, 87 and 89).

The relatively unaltered ultrastructure of the displaced organelles indicates that this was an early event in toxin activity. The unaltered ultrastructure of the chloroplasts suggested that they had incurred very little damage. The mitochondria, which were also visible in these disrupted cells, were not as well defined as ones observed in control tissues but could still be confidently identified (Figs. 87 and 89). The nucleus shown in Figure 86 has an appearance which differs slightly from nuclei in control tissues. It seems to have an increased proportion of lightly staining material in its nucleoplasm but its double membrane envelope appears to be intact.

In addition, apparently undamaged microbodies were observed in these cells which had suffered tonoplast failure.

Continued degradation of the toxin-affected cells likely resulted in the decomposition of the displaced, yet relatively intact, organelles described above. In Figures 90 and 91, degraded chloroplasts, which consisted of bundles of dilated thylakoid stacks, are visible in the disrupted cells. In addition, the dense staining structure at the top of the cell in Figure 90 looks like a remnant of a nucleus which had been severely degraded.

Comparison disruptive treatments

Dehydration treatment. The removal of leaves from plants and the tissue dehydration which ensued resulted in mesophyll cell ultrastructure similar to that found in toxin-treated tissues. Chloroplasts remnants were the only identifiable organelles remaining in the mesophyll cells of leaves which have been detached for 24 hours (Fig 92 and 93) and the cell walls of these cells were invaginated due to dehydration (Fig. 92). The tonoplast, plastid envelope or plasma membranes were not discernable in cells from these tissues and no wall appositions were observed.

The chloroplast remnants were displaced from the periphery of the cell towards the interior; they occupied a larger proportion of the cell volume than chloroplasts in healthy and turgid control tissue, and they still seemed to be arranged in a ring-like pattern. This pattern of chloroplast arrangement suggests that plasmolysis, and not tonoplast disintegration which would likely have caused the chloroplasts to scatter more randomly, may have occurred in these cells. The chloroplasts had a relatively well-preserved internal thylakoid structure (Fig. 93) but had accumulated a large number of dense-staining globules. Also, these chloroplasts lacked the large starch granules found in collapsed toxin-treated cells.

Figure 86. Transmission electron micrograph of transverse section of toxin-infiltrated leaf exposed to the humid environment showing a disrupted mesophyll cell. Note: The nucleoplasm is lightly stained, the chloroplasts are scattered, and the protoplasm appears diluted. Post-fixed with osmium and potassium ferrocyanide. Cultivar Glenlea, 24 h, p.i., bull's eye. Bar = 2 µm.

Figure 87. Transmission electron micrograph of transverse section of toxin-infiltrated leaf exposed to the humid environment showing a portion of a disrupted mesophyll cell. Note: The plasma membrane, the thylakoid membranes and the mitochondrion appear relatively intact whereas the tonoplast appears loose and is broken (arrow). Post-fixed with osmium and potassium ferrocyanide. Cultivar Glenlea, 24 h, p.i., bull's eye. Bar = 1 µm.

Figure 88. Transmission electron micrograph of transverse section of toxin-infiltrated leaf exposed to a humid environment showing disrupted and healthy mesophyll cells. Post-fixed with potassium ferrocyanide and osmium. Cultivar Glenlea, 24 h, p.i., bull's eye. Bar = 5 µm.

Figure 89. Transmission electron micrograph of transverse section of toxin-infiltrated leaf exposed to the humid environment showing a magnification of the junction between a disrupted and a healthy mesophyll cell. Note: The plasma membrane is visible in both cells but the tonoplast seems to have disappeared in the disrupted cell. Post-fixed with osmium and potassium ferrocyanide. Cultivar Glenlea, 24 h, p.i., bull's eye. Bar = 1 µm.

Figure 90. Transmission electron micrograph of transverse section of toxin-infiltrated leaf exposed to the humid environment showing a disrupted mesophyll cell with degraded chloroplasts and nucleus. Post-fixed with osmium and potassium ferrocyanide. Cultivar Glenlea, 24 h, p.i., bull's eye. Bar = 4 µm.

Figure 91. Transmission electron micrograph of transverse section of toxin-infiltrated leaf exposed to the humid environment showing a disrupted mesophyll cell with degraded chloroplasts. Post-fixed with osmium and potassium ferrocyanide. Cultivar Glenlea, 48 h, p.i., bull's eye. Bar = 2 µm.

ch - chloroplast, cr - chloroplast remnant, cw - cell wall, dM - disrupted mesophyll cell, dp - diluted protoplasm, M - mesophyll cell, mi - mitochondrion, nr - nucleus remnant, pd - plasmodesmata, pm - plasma membrane, to - tonoplast, wa - wall apposition. (p.i. - post-infiltration)

ch
to
to
mi
86
87
88
89
90
91
dM
pd
M

It should be noted that the reduced contrast observed in the micrographs of both the dehydrated and plasmolyzed tissues is likely due to the different fixation system employed to process these particular samples which did not preserve and stain membranes well.

Freeze treatment. The freeze treatment resulted in cells which resembled collapsed toxin-treated cells (Figs. 94 and 95). The walls of these cells were very severely deformed and the cells were completely collapsed. There was no remnant of a vacuolar space as the entire cell contents stained very densely. As with all the other treatments so far described, the only structure which could be detected in these degraded cells were the thylakoid stacks. Unlike the collapsed cells from toxin-treated tissue, the collapsed cells of the freeze-treatment did not accumulate any starch granules.

Plasmolysis treatment. The plasmolysis at time of fixation treatment did not cause any significant disruption to cellular ultrastructure (Figs. 96 and 97). The plasma membrane withdrew from the cell wall but organelles did not appear to incur any ultrastructural damage. Chloroplasts, mitochondria and nuclei, although somewhat compressed, were not disorganized by this treatment.

Figure 92. Transmission electron micrograph of transverse section of wheat leaf removed from plant for 24 hours and allowed to desiccate. Note: Cell walls are deformed at the bottom right hand corner and the chloroplasts are the only discernable remnants of cellular ultrastructure. Post-fixed with osmium. Cultivar Glenlea. Bar = 4 µm.

Figure 93. Transmission electron micrograph of transverse section of wheat leaf removed from plant and desiccated for 24 hours showing chloroplasts which have retained thylakoid stacks. Post-fixed with osmium. Cultivar Glenlea. Bar = 1 µm.

Figure 94. Transmission electron micrograph of transverse section of wheat leaf frozen at -20°C and returned to the growth chamber for 48 hours. Note: Cell walls are severely deformed and the cell contents stain densely. Post-fixed with osmium and potassium ferracyanide. Cultivar Erik. Bar = 4 µm.

Figure 95. Transmission electron micrograph of transverse section of wheat leaf frozen at -20°C and returned to the growth chamber for 48 hours showing thylakoids and dense-staining cell contents. Post-fixed with osmium and potassium ferracyanide. Cultivar Erik. Bar = 1 µm.

Figure 96. Transmission electron micrograph of transverse section of wheat leaf plasmolyzed with 2M NaCl at the time of fixation. Note: The cytoplasm has pulled away from the cell wall but internal organization has been preserved. Post-fixed with osmium. Cultivar Glenlea. Bar = 5 µm.

Figure 97. Transmission electron micrograph of transverse section of wheat leaf plasmolyzed with 2M NaCl at the time of fixation showing preserved nucleus, mitochondria, and chloroplasts. Post-fixed with osmium. Cultivar Glenlea. Bar = 0.5 µm.

ch - chloroplast, cr - chloroplast remnant, cw - cell wall, dp - dense staining cell contents, E - epidermal cell, M - mesophyll cell, mi - mitochondrion, nu - nucleus, ts - thylakoid stack, v - vacuole

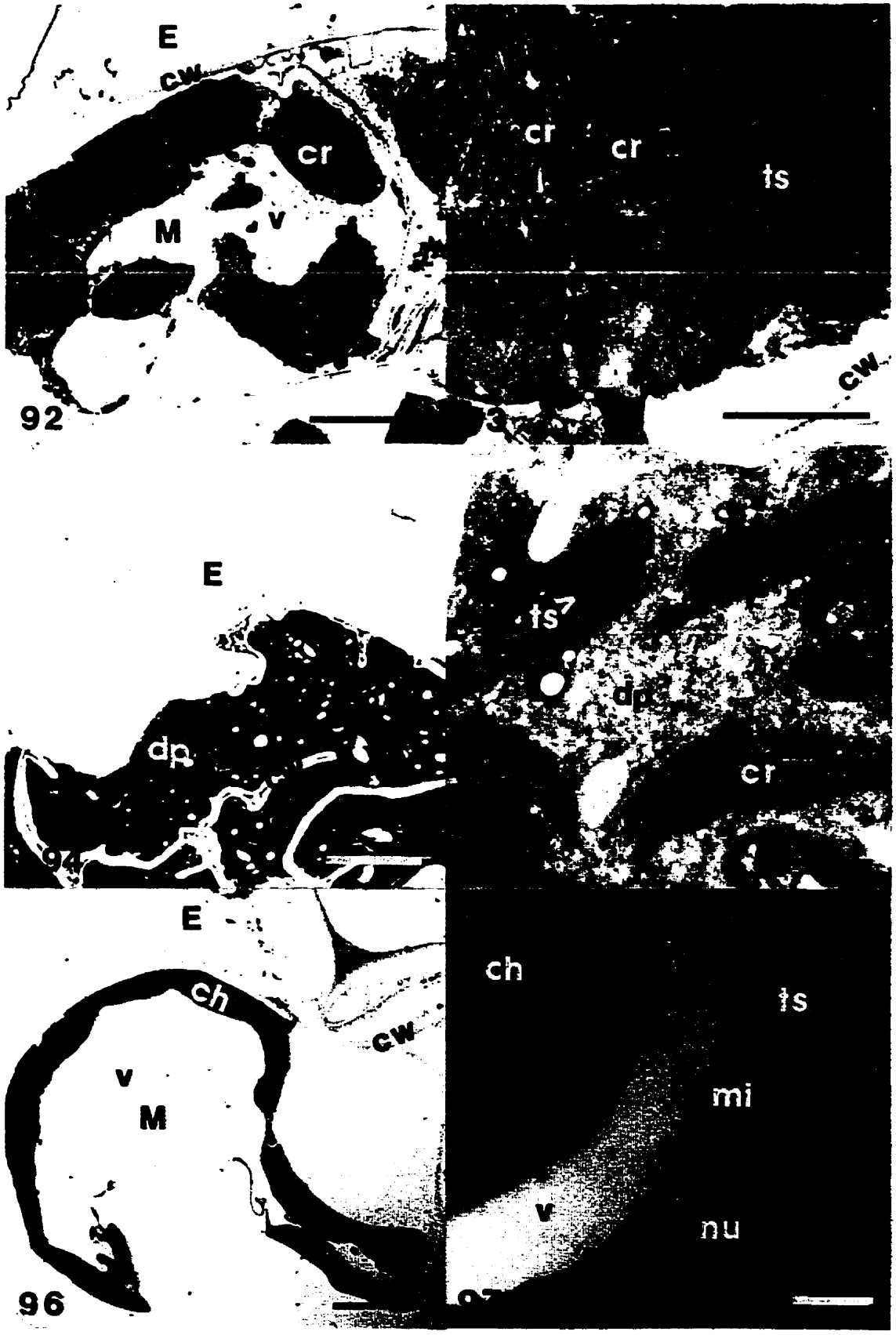
E
cw
cr
M
v
92
cr
cr
ts
cw
E
ts
dp
dp
cr
94
E
ch
cw
v
M
96
ch
ts
mi
v
nu

DISCUSSION

Tan necrosis development and toxin movement in leaf tissues and cells

Following infiltration of low concentrations of PtrToxA into sensitive wheat leaf tissue, necrotic lesions expand outwardly from the centre of the infiltrated region over time. This indicates that the tissues further away from the bull's eye or centre of the infiltration zone react more slowly to the infiltrated toxin. The delayed reaction could be due to the reduced toxin concentration to which the cells away from the bull's eye region are exposed. A gradient in toxin concentration would likely be created during the infiltration process as toxin is filtered or trapped in the sieve-like cell walls. Therefore, cells closest to the bull's eye would be exposed to higher toxin concentrations than cells on the edges of the infiltration region, and these cells would succumb more rapidly to the effects of toxin activity.

The development of toxin symptoms in the upper mesophyll reflects the ease with which the toxin solution flows in this part of the mesophyll. The upper mesophyll is more permeable than the lower because it contains larger intercellular spaces and channels. Therefore, during the infiltration process, the toxin solution will preferentially flow in the upper mesophyll. This would probably expose the upper mesophyll to a higher toxin concentration and lead to earlier symptom development in this region.

PtrToxA, which has presumably been trapped in the cell walls of the apoplasm, would have to diffuse across the cell wall to reach the surface of the plasma membrane. However, unlike most host-specific toxins which are relatively small molecules, PtrToxA diffusion would be impeded by the structure of the cell wall. Using a solute exclusion technique, Carpita *et al.* (1979) found that cell wall pores would allow proteins of about 17 kDa to pass freely. Considering that 17 kDa is the cut-off, that PtrToxA has a molecular weight of 14 kDa, and that the toxin may have an affinity to bind electrostatically to plant cell walls, the movement of the toxin across the cell wall may be slowed. Due to the activity of the plasma membrane H^+-ATPase, the cell wall pH is often between 5.0 and 5.5 (Salisbury and

Ross, 1992), which is in the pH range used to bind PtrToxA to CM-cellulose during cation exchange chromatography in the toxin purification process (Ballance *et al.*, 1989). Therefore, positively charged PtrToxA molecules could bind to the galacturonic acids of plant cell wall pectins, which would be dissociated at physiological pH and therefore negatively charged, and hamper their movement towards the plasma membrane.

The movement of PtrToxA from the mesophyll apoplasm into the vascular bundles would be further impeded by the mestome sheath suberized lamella (O'Brien and Kuo, 1975). Like Casparian strips in roots, suberized mestome sheath walls act as barriers to the diffusion of solutes into the vascular bundle and therefore require that sugars be imported into the vascular bundle via the symplasm (O'Brien and Kuo, 1975). Since PtrToxA is much larger than the sugars which are purportedly blocked by the mestome sheath walls, its diffusion into the vascular tissues would be prevented. Therefore, bundle tissues may not be toxin-insensitive but may simply not have been exposed to any significant concentration of toxin.

Once the toxin has reached the surface of the plasma membrane there are two possible means by which is can affect the toxin-sensitive plant cells. The first means is based on the hypothesis that there are toxin-receptors on the surface of toxin-sensitive cells which bind the toxin and that the binding of the toxin to these putative plasma membrane receptors somehow leads to cell death.

On the other hand if the molecule with which the toxin must interact is within the cell, the toxin must somehow cross the plasma membrane. However, only small uncharged molecules such as water can pass through the plasma membrane and pumps and channels are used to shuttle mineral ions. PtrToxA entry into wheat cells would likely therefore involve endocytosis as is the case for a number of protein toxins in animal cells (Olsnes and Sandvig, 1985). Endocytosis involves the formation of vesicles from the plasma membrane. This process is a component of vesicular transport mechanism involving the endoplasmic reticulum, Golgi apparatus and the vacuole. Endocytosis recovers membrane material, assists in the processing of proteins, and imports ligands which have bound to their specific

surface membrane receptors. Vesicles which are formed by endocytosis will contain a certain amount of extracellular fluid which could include molecules of PtrToxA. Interestingly, many endocytosed vesicles are directed to the vacuole which is an important component of the endomembrane system and which seems to be one of the structures affected in the early stages of toxin activity.

The relatively slow reaction of sensitive wheat tissues to PtrToxA compared to that of other toxins might be explained by the long and tortuous path it must follow. The earliest documented reaction to PtrToxA is electrolyte leakage which is seen only after about 10 hours of toxin exposure (Kwon *et al.*, 1996). Victorin causes electrolyte leakage within 20 to 30 minutes (Keck and Hodges, 1973). Victorin is a small peptide with an unusual cyclic structure and a size equivalent to six amino acids (Wolpert, *et al.*, 1988) and can therefore diffuse more easily in the cell wall and may also cross the plasma membrane more readily. PtrToxA is composed of about 126 amino acids (Ballance *et al.*, 1989) and would slowly diffuse through the wall. Also, if PtrToxA enters via endocytosis, and this is a random and infrequent event, it may take a long time before the toxin penetrates the cell and begins to have its effect.

PtrToxA effect on water relations

One of the conspicuous results of PtrToxA activity is the drying or desiccation of wheat leaf tissue. Also, even though exposure of toxin-treated wheat leaves to a humid environment does not prevent cell death, it does prevent cell collapse and alters the appearance of the toxin-induced necrotic symptoms. Therefore, toxin-activity seems to alter the ability of leaf tissue, particularly in mesophyll and epidermal cells, to control the movement of water.

The simplest hypothesis for water related toxin-activity consists of specific targeting of epidermal cells by PtrToxA and the disruption of the cuticular layer which serves as a barrier to water loss from the interior of the leaf. There are two ways this could occur. Firstly, toxin activity could cause epidermal cells to collapse and this cellular deformation might sufficiently strain the cuticle to create highly

water-conductive fissures. Secondly, toxin activity could cause lysis of the plasmalemma of epidermal cells and the accompanying release of enzymes could potentially digest the waxy cuticle and increase the rate of water loss.

Experiments conducted by Deshpande (1993) support the theory of tissue-specific activity of PtrToxA. In these experiments, undifferentiated callus tissue of a toxin-sensitive wheat cultivar, was unaffected by PtrToxA containing media. The microscopic observations described herein also indicated that epidermal cells sometimes collapsed before the underlying mesophyll was affected.

However, there are a number of facts which do not support this hypothesis. Firstly, the epidermis was not always the first tissue to collapse due to toxin activity. Also, damage to the cuticular layer would likely have resulted in an organized pattern of desiccation inside the leaf. However, collapsed or disrupted mesophyll cells were often relatively randomly interspersed with healthy ones. The fluorescence staining with PAS and calcofluor which did not indicate any degradation, failure or severe deformation of collapsed epidermal exterior cell walls, implies that the cuticular barrier was not significantly compromised. Finally, and most importantly, exposure of the toxin-treated leaves to the high humidity environment, which would have significantly reduced the water loss through the potentially damaged cuticle, did not prevent the development of symptoms nor the disruption of mesophyll cells.

A similar hypothesis would involve the disruption of stomatal aperture allowing uncontrolled water vapor loss. Although it is not possible to comment specifically on the stomatal function, the apparent preservation of stomatal guard cells, even when the remainder of the tissue has completely collapsed, strongly suggests that these cells are operational long after the first toxin has had its primary effects. Also, the thickness of the cell walls surrounding stomatal guard cells would likely seriously impede the diffusion of PtrToxA and therefore prevent any interaction of toxin with the cell.

The first two hypotheses with respect to toxin effect on leaf water relations considered increased water loss as the cause of mesophyll cell collapse. However,

a third hypothesis suggests that water supply to mesophyll and epidermal tissue is reduced by a restriction in the transfer of water from the vascular bundle. This hypothesis again supports the tissue specificity of toxin activity suggested by Deshpande's (1993) experiments. The toxin does seem to affect the parenchymous cells of the outer bundle sheath which surround the vascular bundle. In studies of water pathways, Canny (1986), found that water in the transpiration stream of wheat moved from the xylem into the mestome (inner bundle) sheath cells and then symplastically across the suberized mestome sheath walls into the outer bundle sheath cells via plasmodesmata. Therefore, if the bundle sheath cells were affected first by toxin activity, especially if the plasmodesmata connecting mestome and outer bundle sheath cells were blocked by wall appositions in the mestome sheath cells, water movement out of the bundle and into the surrounding mesophyll might be severely impeded. This in turn could lead to the collapse of mesophyll and epidermal cells but would allow the vascular bundle to function and continue to deliver water and nutrients to regions of the tissue unaffected by the toxin.

However, this third hypothesis regarding the toxin sensitivity of the outer bundle sheath unfortunately is also not without its weaknesses. For example although the experiments conducted by Canny (1990) predicted that most of the transpiration water moved symplastically, they also indicated that the suberized lamella of the mestome sheath were not completely impervious to water and solutes. This means that interruption of symplastic water movement could be at least partially replaced by apoplastic movement of water. Also, outer bundle sheath cells did not usually appear to be damaged before the cells in the surrounding mesophyll or epidermal tissue. Most importantly, if the movement of water from the vascular bundle into toxin-treated leaf regions was impeded by toxin-damaged outer bundle sheath cells, a reduction in overall leaf transpiration would be expected. However, a preliminary transpiration experiment indicated that toxin-treated tissues had an increased rate of transpiration (personal observation) compared with water-infiltrated tissues.

All of the above three hypotheses suggest that the toxin effect on specific

cells; epidermal cells, stomatal guard cells, and outer bundle sheath cells, disrupts water relations in the leaf and indirectly leads to the collapse of mesophyll cells of toxin-treated leaves. This indirect disruption of water relations was also examined in detached wheat leaves allowed to desiccate in the same environmental conditions to which toxin-treated leaves are exposed. In other words, tissues of the detached wheat leaves did not receive any water via the transpiration stream. However, even after 24 hours of this desiccation treatment none of the mesophyll cells appeared as collapsed and damaged as some of those from toxin-sensitive leaves exposed to toxin for the same period of time. The desiccated mesophyll cells were shrunken but still seemed to contain remnants of a central vacuolar region delineated by chloroplasts distributed on the inside of the cell wall which was only slightly deformed. In contrast the contents of severely collapsed toxin-treated cells was very densely staining, showed no signs of any remaining vacuolar region, and had very deformed cell walls. Therefore, comparison of the detached-leaf-desiccation treatment with the PtrToxA treatment suggests that disruption of water movement external to mesophyll cells does not explain the effect of PtrToxA toxin activity in sensitive wheat leaf tissue.

One of the most plausible hypotheses regarding the effect of toxin activity on water relations suggests that the toxin disrupts the tonoplast. This hypothesis is supported by the observation that tonoplast failure was an early symptom of toxin activity.

The vacuole is an important component of the osmoregulatory system of plant cells, not simply because of the large volume it occupies, but because it is used to sequester ions, metabolites, and allelochemicals which generate a significant amount of osmotic pressure (Wink, 1993). Also, the vacuole is important in regulating the cytoplasmic pH (Boller and Wiemken, 1986) which is also critical for osmoregulation because the movement of many solutes, like sucrose and potassium ions, depends on the electrochemical gradient generated by proton pumps located both in the plasma membrane and in the tonoplast (Palmgren, 1991). The vacuole has a higher pH and often a higher concentration of ions,

sugars, and acids than the cytoplasm. Therefore, failure of the tonoplast would increase the cytoplasmic pH and release a number of solutes into the cytoplasm and this would not only interfere with the activity of a number of enzymes but also disrupt the functioning of pumps and carriers located at the plasma membrane.

Consequently, this imbalance would permit the diffusion of a large number of solutes out from the cytoplasm into the intercellular space, followed by the loss of cytoplasmic water. The cell would then collapse leaving only high molecular weight compounds and polymers, which could not diffuse out, inside the cell. This is a relatively accurate description of the appearance of severely collapsed mesophyll cells of toxin-treated sensitive wheat leaf tissue.

Membranes were also damaged in the freeze-thaw treatment conducted with Erik wheat plants. The freezing of Erik plants likely resulted in the formation of extracellular ice which drew most of the water out of the cells. The presence of water in the apoplasm was evident when the leaves thawed because the leaves were flaccid and looked as if they had just been infiltrated with water. The dehydration of the cell interior and the formation of large ice crystals outside the cell would also have severely damaged the cell's membranes. Therefore, upon thawing, cells of frozen tissue will not have been able to re-absorb the intercellular water, and this resulted in the collapsed and desiccated appearance of that tissue. The similarity between collapsed toxin-treated Glenlea and frozen-thawed Erik cells further implies that membrane disruption leading to uncontrolled water loss is an important effect of PtrToxA. Note that although two different wheat cultivars are being compared, it is unlikely that there would have been a cultivar-specific reaction to the drastic freeze-thaw treatment used in this experiment.

Toxin activity and the cell wall

A conspicuous effect of toxin activity is the deformation or collapse of cell walls especially in the late stages of necroses development. This symptom, evident at the microscopic level, suggests some interaction, direct or indirect, of PtrToxA and the cell wall of sensitive wheat tissue. In the following discussion a number of hypotheses regarding this possible interaction will be presented.

In the previous sections it was suggested that the toxin could reach the surface of the plasma membrane in order to interact with a molecule there or somewhere inside the cytoplasm. However, there is evidence that a fungal metabolite can be trapped in the cell wall and still be able to have an effect on the plant cell. Shiraishi *et al.* (1998) suggested that a glycopeptide produced by *Mycospharella pinoides* (molecular weight >70 kDa) was not able to migrate through the cell wall to the surface of the plasma membrane of pea cells yet was still able to elicit a defense reaction in these cells. Shiraishi *et al.* (1998) cite a number of cell wall-bound proteins which elicitor signal molecules could activate leading to a defense response. Therefore, it is possible that the toxin, because of its size and charge, cannot migrate through the cell wall, but can still cause sensitive wheat cells to die by interacting with wall-bound enzymes (Varner and Lin, 1989).

Regardless of where toxin first interacts with sensitive wheat leaf cells, the collapsed appearance of toxin-treated leaf mesophyll and epidermal cells suggests that there is an induction of cell wall degradation by PtrToxA. It is proposed that the following conditions would need to be satisfied for the toxin-induced cell collapse to occur. Firstly, the cell walls, which are capable of holding turgor pressure many times larger than atmospheric pressure, would presumably have lost some structural integrity. Additionally, the cell would have to experience negative turgor pressure in order to pull the walls into the cell's interior and the cell wall would have to be tightly bound to the surface of the plasma membrane. Theoretically, negative turgor pressure could only occur if the combination of osmotic and matric potentials outside the cell were lower than the osmotic pressure inside the cell. The above stated conditions were indirectly examined using the freeze-thaw, desiccation and plasmolysis treatments.

In the freeze-thaw treatment ice formed intercellularly and membranes were damaged. This caused water to be removed from the cell and potentially released hydrolytic enzymes in the intercellular spaces which could have weakened the cell wall. In these tissues, the cells were completely collapsed, the walls were severely deformed, and the cell contents stained very densely. Therefore, the freeze-thaw

treatment created a cellular environment which satisfied all the above-stated conditions required for cell collapse.

In the desiccation treatment, water was gradually removed from the tissue and cells because the supply of water from the transpiration stream was cut-off. However, it does not appear, at least in the early stages of desiccation, that cellular compartmentalization was lost. The mesophyll cells of these tissues were somewhat collapsed, but their cell walls were not as severely deformed as those of collapsed toxin-treated or freeze-thawed leaves. Therefore, water potential outside the cells of desiccated tissue caused the cells to shrink but their cell walls were probably not being degraded by enzymes released from inside the cell.

Finally, in the plasmolysis treatment, the cells were exposed to a very low osmotic potential in the intercellular spaces for a brief moment as fixation was taking place. Consequently, there was not enough time for the walls of these cells to be degraded. The osmolarity of the fixative solution caused the plasma membrane to pull away from the wall as the cytoplasm contracted, but the cell walls were not significantly distorted. In summary, the so-called comparison treatments seemed to support the above-proposed conditions required for cell collapse, namely that wall stiffness was reduced and water was drawn out of the cell.

The importance of wall collapse or degradation has been proposed as a primary or significant event in plant cell death in a number of situations. For example, many plant pathogens are known to secrete hydrolytic enzymes which attack plant cell walls (Bateman, 1976) and the activity of these enzymes often seems to lead to plant cell death. For example, Bucheli *et al.* (1990) found that heat-labile factors, probably proteins, secreted by the rice pathogen *Magnaporthe grisea* solubilizes fragments from maize cell walls which kill maize cells. This cell death could be a type of defense response elicited by the oligosaccharides released by enzyme activity (Walton, 1994). Alternatively, Basham and Bateman (1975) showed that pectic enzymes could kill tobacco cells, not via the wall fragments generated, but possibly through the weakened cell wall unable to support the plasma membrane.

Alteration of wall structure and strength can also occur as part of normal plant development. McQueen-Mason and Cosgrove (1994) described the weakening of hydrogen bonding between cellulose fibrils by expansin proteins which are present in the cell wall. These proteins can putatively control the ability of cells to expand by loosening wall structure. Another example of wall modification involves the induction of endogenous cell wall degrading enzymes by heat in the process of fruit softening (Okolie and Obasi, 1992). However, unlike the above two processes, wall degradation induced by leaf-abscission leads to or is very closely associated with plant cell death. Cellulase expression is induced by ethylene, a plant growth regulator which promotes abscission and fruit ripening (Tucker *et al.*, 1991, and Ferrarese *et al.*, 1995) and cell wall degradation seems to precede cell death in ethylene-induced abscission of geranium petals.

Wall collapse has also been described as an important event in viral infection and in plant cells exposed to fungal metabolites. Kofalvi *et al.* (1995), examined the wall collapse of wheat cells in response to wheat streak mosaic virus infection and their findings indicated the induction of an endoxylanase, a potential corresponding decrease in cross-linking of phenolics to cell wall polymers, and an altered ion content of cell walls which might indirectly weaken them. The folding of geranium root cell walls in response to *Pythium ultimum* fungal filtrates was examined by Desilets *et al.* (1994). Their experiments did not indicate that the wall folding was due to hydrolysis of cellulose or pectin. They agreed with Hanchey's (1981) interpretation of cell wall collapse in toxin treated plant tissues as reflecting a change in wall plasticity or as a result of tissue desiccation but not due to wall degradation as such.

In summary, there is support for the hypothesis that PtrToxA has an early effect on cell wall integrity which could in turn lead to cell death. PtrToxA causes mesophyll and epidermal cells to collapse. PtrToxA may be trapped in the cell wall and have its primary effect there or it may reach the plasma membrane of cytoplasm and trigger processes in the cell wall. Damage to the cell wall has been documented as a significant event preceding or coinciding with cell death.

Hydrolysis of cell walls could decrease the osmotic potential of the intercellular space by releasing a large number of solutes and thereby creating a water potential gradient which would pull water from the cell and cause it to collapse. Polysaccharides released by degradation of the plant cell wall can be a nutritional source for the invading Ptr hyphae. Also, it would be more efficient for the fungus to utilize the plant's endogenous enzymes to release these compounds than to synthesize and export its own hydrolytic enzymes.

In spite of the above evidence suggesting that PtrToxA causes cell death via the cell wall, there are some problems with this theory. Firstly, the PAS and calcofluor staining did not indicate any significant degradation of polysaccharides containing vicinal glycol groups or 1,4-β-linkages respectively. It may be that these two staining techniques were not sensitive to changes in these cell wall polymers or that the changes occurred in other materials present in the cell wall such as lignin, proteins, or even ionic content. Secondly, the collapse of toxin-treated cells is a late event in the symptom development of necrotic lesions. By the time the cells have collapsed, enzymes may have been released by a damaged plasma membrane and water may have been lost from the cell as a consequence of toxin-activity elsewhere in the cell. Additionally, cells which show early symptoms of toxin activity have disrupted contents but do not seem to have damaged walls. Also, it is difficult to imagine that hydrolytic cleavage of cell wall polymers could release enough solutes in the intercellular space leading to a withdrawal of water from the cell's interior because these compounds are generally difficult to digest. Finally, cell collapse has been documented in tissues which have been drought-stressed (Pearce and Beckett, 1987) or exposed to hyperosmotic solutions (Oertli, 1986) but which would not likely have been exposed to any hydrolytic enzymic activity detrimental to wall integrity.

Catabolism of cytoplasm

In this section the degradation or preservation pattern of cytoplasmic ultrastructure is discussed as it may suggest a primary site of action of PtrToxA.

Surprisingly, in all treatments, including PtrToxA infiltration, freeze-thaw,

plasmolysis and desiccation, the thylakoid membranal system was relatively resistant to degradation. This is somewhat contrary to the observations of Freeman *et al.* (1995) which showed that chloroplasts had swollen grana 4 hours after PtrToxA infiltration. The compact organization of thylakoid stacks may have prevented access to these structures by catabolic enzymes in disrupted cells. Also, the double membrane plastid envelope may provide an additional barrier to penetration of the chloroplast by hydrolytic enzymes and may allow the chloroplast to maintain control of the stroma despite disruption in the surrounding cytoplasm. The accumulation of large starch granules in the chloroplasts of many toxin-treated cells indicates that chloroplast integrity was maintained long after the toxin had its first detrimental effects. The independent functioning of the chloroplast in disrupted cells is supported by the theory suggesting that chloroplasts originated as photosynthetic prokaryotes which became endosymbionts within larger cells (Margulis, 1993). This evolutionary theory is partially based on the ability of isolated chloroplasts to transcribe DNA into RNA and to synthesize proteins from amino acids (Hoober, 1984). In addition, isolated chloroplasts have the ability to fix CO_2 into starch (Batz *et al.*, 1995)

The starch accumulation in chloroplasts of toxin-treated tissues, especially in those of collapsed cells, is somewhat counterintuitive. PtrToxA seems to disrupt the ability of sensitive cells to prevent water loss which can be accomplished by solute accumulation and a consequent reduction in osmotic potential. The formation of starch granules would not only reduce the concentration of osmotically active molecules in the chloroplast but may also reduce it in the cytoplasm if precursors of starch synthesis are imported into the chloroplast. This potential change in osmotic potential could aggravate the cellular water loss. However, the opposite reaction has been documented for leaves of soybean (Cortes and Sinclair, 1987) and for leaves of cotton (Ackerson and Hebert, 1981) in response to water stress. It was suggested that the starch accumulation decreased the cellular osmotic volume thereby facilitating osmotic adjustment (Ackerson and Hebert, 1981).

Evidence of tonoplast breakdown as an early symptom of toxin activity was already discussed with respect to disrupted water relations in affected cells. The rupture of the tonoplast would not only have significantly altered the pH and ionic conditions of the cytoplasm, it would also have released a number of hydrolytic enzymes capable of catabolizing the cell contents. The accumulation of densely staining precipitate in the vacuoles of certain toxin-treated cells, particularly epidermal and outer bundle sheath cells, also indicates some disruption of the vacuolar contents may have been an early effect of toxin activity. The collapsed dense staining appearance of frozen-thawed cells, which were likely decompartmentalized by intercellular ice-formation, is similar to the appearance of toxin-treated cells. This similarity further suggests a similar decompartmentalization which occurred in toxin-treated cells due to tonoplast failure.

The effect of PtrToxA on the plasma membrane is more difficult to characterize. In cells where it appeared that the tonoplast had been ruptured, the plasma membrane did not seem to have been broken. In mesophyll cells which were completely collapsed, the density of staining in the cytoplasm made it difficult to discern the presence and condition of the plasma membrane. Kwon *et al.* (1996) developed the electrolyte leakage bioassay based on plasma membrane damage reported by Freeman *et al.* (1995). However, Freeman *et al.* (1995) indicated that chloroplasts were the first structures to be affected by PtrToxA and did not directly address the effect of the toxin on the plasma membrane. In one of their published micrographs the plasma membrane of a severely disrupted mesophyll cell appears slightly invaginated but unbroken. There are however, reasons to believe that the plasma membrane was damaged at some point by toxin activity.

The drastic changes which would have occurred in the cytoplasm following the proposed tonoplastic disruption could have damaged the plasma membrane from the inside. The electrolyte leakage which was detected by Kwon *et al.* (1996) after a few hours of toxin exposure is also suggestive of the failure of the plasma membrane function and possibly of its structure. The collapsed appearance of some of the toxin-treated cells implies that the plasma membrane was incapable of

retaining or regulating solute movement and therefore water loss. Again this is similar to the appearance of frozen-thawed cells which probably had ruptured plasma membranes. Hypothetically, if the plasma membrane fails, the wall becomes the selectively permeable membrane and it permits ions and small molecules such as simple sugars and amino acids but not large polymers and complex structures to diffuse out of the cell. This loss of osmotically active solutes would consequently cause a massive efflux of water. This would leave only dense staining substances like proteins and structures like thylakoid stacks in the collapsed cells. In addition, the dehydration of collapsed cells would likely prevent further degradation of the remaining contents because of the inactivation of hydrolytic enzymes.

It should be noted that once *Pyrenophora tritici-repentis* has penetrated the interior of the leaf that its growth is strictly intercellular (Dushnicky *et al.*, 1996, and Lamari and Bernier, 1989b). The continued growth of the fungus depends on a constant supply of nutrients from the leaf tissue, and since the cells are not penetrated, the nutrients must somehow be released. Toxin activity could be important in this regard by increasing the permeability of the mesophyll cell plasma membranes.

Wall appositions

Wall appositions, formed between the plasma membrane and cell wall of healthy-appearing mesophyll cells in regions immediately opposite to cells which have been collapsed or disrupted due to toxin activity, were observed quite frequently in TEM micrographs. The formation of these structures is not only an interesting, although surprising, reaction of cells which have been treated with PtrToxA, but also might provide some clues as to the activity of this toxin.

Papillae are a type of plant cell wall apposition which forms in response to physical and/or chemical stimuli of invading fungi (Aist, 1976). Another type of wall apposition is the wound plug and its formation can be incited by a number of treatments including pressure, cutting, insertion of microneedles, heat or chemicals. The formation of papillae has often been implicated as a plant disease resistance

mechanism (Sherwood and Vance, 1976, Ride and Pearce, 1979, and Bonhoff *et al.*, 1987) and it may prevent fungal ingress into the cell wall. In addition, papillae and wound plugs may prevent a loss of ions from damaged cells or the movement of enzymes of toxic molecules into them (Wheeler, 1974, and Ride, 1978).

Callose is assumed to be the common constituent of wall appositions (Aist, 1976), but the incorporation of other compounds is more variable. For example, Sherwood and Vance (1976) found papillae of reed canarygrass contained lignin, callose and cellulose but not pectin. On the other hand, while Benhamou and Lafontaine (1995) also found lignin and callose in wall appositions of tomatoes, they detected much less cellulose than pectin. Callose content of wall appositions observed in toxin-treated wheat tissues was confirmed by aniline blue staining. In electron micrographs, structures composed of 1,3-β-glucans, such as callose, should appear electron lucent or unstained (Škalamera and Heath, 1995). However, these wall appositions in TEM micrographs were not electron lucent but rather had a light- to dark-gray appearance. This suggests that these appositions also contained other materials, such as lignin. Lignin has been detected in the papilla of wheat (Ride and Pearce, 1979) and phenolic compounds and lignification were implicated in the thickening of cell walls in the defense reaction of wheat to Ptr infection (Dushnicky *et al.*, 1998). In addition, the cross-linking of lignin to callose in wall appositions is expected to create a more impervious composite with some fungicidal activity (Benhamou and Lafontaine, 1995).

Callose is usually only deposited in response to stress, wounding, or pathogenesis in plants (Ohana *et al.*, 1993). Therefore, there are some specific signals which trigger callose synthesis and its corresponding deposition in wall appositions. Experiments by Foissner (1990) suggest that wall appositions formation is induced in characeaen algal cells by a cytoplasmic influx of calcium ions. Calcium induction of callose synthesis by the plasma membrane bound 1,3-β-glucan synthase has been well documented (Kauss, 1987). It has been proposed that elicitors, such as chitosan, can disrupt the plasma membrane, and thereby allow leakage of electrolytes such as K^+, depolarize the plasma membrane, and

most significantly permit an influx of Ca^{2+} from the apoplasm.

However, toxin-treated tissues have not been invaded by fungi and therefore should not contain any fungal derived elicitors to disrupt the membrane, cause an influx of calcium and thus induce callose deposition. Therefore, if callose deposition was elicited by a compound from outside the cell, it must have been of plant origin. Mathieu *et al.* (1991) found that oligogalacturonides, which are short segments of polygalacturonic acid likely the result of pectin degradation, could depolarize the plasma membrane, acidify the cytoplasm and cause an influx of Ca^{2+}. Hence, the deposition of callose-containing wall appositions in cells neighbouring toxin-collapsed cells supports the previously stated hypothesis for cell wall degradation induced by PtrToxA activity.

An alternative explanation for callose synthesis involves a reported activator of callose synthase, β-furfuryl-β-glucoside (FG) (Ohana *et al.*, 1991) which is located in the vacuole (Ohana *et al.*, 1993). It was shown that lowering of cytoplasmic pH redistributed FG from the vacuole to the cytoplasm and that this redistribution was accompanied by an elicitation of callose synthesis. Tonoplast damage, which was suggested as a result of toxin activity, would create the conditions usually associated with induction of callose synthesis. As mentioned earlier, tonoplast rupture would decrease cytoplasmic pH, release Ca^{2+}, which is one of the ions sequestered in the vacuole, and release FG, an activator of callose synthase.

However, callose was not usually observed in the collapsed or severely disrupted cells, but in their relatively healthy neighbours. The frequent observation of plasmodesmata between collapsed and healthy cells of toxin-treated tissue where wall appositions were formed suggests that cell-to-cell communication may be involved in the deposition of callose. Plasmodesmata, which form a bridge of cytoplasm and endoplasmic reticulum across cell walls, allow relatively free flow of ions, exchange of metabolites and small molecules with a molecular weight less than 850-900 Da (Lucas *et al.*, 1993). Plasmodesmata also appear to be able to traffic plant viruses and endogenously synthesized proteins. Interestingly, 1,3-β-glucan synthase is involved in the regulation of size exclusion limit of

plasmodesmata.

The following hypothesis is therefore proposed to explain the deposition of callose-containing wall appositions. PtrToxA disrupts the tonoplast of a sensitive wheat cell and protons, Ca^{2+} and FG are released into the cytoplasm. These substances can freely diffuse into the neighbouring cell, which has not yet been affected by the toxin, via the plasmodesmata. These signals trigger the synthesis of callose in the unaffected cells and cause the formation of the wall appositions. These wall appositions not only prevent the movement of harmful substances across the cell wall but also seal off the cytoplasmic connection thereby preventing the diffusion of any other potentially damaging substances from the moribund cell, possibly including the toxin itself.

Callose deposition by cells of toxin-treated plant tissues has previously been reported in two other cases. Walton and Earle (1985) observed that susceptible, but not resistant, oat protoplasts formed a callose-containing amorphous extracellular wall material in response to the host-specific toxin victorin. No connection was found between extracellular polysaccharide synthesis and calcium, which is usually an important regulator of this process. It should however be noted that protoplast viability required a minimum concentration of 1 mM $CaCl_2$ and this limited the types of experiments that could be conducted to examine the effect of calcium on wall deposition. Wall deposition was observed within 1 hour of toxin treatment and was prevented by inhibitors of protein and RNA synthesis provided to the cells 12 hours prior to the toxin.

Synthesis of callose-containing extracellular wall material was also described in Japanese pear leaves treated with AK-toxin (Park, 1998). These studies, as was described earlier, indicated ion-leakage from the plasma membranes at the plasmodesmata in response to the toxin and this is where deposition of carbohydrates was observed. Anti-1,3-β-glucan monoclonal antibody indicated a positive reaction at the wall appositions, at the plasma membrane and in the Golgi apparatus. It was suggested that AK-toxin disrupted the plasma membrane, induced hyperfunction of exocytosis to the regions of membrane disruption, and

caused Golgi synthesized glucan to be deposited at the plasmodesmata prior to cell death. The involvement of Golgi apparatus in callose deposition is not supported by the experiments of Škalamera and Heath (1996) which showed that inhibitors of Golgi-associated vesicle transfer did not reduce callose deposition in response to fungal infection. Kauss (1996) suggests that there is much more evidence to support plasma membrane-localized callose synthesis than there is for the Golgi apparatus.

In the cases of victorin and AK-toxin it appeared that wall deposition was a direct result of toxin activity. However, the results of this experiment with PtrToxA suggest that wall appositions are a protective reaction in response to the toxin-induced death of neighbouring cells and not a direct effect of the toxin. This could be viewed as an indication that toxin activity does not impair the ability of cells to defend themselves against fungal invasion. Conversely, it could be argued that the toxin had not yet affected the cells which reacted by forming the wall apposition.

CONCLUSIONS

PtrToxA caused the disruption and collapse of the mesophyll, outer bundle sheath, and epidermal cells. It did not seem to affect the cells within the vascular bundle, including the inner bundle sheath, or the stomatal guard cells. It is proposed that the thicker walls of the mestome sheath and stomatal guard cells prevented the toxin from reaching the cell surface and thereby protected these cells from toxin activity.

PtrToxA may have a primary effect on the tonoplast. Some cells, apparently in the early stages of toxin-induced disruption, had relatively intact organelles distributed throughout their volume indicating that the tonoplast was no longer confining them to perimeter of the cell. These cells also still seemed to have an intact plasma membrane. PtrToxA disrupted the water relations of plant cells and the vacuole is an important component of the osmoregulatory system. The delayed reaction of sensitive wheat leaf cells to toxin activity and the large size of PtrToxA compared to other host-selective toxins suggested a convoluted path followed by the toxin to its site of activity. This path could consist of endocytosis of the toxin into a vesicle followed by the incorporation of this toxin-containing vesicle into the vacuole where it could have its initial detrimental effect. The vacuolar destination for the endocytosed vesicle is probable since the vacuole is a component of the endomembrane system to which vesicles are often directed.

Mesophyll cells in the late stages of toxin-induced necrosis were severely collapsed and had densely staining cytoplasm similar in appearance to cells subjected to the freeze-thaw treatment. PAS and calcofluor staining of the walls of these cells did not indicate a significant loss of polysaccharides containing vicinal glycols or cellulose respectively. It therefore does not appear that the toxin had any detrimental effect on the structure of cell walls which would have lead to death of these cells. There were large starch granules interspersed within the thylakoid remnants of these collapsed cells. This suggests that the chloroplasts were not the primary sites of PtrToxA activity.

Wall appositions were deposited between the plasma membrane and cell

wall of healthy-appearing cells in regions opposite cells which had been damaged by toxin activity. These wall appositions reacted positively with aniline blue indicating the presence of callose. Many of these appositions occurred in the vicinity of plasmodesmata connecting the healthy and toxin-affected cells and they seemed to act as a seal between these cells. These observations lead to a hypothesis further involving PtrToxA-induced tonoplast damage. It was proposed that the tonoplast of the affected cell was damaged by the PtrToxA activity and that this released substances which activate callose synthesis into the cytoplasm. These elicitor substances diffused into the healthy-appearing cell via the plasmodesmata and initiated callose deposition at the surface of its plasma membrane.

Immunogold labelling is a microscopic technique which could verify the validity of the hypothesis suggesting that the tonoplast is the site of action for PtrToxA. It could also show whether or not PtrToxA is able to diffuse across the cell walls of guard cells or of the mestome sheath. If the tonoplast hypothesis is valid, labelling should be observed in vesicles and in the vacuole. However, it is possible that the toxin binds to a receptor on the surface of the plasma membrane and triggers a signal inside the cell.

Finally, the effect of PtrToxA on isolated tonoplast from wheat cells might also provide some valuable insight. For example PtrToxA might alter the permeability of the tonoplast to protons and thereby disrupt the electrochemical potential across this membrane.

LITERATURE CITED

Abbas, H.K., Duke, S.O., and Paul, R.N. 1995. AAL-toxin, a potent natural herbicide which disrupts sphingolipid metabolism of plants. Pestic. Sci. 43:181-187.

Ackerson, R.C., and Hebert, R.R. 1981. Osmoregulation in cotton in response to water stress. Plant Physiol. 67:484-488.

Adee, E. A., and Pfender, W. F. 1989. The effect of primary inoculum level of *Pyrenophora tritici-repentis* on tan spot epidemic development in wheat. Phytopathology 79:873-877.

Aist, J.R. 1976. Papillae and related wound plugs of plant cells. Ann. Rev. Phytopathol. 14:145-163.

Akimatsu, K., Kohmoto, K., Otani, H., and Nishimura, S. 1989. Host-specific effects of toxin from the rough lemon pathotype of *Alternaria alternata* on mitochondria. Plant Physiol. 89:925-931.

Alexandratos, N. 1995. World Food and Agriculture: a 20-Year Perspective. In: World Agriculture: Towards 2010 An FAO Study, ed. N. Alexandratos. pp. 73-145. FAO of the U. N. and John Wiley and Sons, Toronto. 488 pp.

Anderson, J. A., Effertz, R. J., Faris, J. D., Francl, L. J., Meinhardt, S. W., and Gill, B. S. 1999. Genetic analysis of sensitivity to a *Pyrenophora tritici-repentis* necrosis-inducing toxin in durum and common wheat. Phytopathology 89:293-297.

Anon. 1999. Grain trade of Canada 1997-98. Catalogue number 22-201-XPB. Statistics Canada, Ottawa.

Ballance, G. M., Lamari, L., and Bernier, C. C. 1989. Purification and characterization of a host-selective necrosis toxin from *Pyrenophora tritici-repentis*. Physiol. Mol. Plant Pathol. 35:203-213.

Ballance, G. M., Lamari, L., Kowatsch, R., and Bernier, C. C. 1996. Cloning, expression and occurrence of the gene encoding the Ptr necrosis toxin from *Pyrenophora tritici-repentis*. Molecular Plant Pathology On-Line, http://www.bspp.org.uk/mppol/1996/1209ballance.

Barton, R. 1966. Fine structure of mesophyll cells in senescing leaves of *Phaseolus*. Planta 71:314-325.

Basham, H.G., and Bateman, D.F. 1975. Killing of plant cells by pectic enzymes: the lack of direct injurious interaction between pectic enzymes or their soluble reaction products and plant cells. Phytopathology 65:141-153.

Bateman, D.F. 1976. Plant cell wall hydrolysis by pathogens. p79-103. In: Biochemical aspects of plant-parasite relationships. Friend, J., and Threlfall, D.R. eds. Academic Press, London.

Batz, O., Scheibe, R., Neuhaus, H.E. 1993. Purification of chloroplasts from fruits of green pepper (*Capsicum anuum* L.) And characterization of starch synthesis. Planta 196:50-57.

Benhamou, N., and Lafontaine, P.J. 1995. Ultrastructural and cytochemical characterization of elicitor-induced structural responses in tomato root tissues infected by *Fusarium oxysporum* f.sp. *radicis-lycopersici*. Planta 197:89-102.

Boller, T., and Wiemken, A. 1986. Dynamics of vacuolar comparmentation. Ann. Rev. Plant Physiol. 37:137-164.

Bonhoff, A., Reith, B., Golecki, J., Grisebach, H. 1987. Race cultivar-specific differences in callose deposition in soybean roots following infection with *Phytophthora megasperma* f.sp. *glycinea*. Planta 172:101-105.

Brosch, G., Ransom, R., Lechner, T., Walton, J.D., and Loidl, P. 1995. Inhibition of maize histone deacetylases by HC toxin, the host-selective toxin of *Cochliobolus carbonum*. Plant Cell 7:1941-1950.

Bucheli, P., Doares, S.H., Albersheim, P., and Darvill, A. 1990. Host-pathogen interactions XXXVI. Partial purification and characterization of heat-labile molecules secreted by the rice blast pathogen that solubilize plant cell wall fragments that kill plant cells. Physiol. Mol. Plant Pathol. 36:159-173.

Campbell, N.A. 1993. Protists and the origin of eukaryotes. pp 533-558. In: Biology 3rd edition. The Benjamin/Cummings Publishing Company, Inc. Don Mills, Ontario.

Canny, M.J. 1986. Water pathways in wheat leaves. III. The passage of the mestome sheath and the function of the suberized lamellae. Physiol. Plant. 66:337-347.

Canny, M.J. 1990. Rates of apoplastic diffusion in wheat leaves. New Phytol. 116:263-268.

Carpita, N., Sabularse, D., Montezinos, D., Delmer, D.P. 1979. Determination of the pore size of cell walls of living plant cells. Science 205:1144-1147.

Ciuffetti, L. M., Tuori, R. P., Gaventa, J. M. 1997. A single gene encodes a selective toxin causal to the development of tan spot of wheat. Plant Cell 9:135-144.

Ciuffetti, L. M., Francl, L. J., Ballance, G. M., Bockus, W. W., Lamari, L., Meinhardt, S. W., and Rasmussen, J. B. 1998. Standardization of toxin nomenclature in the *Pyrenophora tritici-repentis*/wheat interaction. Can. J. Plant Pathol. 20:421-424.

Cohen, J. E. 1995. Estimates of human carrying capacity: A survey of four centuries. In: How many people can the earth support? pp. 212-237. W. W. Norton & Company, Inc., New York. 532 pp.

Cortez, P.M., and Sinclair, T.R. 1987. Osmotic potential and starch accumulation in leaves of field-grown soybean. Crop Sci. 27:80-84.

Deacon, J.W. 1997a. Nutrition. p.90-103. In: Modern Mycology. Blackwell Science Ltd., London.

Deacon, J.W. 1997b. Fungi as plant parasites. p.224-253. In: Modern Mycology. Blackwell Science Ltd., London.

Deshpande, U. S. 1993. Effects and mechanism of action of Ptr (*Pyrenophora tritici-repentis*) necrosis toxin on wheat. M. Sc. Thesis, 1993, The University of Manitoba, Winnipeg.

Desilets, H., Benhamou, N., and Bélanger, R.R. 1994. A comparitive study of histological and ultrastructural alterations induced by *Pythium ultimum* or its metabolites on geranium (*Pelargonium*) roots. Physiol. Mol. Plant Pathol. 45:21-36.

Dewey, R.E., Levings, C.S., and Timothy, D.H. 1986. Novel recombinations in the maize mitochondrial genome produce a unique transcriptional unit in the texas male-sterile cytoplasm. Cell 44:439-449.

Dewey, R.E., Siedow, J.N., Timothy, D.H., and Levings C.S. III 1988. A 13-kilodalton maize mitochondrial protein in *E. coli* confers sensitivity to *Bipolaris maydis* toxin. Science 239:293-295.

DeWolf, E. D., Effertz, R. J., Ali, S., and Francl, L. J. 1998. Vistas of tan spot research. Can. J. Plant Pathol. 20:349-370.

Dhingra, O.D. and Sinclair, J.B. 1985. Basic Plant Pathology Methods. CRC Press, Boca Raton, Fla, pp. 355.

Drechsler, C. 1923. Some graminicolous species of *Helminthosporium*. J. Agric. Res. 24:641-740.

Dukes, J., Toma, R. B., and Wirtz, R. 1995. Cross-cultural and nutrional values of bread. Cereal Foods World 40:384-385.

Dushnicky, L. G., Ballance, G. M., Sumner, M. J., and MacGregor, A. W. 1996. Penetration and infection of susceptible and resistant wheat cultivars by a necrosis toxin-producing isolate of *Pyrenophora tritici-repentis*. Can J. Plant Pathol. 18:392-402.

Dushnicky, L.G., Ballance, G.M., Sumner, M.J., and MacGregor, A.W. 1998. The role of lignification as a resistance mechanism in wheat to a toxin-producing isolate of *Pyrenophora tritici-repentis*. Can. J. Plant Pathol. 20:35-47.

Effertz, R.J., Meinhardt, S.W., Anderson, J.A., Jordahl, J.G., and Francl, L.J. Identification of a chlorosis-inducing toxin from *Pyrenophora tritici-repentis* and chromosomal location of a gene conditioning insensitivity in wheat. (Abstract) Phytopathology 88:S25.

Eschrich, W., and Currier, H.B. 1964. Identification of callose by its diachrome and fluorochrome reactions. Stain Tech. 39:303-307.

Evans, L.E., Shebeski, R.C., Briggs, K.G., and Zuzens, D. 1972. Glenlea red spring wheat. Can. J. Plant Sci. 52:1081-1082.

Faris, J. D., Anderson, J. A., Francl, L. J., and Jordahl, J. G. 1996. Chromosomal Location of a Gene Conditioning Insensitivity in Wheat to a Necrosis-Inducing Culture Filtrate from *Pyrenophora tritici-repentis*. Phytopathology 86:459-463.

Ferrarese, L., Trainotti, L., Moretto, P., Polverino de Laureto, P., Rascio, N., and Casadoro, G. 1995. Differential ethylene-inducible expression of cellulase in pepper plants. Plant Mol. Biol. 29:735-747.

Fling, S.P. and Gregerson, D.S. 1986. Peptide and protein molecular weight determination by electrophoresis using a high-molarity Tris buffer system without urea. Anal. Biochem. 155:83-88.

Foissner, I. 1990. Wall appositions induced by ionophore A23187, $CaCl_2$, $LaCl_3$, and nifedipine in characean cells. Protoplasma 154:80-90.

Freeman, T., Rasmussen, J., Francl, L., and Meinhardt, S. 1995. Wheat necrosis induced by *Pyrenophora tritici-repentis* toxin. Pages 990-991 in G. W. Bailey, M. H. Ellisman, R. A. Hennigar, and N. J. Zaluzec, eds., Proceedings of Microscopy and Microanalysis 1995. Jones and Begell Publishers, New York.

Gamba, F. M., Lamari, L., Brûlé-Babel, A. L. 1998. Inheritance of race-specific necrotic and chlorotic reactions induced by *Pyrenophora tritici-repentis* in hexaploid wheats. Can. J. Plant Pathol. 20:401-407.

Gengenbach, B.G., Miller, R.J. Koeppe, D.E. and Arntzen, C.J. 1973. The effect of toxin from *Helminthosporium maydis* (race T) on isolated corn mitochondria: swelling. Can. J. Bot. 51:2119-2125.

Gooding, M. J., and Davies, W. P. 1997. An introduction to the utilization, development and production of wheat. In: Wheat production and utilization systems, quality and the environment. pp. 1-60. CAB International, New York. 355 pp.

Hagborg, W.A.F. 1970. A device for injecting solutions and suspensions into thin leaves of plants. Can. J. Bot. 48:1135-1136.

Hanchey, P. 1981. Ultrastructural effects. In: Toxins in plant disease. Durbin, R.D. ed. Academic Press. New York/London/Toronto/Sydney/San Fransisco.

Hanchey, P., and Wheeler, H. 1968. Pathological changes in ultrastructure: false plasmolysis. Can. J. Bot. 47:675-678.

Hoober, J.K. 1984. Chloroplasts. Plenum. New York. 280 pp.

Hosford, R. M. 1971. A form of *Pyrenophora trichostoma* pathogenic to wheat and other grasses. Phytopathology 61:28-32.

Hosford, R. M. 1972. Propagules of *Pyrenophora trichostoma*. Phytopathology 62:627-629.

Hughes, J. and McCully, M.E. 1975. The use of an optical brightener in the study of plant structure. Stain Tech. 50:319-329.

Jones, D.R., Graham, W.G., and Ward, E.W.B. 1975. Ultrastructural changes in pepper cells in an incompatible interaction with *Phytophthora infestans*. Phytopathology 65:1274-1285.

Kauss, H. 1987. Some aspects of calcium-dependent regulation in plant metabolism. Ann. Rev. Plant Physiol. 38:47-72.

Kauss, H. 1996. Callose synthesis. pp77-92. In: Membranes: specialized functions in plants. Smallwood, M., Knox, J.P., and Bowles, D.J. eds. BIOS Scientific Publishers Ltd., Oxford, UK.

Keck, R.W., and Hodges, T.K. 1973. Membrane permeability in plants: changes induced by host-specific pathotoxins. Phytopathology 63:226-230.

Keon, J.P.R. 1985. Cytological damage and cell wall modification in cultured apple cells following exposure to pectin lyase from *Monilinia fructigena*. Physiol. Plant Pathol. 26:11-29.

Kirschenbaum, D.M. 1975. Molar absorptivity and A1%/1 cm values for proteins at selected wavelenghts of the ultraviolet and visible regions. Anal. Biochem. 68:465-484.

Kofalvi, S.A., Gao, J.-G., and Nassuth, A. 1995. Biochemical investigation into the wall collapse of wheat leaf cells caused by wheat streak mosaic virus infection. Physiol. Mol. Plant Pathol. 47:379-389.

Kohmoto, K., Kondoh, Y., Kohguchi, T., and Otani, H. 1984. Ultrastructural changes in host leaf cells caused by host-selective toxin of *Alternaria alternata* from rough lemon. Can. J. Bot. 62:2485-2492.

Kohmoto, K., Otani, H., Kodama, M., and Nishimura, S. 1989. Host recognition: can accessibility to fungal invasion be induced by host-specific toxins without necessitating necrotic cell death? p. 249-265. In: Phytotoxins and plant pathogenesis. Graniti, A. ed. Springer-Verlag. Berlin.

Krupinsky, J. M. 1982. Observations on the host range of isolates of *Pyrenophora trichostoma*. Can. J. Plant Pathol. 4:42-46.

Kwon, C. Y., Rasmussen, J. B., Francl, L. J., and Meinhardt, S. W. 1996. A quantitative bioassay for necrosis toxin from *Pyrenophora tritici-repentis* based on electrolyte leakage. Phytopathology 86:1360-1363.

Kwon, C. Y., Rasmussen, J. B., and Meinhardt, S. W. 1998. Activity of Ptr ToxA from *Pyrenophora tritici-repentis* requires host metabolism. Physiol. Mol. Plant Pathol. 52:201-212.

Lai, W., and Srivastava, L.M. 1976. Nuclear changes during differentiation of xylem vessel elements. Cytobiologie 12:220-243.

Lamari, L., and Bernier, C. C. 1989a. Evaluation of wheat lines and cultivars to tan spot [*Pyrenophora tritici-repentis*] based on lesion type. Can. J. Plant Pathol. 11:49-56.

Lamari, L., and Bernier, C. C. 1989b. Virulence of isolates of *Pyrenophora tritici-repentis* on 11 wheat cultivars and cytology of the differential host reactions. Can. J. Plant Pathol. 11:284-290.

Lamari, L., and Bernier, C. C. 1989c. Toxin of *Pyrenophora tritici-repentis*: host-specificity, significance in disease, and inheritance of host reaction. Phytopathology 79:740-744.

Lamari, L., and Bernier, C. C. 1991. Genetics of tan necrosis and extensive chlorosis in tan spot of wheat caused by *Pyrenophora tritici-repentis*. Phytopathology 81:1092-1095.

Lamari, L., and Bernier, C. C. 1994. Temperature-induced resistance to tan spot [*Pyrenophora tritici-repentis*] of wheat. Can. J. Plant Pathol. 16:279-286.

Lamari, L., Bernier, C. C., and Smith R. B. 1991. Wheat genotypes that develop both tan necrosis and extensive chlorosis in response to isolates of *Pyrenophora tritici-repentis*. Plant Disease 75:121-122.

Lamari, L., Ballance, G. M., Orolaza, N. P., and Kowatsch, R. 1995. *In planta* production and antibody neutralization of the Ptr necrosis toxin from *Pyrenophora tritici-repentis*. Phytopathology 85:333-338.

Larez, C. R., Hosford, R. M., and Freeman, T. P. 1986. Infection of wheat and oats by *Pyrenophora tritici-repentis* and initial characterization of resistance. Phytopathology 76:931-938.

Lee, T. S., and Gough, F. J. 1984. Inheritance of Septoria leaf blotch (*S. tritici*) and Pyrenophora tan spot (*P. tritici-repentis*) resistance in *Triticum aestivum* cv. Carifen 12. Plant Disease 68:848-851.

Lehninger, A.L., Nelson, D.L., and Cox, M.M. 1993. Carbohydrate biosynthesis. p. 598-641. In: Principles of Biochemistry. Worth Publishers, Inc. New York.

Levings, C.S. III, and Siedow, J.N. 1992. Molecular basis of disease susceptibility in the Texas cytoplasm of maize. Plant Mol. Biol. 19:134-147.

Loegering, W. Q. 1978. Current concept in interorganismal genetics. Ann. Rev. Phytopathol. 16:309-333.

Lucas, W.J., Ding, B., and van der Shoot, C. 1993. Plasmodesmata and the supracellular nature of plants. New Phytol. 125:435-476.

Luz, W. C. da, and Berstrom G.C. 1986. Evaluation of triadimenol seed treatment for early season control of tan spot, powdery mildew, spot blotch and septoria nodorum spot on spring wheat. Crop Protection 5:83-87.

Maeda, H., and Ishida, N. 1967. Specificity of binding of hexopyranosyl polysaccharides with fluorescent brightener. J. Biochem. 62:276-278.

Margulis, L. 1993. Symbiosis in cell evolution: microbial communities in the Archean and Proterozoic eons. 2nd ed. W.H. Freeman and Company. New York. 452 pp.

Martin, J.S., Green, R.D., Cotter, T.G. 1994. Dicing with death: dissecting the components of the apoptosis machinery. Trends Biol. Sci. 19:26-30.

Mathieu, Y., Kurkdjian, A., Xia, H., Guern, J., Koller, A., Spiro, M.D., O'Neill, M., Albersheim, P., and Darvill, A. 1991. Membrane responses induced by oligogalacturonides in suspension-cultured tobacco cells. Plant J. 1:333-343.

McCully. M.E., and O'Brien, T.B. 1981. The study of plant structure: principles and selected methods. Termarcarphi Pty. Ltd., Melbourne, Australia. 357 pp.

McQueen-Mason, S., and Cosgrove, D.J. 1994. Disruption of hydrogen bonding between plant cell wall polymers by proteins that induce wall extension. Proc. Natl. Acad. Sci. USA 91:6574-6578.

Meeley, R.B., Johal, G.S., Briggs, S.P., and Walton, J.D. 1992. A biochemical phenotype for a disease resistance gene of maize. Plant Cell 4:71-77.

Mehta, Y. R., Riede, C. R., Campos, L. A. C., and Kohli, M. M. 1992. Integrated management of major wheat diseases in Brazil: an example for the Southern Cone region of Latin America. Crop Protection 11:517-524.

Meyer, S.L.F.,and Heath, M.C. 1987a. A comparison of the death induced by fungal invasion or toxic chemicals in cowpea epidermal cells. I. Cell death induced by heavy metal salts. Can. J. Bot. 66:613-623.

Meyer, S.L.F., and Heath, M.C. 1987b. A comparison of the death induced by fungal invasion or toxic chemicals in cowpea epidermal cells. II. Responses induced by *Erisiphe cichoracearum*. Can. J. Bot. 66:624-634.

Miller, R.J., and Koeppe, D.E. 1971. Southern corn leaf blight: susceptible and resistant mitochondria. Science 173:67-69.

Mittelheuser, C.J., and Van Steveninck, R.F.M. 1971. The ultrastructure of wheat leaves. I. Changes due to natural senescence and the effects of kinetin and ABA on detached leaves incubated in the dark. Protoplasma 73:239-252.

Mittler, R., and Lam, E. 1997. Characterization of nuclease activities and DNA fragmentation induced upon hypersensitive response cell death and mechanical stress. Plant Mol. Biol. 34:209-221.

Morrall, R. A. A., and Howard, R. J. 1975. The epidemiology of leaf spot disease in a native prairie. II. Airborne spore populations of *Pyrenophora tritici-repentis*. Can. J. Bot. 53:2345-2353.

Navarre, D.A., and Wolpert, T.J. 1995. Inhibition of the glycine decarboxylase multienzyme complex by the host-selective toxin victorin. Plant Cell 7:463-471.

O'Brien, T.P., and Kuo, J. 1975. Development of the suberized lamella in the mestome sheath of wheat leaves. Aust. J. Bot. 23:783-794.

Oertli, J.J. 1986. The effect of cell size on cell collapse under negative turgor pressure. J. Plant Physiol. 124:365-370.

Ohana, P., Delmer, D.P., Volman, G., Steffens, J.C., Matthews, D.E., and Benziman, M. 1991. β-Furfuryl-β-glucoside: an endogenous activator of higher plant UDP-glucose:(1->3)-β-glucan synthase. Biological activity, distribution, and *in vitro* synthesis. Plant Physiol. 98:708-715.

Ohana, P., Benziman, M., and Delmer, D.P. 1993. Stimulation of callose synthesis in vivo correlates with changes in intracellular distribution of the callose synthase activator β-furfuryl-β-glucoside. Plant Physiol. 101:187-191.

Ojanperä, K., Sutinen, S., Pleijel, H., and Selldén, G. 1992. Exposure of spring wheat, *Triticum aestivum* L., cv. Drabant, to different concentrations of ozone in open-top chambers: effects on the ultrastructure of flag leaf cells. New Phytol. 120:39-48.

Okolie, P.H., and Obasi, B.N. 1992. Implication of cell wall degrading enzymes in the heat-induced softening of the African Pear (*Dacryodes edulis* (G Don) H J Lam). J. Sci. Food Agric. 59:59-63.

Olsnes, S., and Sandvig, K. 1985. Toxins. p. 195-234. In: Endocytosis. Pastan, I., and Willingham, M.C. eds. Plenum Press, New York and London.

Otani, H. Nishimura, S., and Kohmoto, K. 1973. Nature of specific susceptibility to *Alternaria kikuchiana* in Nijisseiki cultivar among Japanese pears. (II). J. Faculty Agric., Tottori University 8:14-20.

Otani, H., Kohmoto, K., and Nishimura, S. 1989. Action sites for AK-toxin produced by the Japanese pear pathotype of *Alternaria alternata*. p. 107-120. In: Host-specific toxins: recognition and specificity factors in plant disease. Kohmoto, K., and Durbin, R.D., eds. Tottori University Press, Tottori.

Otani, H., Kohmoto, K., Kodama, M., and Nishimura, S. 1991. Role of host-specific toxins in the pathogenesis of *Alternaria alternata*. p139-149. In: Molecular strategies of pathogens and host plants. Patil, S.S. ed. Springer-Verlag, New York.

Otani, H., Kohmoto, K., and Kodama, M. 1995. *Alternaria* toxins and their effects on host plants. Can. J. Bot. 73(Suppl. 1):S453-S458.

Palmgren, M.G. 1991. Regulation of plant plasma membrane H^+-ATPase activity. Physiol. Plant. 83:314-323.

Park, P. 1977a. Effects of the host-specific toxin and other toxic metabolites produced by *Alternaria kikuchiana* on ultrastructure of leaf cells of Japanese pear. Ann. Phytopathol. Soc. Japan 43:15-25.

Park, P. 1977b. Ultrastructural and cytochemical changes in unit membrane of membranous inclusions observed in cells of Japanese pear leaves treated with *Alternaria kikuchiana*-toxin. Ann. Phytopathol. Soc. Japan 43:475-478.

Park, P. 1977c. Origin of inclusive materials between cell walls and invaginated plasma membranes in cells of susceptible leaves of Japanese pear treated with a host-specific toxin from *Alternaria alternata* Tanaka. Physiol. Plant Pathol. 11:39-42.

Park, P. 1998. The accelerated effects of AK-toxin I on exocytosis and endocytosis of susceptible Japanese pear leaves. In: Molecular genetics of host-specific toxins in plant disease. Kohmoto, K., and Yoder, O.C. eds. Kluwer Academic Publishers, Dordrecht/Boston/London.

Park, P., Fukutomi, M., Akai, S. and Nishimura, S. 1976. Effect of the host-specific toxin from *Alternaria kikuchiana* on the ultrastructure of plasma membranes of cells in leaves of Japanese pear. Physiol. Plant Pathol. 9:167-174.

Park, P., Nishimura, S., Kohmoto, K., Otani, H., and Tsujimoto, K. 1981. Two action sites of AM-toxin I produced by apple pathotype of *Alternaria alternata* in host cells: an ultrastructural study. Can. J. Bot. 59:301-310.

Park, P., Ohno, T., Nishimura, S., Kohmoto, K., and Otani, H. 1987. Leakage of sodium ions from plasma membrane modification, associated with permeability change, in host cells treated with a host-specific toxin from a Japanese pear pathotype of *Alternaria alternata*. Can. J. Bot. 65:330-339.

Pearce, A.G.E. 1968. Histochemistry: Theoretical and applied. Volume 1. 3rd ed. J. & A. Churchill Ltd., London. 759 pp.

Pearce, R.S., and Beckett, A. 1987. Cell shape in leaves of drought-stressed barley examined by low temperature scanning electron microscopy. Ann. Bot. 59:191-195.

Pearce, R.S., and McDonald, I. 1977. Ultrastructural damage due to freezing followed by thawing in shoot meristem and leaf mesophyll cells of tall fescue (*Festuca arundinacea* Schreb.). Planta 134:159-168.

Pringle, R.B. and Braun, A.C. 1957. The isolation of the toxin of *Helminthosporium victoriae*. Phytopathology 47:369-376.

Quartacci, M.F., Forli, M., Rascio, N., Vecchia, F.D., Bochicchio, A., and Navari-Izzo, F. 1997. Desiccation-tolerant *Sporobolus stapfianus*: lipid composition and cellular ultrastructure during dehydration and rehydration. J. Exp. Bot. 48:1269-1279.

Raven, P.H., Evert, R.F., and Eichhorn, S.E. 1992. Plants and people. p.686-712. In: Biology of Plants. 5th ed. Worth Publishers, Inc., New York. 791 pp.

Rees, R. G. and Platz, G. J. 1979. The occurrence and control of yellow spot of wheat in north-eastern Australia. Aust. J. Exp. Agric. An. Husb. 19:369-372.

Rees, R. G., and Platz, G. J. 1980. Effects of yellow spot on wheat: comparison of epidemics at different stages of crop development. Aust. J. Agric. Res. 34:39-46.

Revelle, R. 1976. The resources available for agriculture. Sci. Am. 235:165-178.

Ride, J.P. 1978. The role of cell wall alterations in resistance to fungi. Ann. Applied Biol. 89:302-306.

Ride, J.P., and Pearce, R.B. 1979. Lignification and papillla formation at sites of attempted penetration of wheat leaves by non-pathogenic fungi. Physiol. Plant Pathol. 15:79-92.

Roberts, D. A., and Boothroyd, C. W. 1984. Prologue to Part I: The nature and consequences of disease in Plants. In: Fundamentals of plant pathology, 2nd ed., pp. 6-14. W. H. Freeman and Company, New York. 432 pp.

Roel G.L. of den Camp, and Kuhlemeier, C. 1997. Aldehyde dehydrogenase in tobacco pollen. Plant Mol. Biol. 35:355-365.

Ruzin, S.E. 1999. Plant microtechnique and microscopy. Oxford University Press. New York. 322 pp.

Salisbury, F.B., and Ross, C.W. 1992. Absorption of mineral salts. pp 136-160. In: Plant Physiology. 4th ed. Wadsworth Publishing Co., Belmont, California.

Scheffer, R. P. 1991. Role of toxins in evolution and ecology of plant pathogenic fungi. Experientia 47:804-811.

Scheffer, R. P., and Livingston, R. S. 1984. Host-selective toxins and their role in plant diseases. Science 223:17-21.

Scheffer, R.P., and Samaddar, K.R. 1970. Host-specific toxins as determinants of pathogenecity. Recent Adv. Phytochem. 3:123-142.

Scheffer, R.P., and Yoder, O.C. 1970. Host-specific toxins and selective toxicity. p. 251-269. In: Phytotoxins in plant diseases; proceedings of the NATO advanced study institute, Pugnochiuso, Italy. Wood, R.K.S, Ballio, A., and Graniti, A. eds. Academic Press, London, New York.

Schilder, A. M. C. and Bergstrom, G. C. 1995. Seed transmission of *Pyrenophora tritici-repentis*, causal fungus of tan spot of wheat. Euro. J. Plant Pathol. 101:81-91.

Schwartzman, R.A., and Cidlowski, J.A. 1993. Apoptosis: the biochemistry and molecular biology of programmed cell death. Endocr. Rev. 14:133-151.

Shaw, M., and Manocha, M.S. 1965. Fine structure in detached, senescing wheat leaves. Can. J. Bot. 43:747-755.

Sherwood, R.T., and Vance, C.P. 1976. Histochemistry of papillae formed in reed canarygrass leaves in response to noninfecting pathogenic fungi. Phytopathology 66:503-510.

Shimomura, N., Park, P., Otani, H., Kodama, M., and Kohmoto, K. 1992. Effects of light and SH-reagent on ultrastructural changes in leaf cells induced by AM-toxin from *Alternaria alternata* apple pathotype. Ann. Phytopathol. Soc. Jpn. 58:305-309.

Shiraishi, T., Kiba, A., Inata, A., Sugiura, T., Toyoda, K., Ichinose, Y., and T. Yamada. 1998. Plant cell wall with the suppressor may play a crucial role in determining specificity. In: Molecular genetics of host-specific toxins in plant disease. Kohmoto, K., and Yoder, O.C. eds. Kluwer Academic Publishers, Dordrecht/Boston/London.

Shoemaker, R. A. 1962. Drechslera Ito. Can. J. Bot. 40:809-836.

Sim IV, T., Willis, W. G., and Eversmeyer, M. G. 1988. Kansas plant disease survey. Plant Disease 72:832-836.

Škalamera, D., and Heath, M.C. 1995. Changes in the plant endomembrane system associated with callose synthesis during the interaction between cowpea (*Vigna unguiculata*) and the cowpea rust fungus (*Uromyces vignae*). Can. J. Bot. 73:1731-1738.

Škalamera, D., and Heath, M.C. 1996. Cellular mechanisms of callose deposition in response to fungal infection or chemical damage. Can. J. Bot. 74:1236-1242.

Smith, M.M., and McCully, M.E. 1978a. Enhancing aniline blue fluorescent staining of cell wall structures. Stain Tech. 53:79-85.

Smith, M.M., and McCully, M.E. 1978b. A critical evaluation of the specificity of aniline blue induced fluorescence. Proplasma 95:329-354.

Srivastava, L.M., Singh, A.P. 1972. Certain aspects of xylem differentiation in corn. Can. J. Bot. 50:1795-1804.

Stock, W. S., Brûlé-Babel, A. L., and Penner, G. A. 1996. A gene for resistance to a necrosis-inducing isolate of *Pyrenophora tritici-repentis* located on 5BL of *Triticum aestivum* cv. Chinese Spring. Genome 39:598-604.

Stover, R. W., Francl, L. J., and Jordahl, J. G. 1996. Tillage and fungicide management of foliar diseases in a spring wheat monoculture. J. Prod. Agric. 9:261-265.

Strauss, S.J., Kim, K.S., and Murry, L.E. 1982. Light and electron microscopy of plant leaf cells after short-term exposure to bromine gas. Phytopathology 72:793-800.

Strelkov, S. E., Lamari, L., and Ballance, G. M. 1999. Characterization of a host-specific protein toxin (Ptr ToxB) from *Pyrenophora tritici-repentis*. Mol. Plant Microbe Interactions 12:728-732.

Sutherland, J., and McCully, M.E. 1976. A note on the structural changes in the walls of pericycle cells initiating lateral root meristems in *Zea mays*. Can. J. Bot. 54:2083-2087.

Tabira, H., Otani, H., Shimomura, N., Kodama, M., Kohmoto, K., and Nishimura, S. 1989. Light-induced insensitivity of apple and Japanese pear leaves to AM-toxin from *Alternaria alternata* apple pathotype. Ann. Phytopathol. Soc. Jpn. 55:567-578.

Tadege, M., and Kuhlemeier, C. 1997. Aerobic fermentation during tobacco pollen development. Plant Mol. Biol. 35:343-354.

Taunton, J., Hassig, C.A., and Schreiber, S.L. 1996. A mammalian histone deacetylase related to the yeast transcriptional regulator Rpd3p. Science 272:408-411.

Tekauz, A. 1976. Distribution, severity, and relative importance of leaf spot diseases of wheat in western Canada in 1974. Can. Plant Dis. Survey 56:36-40.

Tekauz, A., Platford, R. G., and English, N. C. 1982. Tan spot of wheat. Proceedings of Manitoba Agronomists. pp. 60-65.

Thomson, W.W., and Platt, K.A. 1997. Conservation of cell order in desiccated mesophyll of *Selaginella lepidophylla* ([Hook and Grev.] Spring). Ann. Bot. 79:439-447.

Tomás, A., and Bockus, W. W. 1987. Cultivar-specific toxicity of culture filtrates of *Pyrenophora tritici-repentis*. Phytopathology 77:1337-1340.

Tucker, M.L., Baird, S.L., and Sexton, R. 1991. Bean leaf abscission: tissue-specific accumulation of a cellulase mRNA. Planta 186:52-57.

Varner, J.E., and Lin, L.-S. 1989. Plant cell wall architecture. Cell 56:231-239.

Walton, J.D. 1994. Deconstructing the cell wall. Plant Physiol. 104:1113-1118.

Walton, J. D. 1996. Host-selective toxins: agents of compatibility. Plant Cell 8:1723-1733.

Walton, J.D., and Earle, E.D. 1985. Stimulation of extracellular polysaccharide synthesis in oat protoplasts by the host-specific phytotoxin victorin. Planta 165:407-415.

Walton, J. D., and Panaccione, D. G. 1993. Host-selective toxins and disease specificity: perspectives and progress. Ann. Rev. Phytopathol. 31:275-303.

Wang, H., Li, J., Bostock, R.M., and Gilchrist, D.G. 1996. Apoptosis: A functional paradigm for programmed plant cell death induced by a host-selective phytotoxin and invoked during development. Plant Cell 8:375-391.

Wheeler, H. 1974. Cell wall and plasmalemma modification in diseased and injured plant tissue. Can. J. Bot. 52:1005-1009.

Wink, M. 1993. The plant vacuole: a multifunctional compartment. J. Exp. Bot. 44:231-246.

Wise, R.P., Fliss, A.E., Pring, Gengenbach, B.G. 1987. Urf13-T of T cytoplasm maize mitochondria encodes a 13 kD polypeptide. Plant Mol. Bio. 9:121-126.

Wodzicki, T.J., and Humphreys, W.J. 1973. Maturing pine tracheids. J. Cell Biol. 56:263-265.

Wolpert, T.J., Macko, V., Acklin, W., and Arigoni, D. 1988. Molecular features affecting the biological activity of the host-selective toxins from *Cochliobolus victoriae*. Plant Physiol. 88:37-41.

Wolpert, T.J., and Macko, V. 1989. Specific binding of victorin to a 100-kDa protein from oats. Proc. Natl. Acad. Sci. USA 86:4092-4096.

Wolpert, T.J., Navarre, D.A., Moore, D.L., and Macko, V. 1994. Identification of the 100 kD victorin binding protein from oats. Plant Cell 6:1145-1155.

Wyllie, A.H., Morris, R.G., Smith, A.L., and Dunlop, D. 1984. Chromatin cleavage in apoptosis: association with condensed chromatin morphology and dependence on macromolecular synthesis. J. Path. 142:67-77.

Yoder, O. C. 1980. Toxins in Pathogenesis. Ann. Rev. Phytopathol. 18:103-129.

Yoder, O.C., and Scheffer, R.P. 1973. Effects of *Helminthosporium carbonum* toxin on nitrate uptake and reduction by corn tissue. Plant Physiol. 52:513-517.

Yoshida, M. and Sugita, K. 1992. A novel tetracyclic peptide, trapoxin, induces phenotypic change from transformed to normal in *sis*-oncogene transformed NIH3T3 cells. Jpn. J. Cancer Res. 83:324-328.

Zhang, H.-F., Francl, L. J., Gordahl, J. G., and Meinhardt, S. W. 1997. Structural and physical properties of a necrosis-inducing toxin from *Pyrenophora tritici-repentis*. Phytopathology 87:154-160.